

General Disclaimer

One or more of the Following Statements may affect this Document

- This document has been reproduced from the best copy furnished by the organizational source. It is being released in the interest of making available as much information as possible.
- This document may contain data, which exceeds the sheet parameters. It was furnished in this condition by the organizational source and is the best copy available.
- This document may contain tone-on-tone or color graphs, charts and/or pictures, which have been reproduced in black and white.
- This document is paginated as submitted by the original source.
- Portions of this document are not fully legible due to the historical nature of some of the material. However, it is the best reproduction available from the original submission.

NASA CR-135177

SRD-77-059



BASIC NOISE RESEARCH PROGRAM

- FAN NOISE -

**EFFECT OF INLET DISTURBANCES ON FAN INLET NOISE
DURING A STATIC TEST**

by K.L. Bekofske, R.E. Sheer, and J.C.F. Wang

(NASA-CR-135177) EFFECT OF INLET
DISTURBANCES ON FAN INLET NOISE DURING A
STATIC TEST (General Electric Co.) 89 p
HC A05/MF A01 CSCL 20A

N77-21091

G3/07

Unclassified
44467

GENERAL ELECTRIC COMPANY

prepared for



NATIONAL AERONAUTICS AND SPACE ADMINISTRATION

NASA Lewis Research Center

Contract NAS 3-17853

1 Report No NASA CR-135177	2 Government Accession No.	3. Recipient's Catalog No.
4. Title and Subtitle BASIC NOISE RESEARCH PROGRAM - FAN NOISE - EFFECT OF INLET DISTURBANCES ON FAN INLET NOISE DURING A STATIC TEST		5. Report Date April 1977
7. Author(s) K.L. Bekofske, R.E. Sheer, Jr., and J.C.F. Wang		6. Performing Organization Code
9. Performing Organization Name and Address General Electric Company Corporate Research and Development Schenectady, New York		8. Performing Organization Report No SRD-77-059
12. Sponsoring Agency Name and Address National Aeronautics and Space Administration Washington, D.C. 20456		10. Work Unit No.
15. Supplementary Notes Project Manager, James H. Dittmar, NASA Lewis Research Center, Cleveland, Ohio		11. Contract or Grant No. NAS 3-17853
16. Abstract		13. Type of Report and Period Covered Contractor Report
17. Key Words (Suggested by Author(s)) Aircraft engine noise Fan noise Inlet distortion Inlet disturbance Inlet turbulence Ground vortex		18. Distribution Statement Unclassified - unlimited
19. Security Classif. (of this report) Unclassified	20. Security Classif. (of this page) Unclassified	21. No. of Pages 84
22. Price*		

TABLE OF CONTENTS

<u>Section</u>		<u>Page</u>
1	SUMMARY	1
2	INTRODUCTION	3
3	TEST DESCRIPTION	7
	Test Facility Description.	7
	Instrumentation.	8
	Test Procedure	10
	Data Recording and Reduction	14
4	TEST RESULTS	19
	Hot Film Results	19
	Acoustic Results	27
5	DISCUSSION OF RESULTS	39
6	CONCLUSIONS	41
7	ACKNOWLEDGMENTS	42
	Appendix I - HOT FILM SYSTEM	43
	Appendix II - TABULATION OF ONE-THIRD-OCTAVE ACOUSTIC DATA	47
	Appendix III - REFERENCES	83

LIST OF ILLUSTRATIONS

<u>Figure</u>		<u>Page</u>
1	Comparison of Flight and Projected Static Inlet Noise Spectra ⁽¹⁾	3
2	Inlet Flow Disturbances Which Occur During Ground Static Tests	4
3	Schematic of the Aero/Acoustic Laboratory	7
4	Overall View of the Aero/Acoustic Laboratory	8
5	Test Vehicle Fan Performance Map	9
6	Test Vehicle Layout	10
7	Instrumentation Probe Support and Circumferential Actuator System .	11

LIST OF ILLUSTRATIONS (Cont'd)

<u>Figure</u>		<u>Page</u>
8	Instrumentation Probe Support and Circumferential Actuator System Installed on Test Vehicle	11
9	Schematic of Simulated Ground Plane Locations.	12
10	Simulated Ground Plane Installed in Anechoic Chamber for Z/D = 0.9 Configuration	13
11	Block Diagram of Hot-Film Measurement System for Stationary or Movable Probe	15
12	Interpretation of X-Probe Hot-Film Velocity Measurements.	16
13	Inlet Disturbances Arising Along the Exterior Cowl as Ambient Air Is Drawn into the Inlet	19
14	Baseline Configuration Circumferential Hot-Film Mappings Showing Wakes Shed by Several Disturbances on Exterior Cowl	20
15	On-Line Inlet Mean and Turbulent Velocity Profiles with Ground Plane at Z/D = 0.9; 69% Speed.	21
16	On-Line Inlet Mean and Turbulent Velocity Profiles for the Porous Chamber Configuration (baseline) at 69% Speed	24
17	Comparison of Turbulent Velocity Profiles for Ground Plane, Nonporous Chamber and Porous Chamber Configurations at 69% Speed.	25
18	Comparison of Integrated Turbulence Length Scales for the Porous and Nonporous Chamber Configurations at 69% Speed.	25
19	Typical Circumferential Velocity Space-Time Cross-Correlation Measurements with Respect to a Stationary Hot-Film Probe at 150	26
20	Typical Autopower Spectra of Circumferential Velocity Measurement.	27
21	Blade Passing Frequency SPL Directivity; 54% Corrected Speed	28
22	Blade Passing Frequency SPL Directivity; 69% Corrected Speed	28
23	Blade Passing Frequency SPL Directivity; 86% Corrected Speed	29
24	Blade Passing Frequency SPL Directivity; 90% Corrected Speed	29
25	Blade Passing Frequency SPL Directivity; 100% Corrected Speed	30
26	Baseline and Ground Plane PWL Spectra for 54% Corrected Speed	31
27	Baseline and Ground Plane PWL Spectra for 69% Corrected Speed	31
28	Baseline and Ground Plane PWL Spectra for 86% Corrected Speed	32
29	Baseline and Ground Plane PWL Spectra for 90% Corrected Speed	32
30	Baseline and Ground Plane PWL Spectra for 100% Corrected Speed	33

LIST OF ILLUSTRATIONS (Cont'd)

<u>Figure</u>		<u>Page</u>
31	54% Speed PWL Increase Due to Ground Plane	33
32	69% Speed PWL Increase Due to Ground Plane	34
33	86% Speed PWL Increase Due to Ground Plane	34
34	90% Speed PWL Increase Due to Ground Plane	35
35	100% Speed PWL Increase Due to Ground Plane	35
36	Blade-Passage-Tone PWL Increase for Ground Plane and Nonporous Chamber Configurations Compared with Baseline	36
37	Conceptual Sketch of Flared Inlet with Exterior Cowl Boundary Layer Suction	40
38	X-Hot-Film Calibration (A + B) Flow at 45 ⁰ to the Sensors	44
39	Effect of Time Delay Window Length on the Turbulence Length Scale Measurement for an Exponential Covariance Function	46

Section 1

SUMMARY

There is evidence that forward radiated fan noise data taken during static test situations do not agree with aircraft engine flight data. In particular, static tests generally produce a significantly higher tone at blade passage frequency than that measured during flight. The present report describes an experimental program carried out to investigate two types of inlet disturbances which may be partially responsible for this discrepancy—large-scale turbulence and inlet vortices.

The anechoic chamber employed for these tests nominally drew air through the floor, ceiling, and all walls (except the wall in the immediate vicinity of the fan inlet duct). The baseline chamber was thus designed to provide a porous-box type of arrangement. Far-field acoustic measurements were made to determine the baseline forward radiated fan noise. In addition, a pair of cross-element hot-film probes provided measurements of the axial and transverse mean velocities and turbulence intensities of the inlet flow field ahead of the rotor. One of the hot-film probes was mounted on an actuator which allowed circumferential mapping around a 180° arc within the inlet. Similarly, inlet flow field mappings ahead of the rotor were carried out while the artificially created inlet vortices or large-scale turbulence were present, to determine the change in the flow and turbulence structure caused by these distortions. The extent of the influence of the artificially created inlet disturbances on the measured forward-radiated fan noise was obtained by direct comparison of their far-field acoustic results with the baseline measurements.

Far-field acoustic results indicated significant increases (up to 4 dB) in the blade passage tone levels for subsonic tip speeds when the distortions were present. The noise level changes were insignificant at supersonic speeds because of the domination of multiple pure tones.

The ground vortices were generated by installing a simulated ground plane directly beneath the fan inlet. The hot-film results obtained with this arrangement clearly showed the orientation and location of the incoming ground vortices and the associated increases in both axial and transverse turbulence intensities.

The large-scale inlet turbulence was achieved by eliminating the porous-box feature of the test chamber. Turbulence length scales were increased by a factor of 2 to 4 with this arrangement. Further analyses of the hot-film data showed evidence of the eddy stretching which usually occurs during static testing.

Substantial inlet distortions were also detected during the testing of the baseline, porous chamber configuration. These disturbances were attributed to a reverse flow that occurred on the exterior cowl of the test setup. Because the baseline was contaminated in this manner, the increased noise levels due to the intentionally generated disturbances were not as great as they otherwise might have been. In a follow-up program, an attempt is being made to eliminate the disturbances related to the exterior cowl.

Section 2

INTRODUCTION

The initial measurement of the acoustic signature of a developmental aircraft engine is commonly made during a static test situation. It is then normal procedure to use these data to project to an in-flight situation in order to predict the actual noise level during flight conditions. However, it has been established (Refs. 1-3) that, even with all known corrective factors (e.g., dynamic effect and atmospheric attenuation) applied to the static measurements, projections of forward radiated noise based on static tests are at variance with actual aircraft engine flight data. An example of such a projection (Ref. 1) is shown in Figure 1, where General Electric CF6-6 ground static engine data were used to predict the DC10-10 flight sound pressure levels. In the forward (inlet) quadrant, such as the approach condition shown in Figure 1, a significant discrepancy occurs. In particular, the static tests generally yield a significantly noisier blade-passage-frequency (BPF) tone and higher (harmonic) frequencies than are actually measured in flight. The difference at BPF for the low power setting shown in Figure 1 is about 8 dB. At higher speeds (takeoff conditions) the effect is generally less, about 2 to 4 dB. Since it is believed that the fan inlet noise is being reduced in going from static to flight conditions, earlier assessments of fan inlet noise based on static data have probably been misleading.

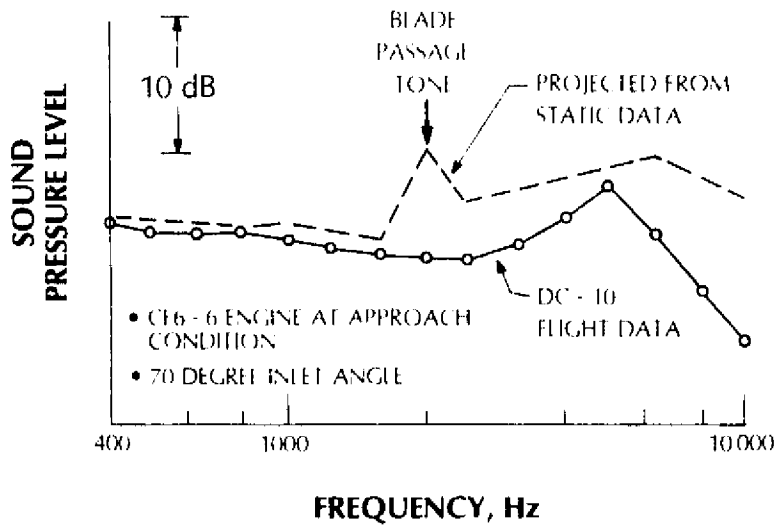


Figure 1. Comparison of Flight and Projected Static Inlet Noise Spectra⁽¹⁾

There are several aspects to the impact of the incorrect evaluation of fan inlet noise levels in aircraft engines. For instance, some potentially worthwhile fan source noise reduction concepts may have been given less consideration than they deserved, or been actually abandoned, because the noise generation during static test was dominated by a source not present in flight. Some source noise reduction concepts, such as the proper selection of vane-blade ratios, increased vane-blade spacings, and vane lean, rely heavily on reducing the rotor-stator interaction as a source noise mechanism (Ref. 4). However, some negative reaction to these methods of source noise reduction may have resulted because, when they were tested statically, the fan inlet noise was dominated by the interaction of the rotor with inlet disturbances, rather than rotor-stator interaction.

A further disturbing ramifications of the static-to-flight noise level discrepancy is the possible misuse of engine development funds due to the improper identification of the source of a noise problem. This might result in the investigation of a problem when, in fact, none exists.

There may be an initial opposition to all static engine acoustic tests based on the above considerations. Yet the static test remains a necessary ingredient in any fan noise reduction program, for practical as well as economic reasons. Therefore, instead of eliminating all static acoustic tests, it is important to explore and remove the causes of the static-to-flight discrepancy, with the objective to give more certainty to aircraft engine flight noise projections. Several methods of simulating flight in a static situation have been attempted (Refs. 5, 6) but to date each one seems to have its own drawbacks.

Several explanations have been given for the decrease in fan inlet noise level during flight, the so-called "in-flight effects." (The commonly used expression "in-flight effects" is actually misleading; it is the increase in noise levels during static tests, not the decrease during flight, which causes the static-to-flight discrepancy.) These explanations all relate to the widely accepted belief that the inlet flow disturbances that are ingested by the engine and interact with the rotor while it is being tested statically, leading to rotor interaction noise, do not occur or are greatly reduced during flight. Cumpsty and Lowrie (Ref. 7) demonstrated that the alteration in character of inlet disturbances with forward speed can indeed produce significant in-flight reductions of BPF tones compared with the levels recorded during static tests. Several sources have been commonly suggested for the inflow disturbances during ground static tests (Figure 2): wakes shed from test-stand supports; ambient air turbulence (including wind disturbances); and ground vortices.

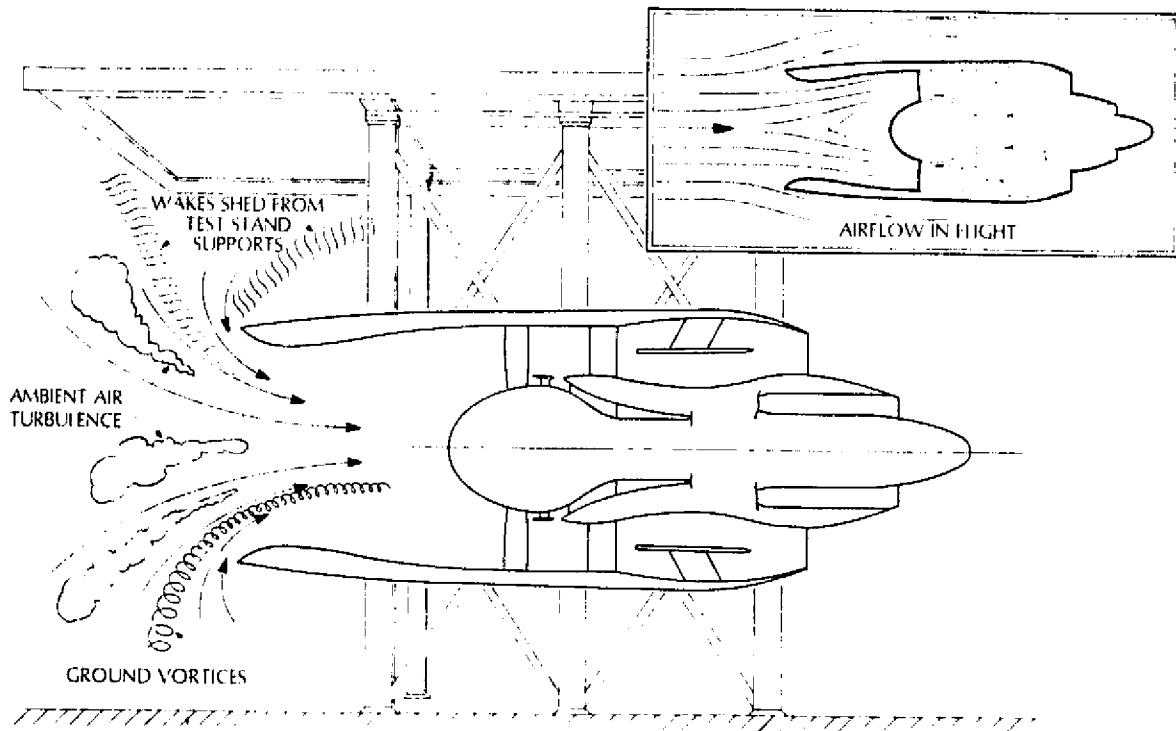


Figure 2. Inlet Flow Disturbances Which Occur During Ground Static Tests

Many researchers (Refs. 8-14) have suggested how one or more of these disturbances can lead to increases in the BPF pure tone and its harmonics. It was observed during ground static tests carried out at NASA Lewis Research Center (Ref. 8) that wakes shed by support structures can lead to substantially higher BPF tone levels. Essentially the same fan was tested in rear drive and front drive. During the front-drive installation, distortion of inlet airflow by a test-stand support structure resulted in more nonuniform inflow. Accompanying far-field acoustic measurements indicated more than a 10 dB increase in fan-generated BPF tone sound pressure level (SPL) above the cleaner rear-drive installation.

An investigation carried out at NASA Ames Research Center (Ref. 9) indicated the significance of the role played by the length scale of fan inlet turbulence on rotor-generated noise. It was found that the reduction of the ambient turbulence length scale to less than one rotor pitch was accompanied by approximately a 10 dB reduction in the sound pressure level of the BPF tone and its first harmonic. Hanson (Ref. 10-12) has pointed out that, when an engine is being tested statically outdoors, ambient air is being drawn into the inlet from all directions as in classical sink flow. Therefore, atmospheric turbulence eddies, which are initially almost isotropic, are stretched into long, thin "sausages" of turbulence (Figure 2). Hanson has been very successful in measuring such disturbances.

These stretched eddies appear to the rotor as almost steady distortions and are a highly effective mechanism of noise generation as they interact with the rotor. This noise mechanism does not exist during flight, since air ingested by the engine originates in a comparatively small cylindrical tube ahead of the inlet, with minimal eddy stretching (Figure 2, inset). Additional experiments at NASA Ames, carried out in a wind tunnel in an attempt to simulate the effects of flight, further demonstrated the importance of inflow turbulence on fan inlet tone noise (Ref. 5). Again, an increase in the turbulence length scale was accompanied by an increase in the blade-passage-frequency SPI level.

Ground vortices, when they exist, can also produce a type of almost steady inlet distortion on the rotor. The existence and strength of ground vortices depend on such factors as inlet height above the ground and ambient wind conditions. The impact which these ground vortices have on fan inlet noise is likely to be similar to the influence of the stretched inflow turbulence described above. This has recently been demonstrated by Hodder (Ref. 14).

The experimental program described in this report was performed at General Electric Corporate Research and Development in order to further investigate some of these possible causes for the static-to-flight noise discrepancy and help answer the fundamental question of in-flight cleanup. The main objective of this program was to provide data which would determine the extent of the influence of inlet ground vortices and large-scale turbulence on the forward radiated fan noise measured at a static test facility. An aerodynamic investigation of fan inlet disturbances was performed in conjunction with acoustic measurements. While inlet ground vortices or large-scale inlet turbulence were being generated intentionally in an anechoic test chamber, far-field noise measurements were taken. In addition, by means of a specially built actuator device, circumferential and radial mappings of the inlet were carried out with hot-film equipment in order to determine the change in the inlet flow caused by such inflow disturbances.

Section 3

TEST DESCRIPTION

TEST FACILITY DESCRIPTION

The test program was conducted in an anechoic chamber at the Aero/Acoustic Laboratory of General Electric Corporate Research and Development, in Schenectady, New York. Figure 3 is a schematic diagram of the facility, and Figure 4 is a photograph showing the inside of the facility. This anechoic chamber was carefully designed to simulate free-field acoustic operation. All walls, floor, and ceiling are covered with an array of 0.71 m (28 in.) high polyurethane foam wedges, to provide less than ± 1 dB standing wave ratio at 200 Hz. A distinguishing feature of the facility is that the walls, floor, and ceiling are porous. This porous-box arrangement is achieved by a manifolding system whereby flow is distributed from a filter house through 15.2 cm (6 in.) deep, U-shaped channels surrounding the chamber. The array of foam wedges is secured to the tops of the channels, and airflow enters the chamber by passing through small openings between the wedges. Such an aspirating chamber arrangement is intended to significantly reduce inflow distortion to the fan. The anechoic chamber is approximately 10.7 m (35 ft) wide by 7.6 m (25 ft) long by 3.1 m (10 ft) high, measured from the tips of the foam wedges.

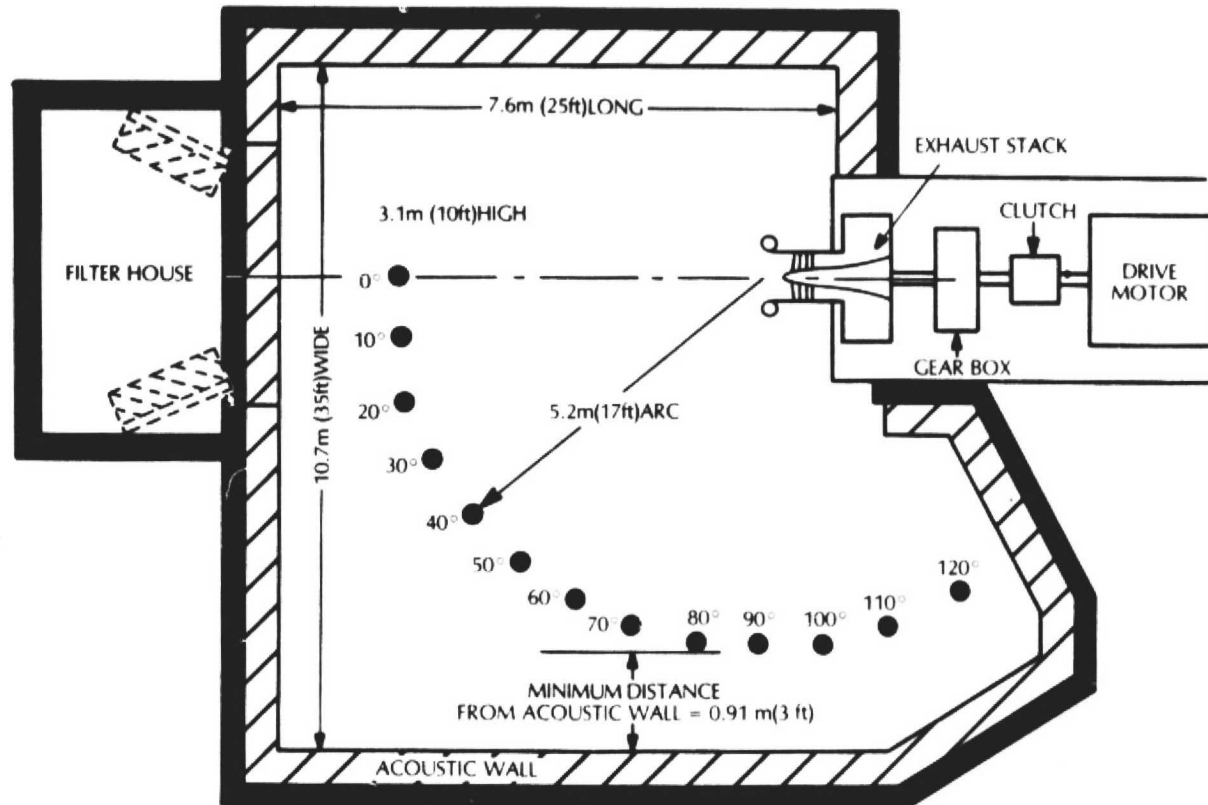


Figure 3. Schematic of the Aero/Acoustic Laboratory

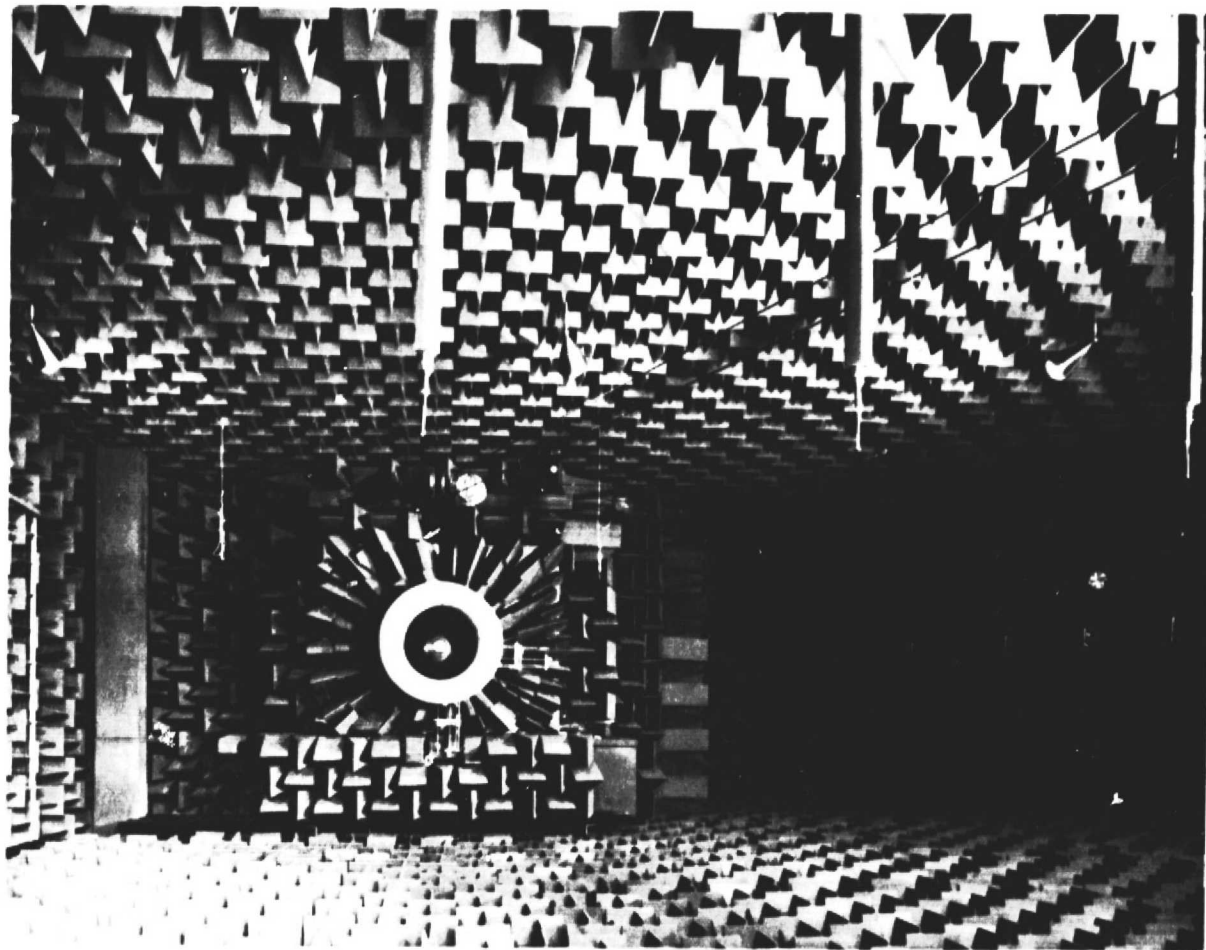


Figure 4. Overall View of the Aero/Acoustic Laboratory

The test vehicle used in this investigation was the NASA Lewis 0.504 m (20 in.) diameter fan model designated as Rotor 11. The stator set and casing were manufactured by General Electric. The overall stage has the design characteristics indicated in Table 1 and the fan performance map is shown in Figure 5. This test vehicle supplied both the air flow and sound source.

The fan inlet was a cylindrical hardwall duct with a length-to-diameter ratio of approximately 0.8. A vehicle layout drawing is shown in Figure 6. All configurations were tested with the standard GE bellmouth, shown in Figures 4 and 6.

INSTRUMENTATION

Both acoustic and aerodynamic measurements were made. The former involved anechoic chamber far-field noise measurements, which were provided by an array of twelve 0.635 cm (0.25 in.) diameter far-field microphones (B&K 4135) located on a 5.2 m (17 ft) radius arc, centered one rotor diameter upstream of the rotor front face. The microphones were arranged at 10° intervals from 0° to 110° relative to the fan centerline (see Figure 3).

Table 1
TEST FAN STAGE DESIGN CHARACTERISTICS

Rotor Inlet Tip Diameter	0.504m (19.84in)
Pressure Ratio	1.574
Rotor Blade Number	44
Stator Vane Number	86
Vane/Blade Ratio	1.95
Inlet Guide Vanes	None
Rotor Inlet Hub Tip Radius Ratio	0.50
Rotor-Stator Tip Spacing	1.27 Rotor Chords
Rotor Rotative Speed	16100 RPM
Rotor Tip Speed	424.9 m/sec (1394ft/sec)
Rotor Tip Inlet Relative Mach. No.	1.394
Rotor Chord (Midspan)	4.62 cm (1.817in)
Stator Chord (Midspan)	4.06 cm (1.597 in)
Rotor Aspect Ratio	2.5
Stator Aspect Ratio	2.3
Rotor Tip Solidity	1.298
Stator Tip Solidity	1.270
Corrected Inlet Weight Flow	29.5 Kg/sec (65 lb/sec)
Adiabatic Efficiency	85.5% (80.9% Measured)

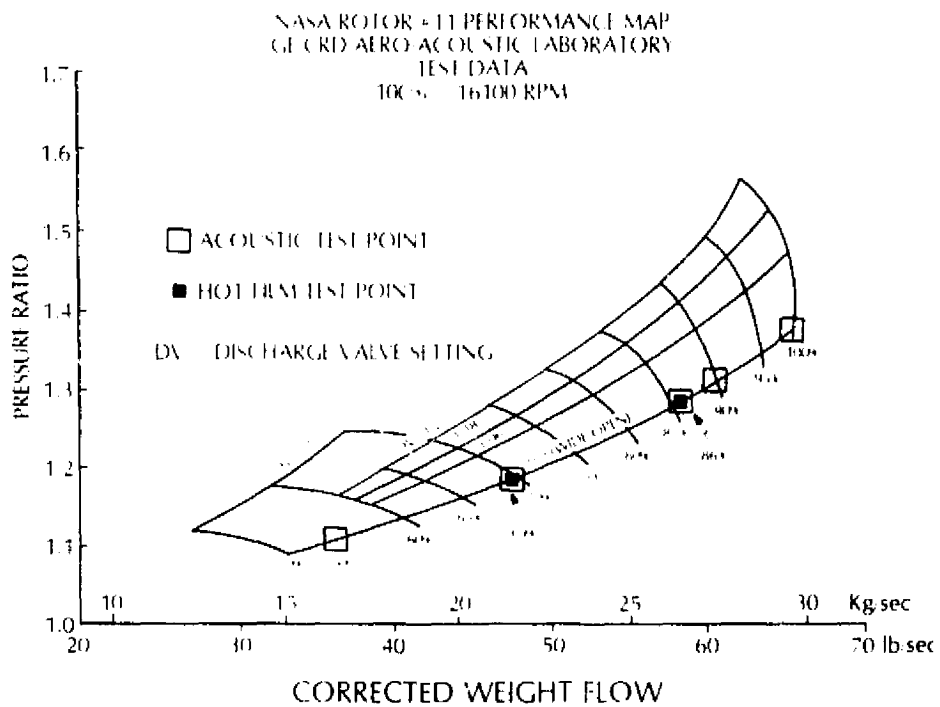


Figure 5. Test Vehicle Fan Performance Map

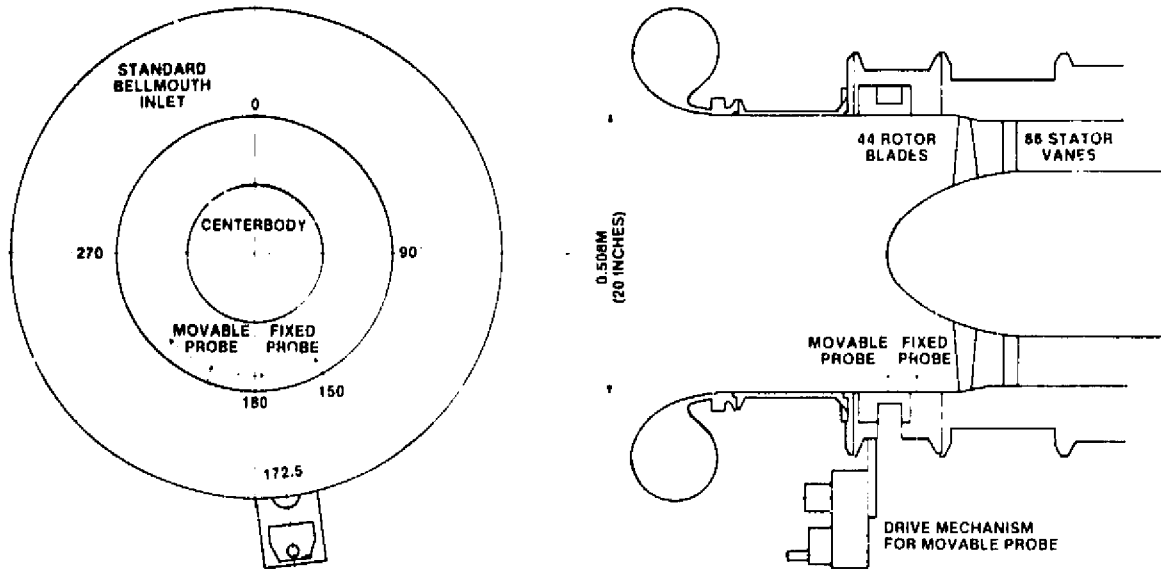


Figure 6. Test Vehicle Layout

Aerodynamic measurements were taken to determine the fan performance. The instrumentation included four total pressure/total temperature five-element rakes, located downstream of the stator, and a 0.56 m (22 in.) diameter orifice in the discharge piping to measure pressure ratio and mass flow.

Inlet turbulence was measured to provide radial and circumferential mappings of the flow approaching the rotor. Axial and transverse inlet velocities and turbulence levels were measured by cross hot-film probes (X-probes). Two X-probes were employed simultaneously during each test. One probe was mounted on a motor-driven actuator mechanism which, after installation on the test vehicle and calibration, was capable of being remotely rotated circumferentially over slightly more than 180° to within $\pm 1^\circ$ accuracy. This actuator mechanism is indicated in Figure 6 and shown in the photographs presented as Figures 7 and 8. The angular location of the rotating hot-film probe was measured by a potentiometer. The second X-probe was mounted on a fixed retainer on the shroud wall (Figure 8). The hot-film probe retainer and the circumferential actuator system could be incorporated into the inlet outer wall at any desired angular orientation. During the test program, however, the stationary probe was used as a reference and located at $\theta = 150^\circ$, forward-looking-aft (FLA), near the bottom of the inlet (see Figure 6). The rotating hot-film probe was movable with respect to the reference probe from $\theta = 82.5^\circ$ to 262.5° FLA or, in some cases, from 112.5° to 292.5° FLA. The stationary and the rotating probes were positioned at 6.9 cm (2.7 in.) and 11.4 cm (4.5 in.), respectively, upstream of the rotor face. Both probes were indexed manually to various radial immersions in 0.635 cm (0.25 in) steps. This radial indexing could be done only while the vehicle was sitting at idle speed or shut down.

TEST PROCEDURE

Three chamber configurations were tested. These can be described briefly as follows:

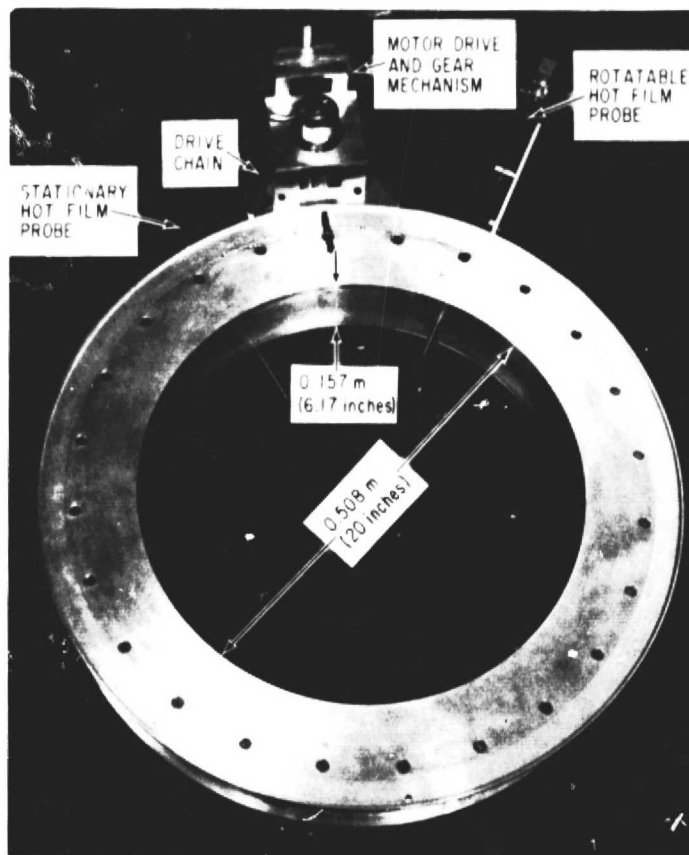


Figure 7. Instrumentation Probe Support and Circumferential Actuator System



Figure 8. Instrumentation Probe Support and Circumferential Actuator System Installed on Test Vehicle

- a. Rotor 11 was first tested in the Aero/Acoustic Laboratory in what is referred to as the baseline configuration. All walls, floor, and ceiling of the anechoic chamber were aspirating and the standard hardwall inlet installed (Figure 6). This configuration was tested at the beginning and near the end of the test program.
- b. In order to investigate the effect of an incoming ground vortex on the inlet noise of the fan stage, two configurations were tested with a 2.44 m by 2.44 m (8 ft x 8 ft) simulated horizontal ground plane situated beneath the fan inlet (see Figures 9 and 10). The air inflow manifolding to the anechoic chamber floor was blocked during the testing of these configurations. It was found that an auxiliary blower providing a crosswind was not necessary to trigger the ground vortex. The condition for the generation and ingestion of the strongest ground vortices was determined to be with the ground plane situated as close as possible to the inlet bellmouth. This corresponded to $Z/D = 0.9$, where Z = height of the inlet centerline above the ground plane, and D = inlet diameter. A schematic diagram of this test configuration is shown in Figure 9 and a photograph in Figure 10. The fan was also tested with the minimum Z/D ratio and, hence, the strongest vortex that might be encountered in normal aircraft engine operation. An A300B Airbus with a CF6-50C engine was geometrically simulated with respect to the ground plane. With the aircraft at rest, the engine inlet centerline is $Z = 1.16D$ above the ground. Therefore, for the 0.504 m (20 in.) diameter inlet being tested, the simulated ground plane was situated 0.59 m (23.2 in.) below the fan centerline. This situation also is indicated schematically in Figure 9.

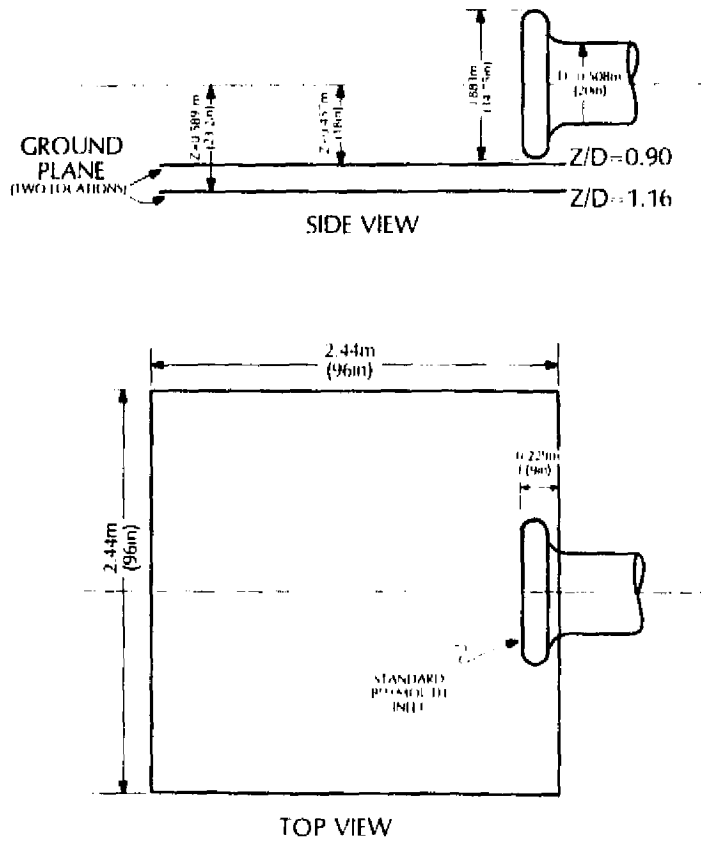


Figure 9. Schematic of Simulated Ground Plane Locations

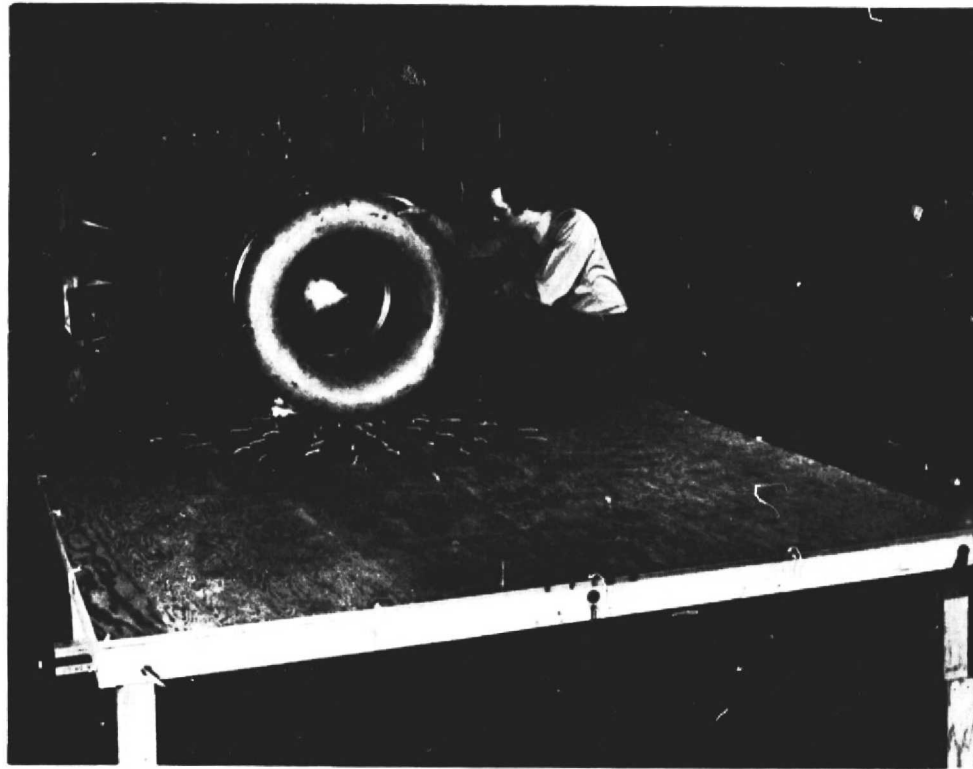


Figure 10. Simulated Ground Plane Installed in Anechoic Chamber for Z/D = 0.9 Configuration

- c. Finally, Rotor 11 was tested with the anechoic chamber modified so that flow was admitted only through the doors leading from the filter house (see Figure 3). All manifolding to the floor, ceiling, and walls was blocked. It was expected that with this method of airflow entrance into the anechoic chamber, the axial scale of the flow turbulence structure into the fan would increase.

Aerodynamic measurements were taken prior to measuring other test data. The conditions for these tests are shown in the fan performance map presented as Figure 5. Each of the configurations described above was tested at the wide-open ($DV = 0$) discharge valve throttle setting (see Figure 5). A test point was reached by adjusting the fan speed to achieve the correct operating point on the fan performance map. The proper physical fan speed was determined as a function of ambient temperature to assure that each test point was at the appropriate corrected fan speed.

Hot-film data were measured at two fan speeds: 69% and 86% corrected speeds. The lower speed (subsonic tip speed, $U_T = 293$ m/sec [962 ft/sec]) is typical of approach conditions; the higher speed (supersonic tip speed, $U_T = 365$ m/sec [1199 ft/sec]) is typical of takeoff conditions for current CTOL engines. Hot-film data were recorded for post-test analyses (auto- and/or cross-correlations) only where deemed necessary. During hot-film measurements, the stability of test conditions and instrumentation drift were checked at several repeat points at different times.

For each hot-film test, preliminary on-line circumferential mappings of mean velocity and turbulence intensity in the inlet ahead of the rotor were obtained at several radial positions between the shroud wall and the centerbody (stationary and movable probes at the same radius). Based on the results of these preliminary axial and transverse mean flow and turbulence level measurements, two radial immersions were selected -- 12.7 cm (0.5 in.), and 3.81 cm (1.5 in.) -- at which to record hot-film measurements for each test condition on magnetic tape for off-line data analyses. These immersions were characteristic of boundary-layer and free-stream flow, respectively.

Acoustic test points included 54, 69, 86, 90, and 100% corrected speeds. The three lowest speeds were selected so that the corresponding blade passing frequencies would lie near the centers of the 6300, 8000, and 10,000 Hz 1/3-octave bands, respectively, for operating conditions in the -5 to 30°C (23 to 86°F) ambient temperature range, which was encountered during the test period. Far-field acoustic data repeat points were taken at 69% and 86%, and the data were found to be very repeatable. All acoustic data to be presented for 69% and 86%, therefore, will represent the average of two readings for each configuration. No inlet probes were installed during measurement of any far-field acoustic data.

In addition to the above aerodynamic and acoustic measurements, some flow visualization, using freely moving tufts, was used to determine the general character of the inlet flow and, in particular, the existence and character of any ground vortices or other flow disturbances in the neighborhood of the fan inlet. These were videotaped for post-test comparisons and analyses.

DATA RECORDING AND REDUCTION

Fan operation was stabilized to steady state before initiating any data recording. After stabilization, the following operational parameters were logged:

- Inlet Configuration
- Barometric Pressure
- Run Number/Reading Number
- Date/Time
- Chamber Pressure and Temperature
- Rotor Speed (rpm)
- Discharge Valve Position
- Shaft, Gear, and Casing Vibrations
- Bearing Temperature

Basic pressure data were individually sampled through use of a 48 channel Scanivalve system. Temperature data were sampled directly through a Hewlett-Packard (HP) crossbar scanner and digital voltmeter.

The hot-film probes were calibrated prior to the start of the test series, prior to the start of each new configuration, and whenever a change in a probe characteristic was noticed. A schematic of the hot-film anemometer arrangement, its data acquisition and reduction systems, is shown in Figure 11. The signals from an X-probe, A and B, were linearized via a dual channel TSI model 1054 anemometer, then input to a TSI model 1063

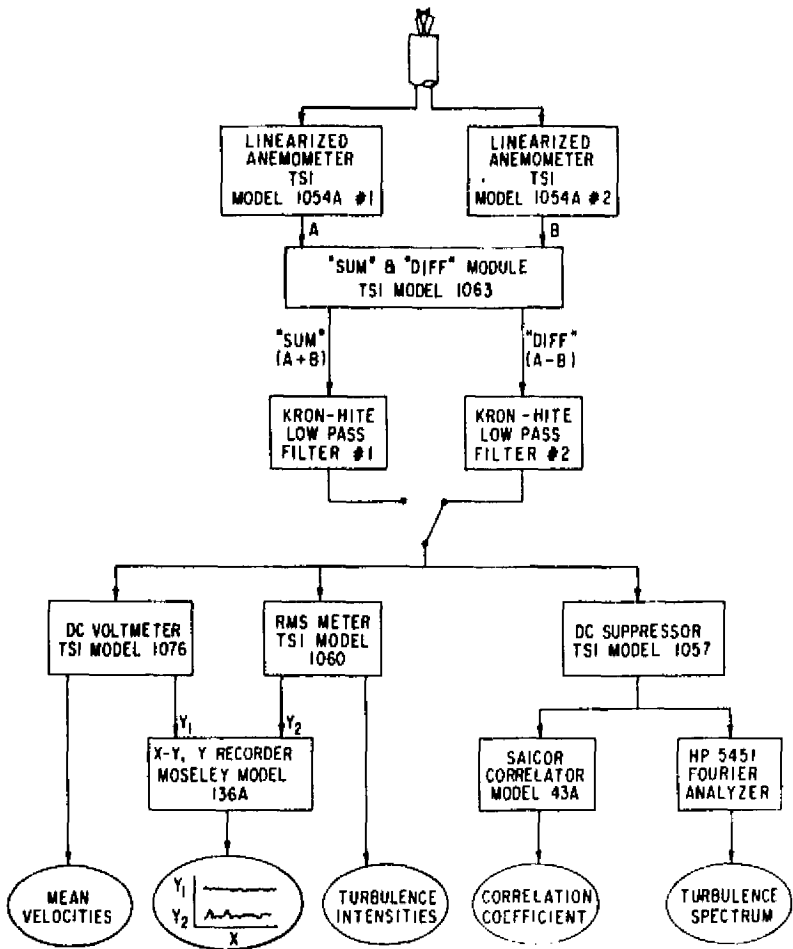
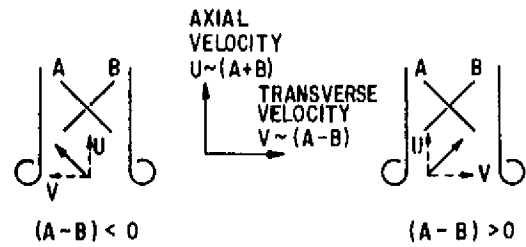


Figure 11. Block Diagram of Hot-Film Measurement System for Stationary or Movable Probe

sum-difference module. The sum (A+B) and the difference (A-B) outputs from the sum-difference module represented respectively the axial (U) and the circumferential (V) velocity components of the flow. The interpretation of the circumferential velocity direction from the (A-B) measurement is shown in Figure 12 (a). The vortex patterns indicated in Figure 12 (b) will be explained later. Calibrations of the X-probes up to 150 m/sec (500 ft/sec) with a standard ASME nozzle flow were performed on each hot-film individually, followed by the sum-difference module outputs. The hot-film signals were analyzed on-line for system check and preliminary observations and reduced off-line for extensive analyses.

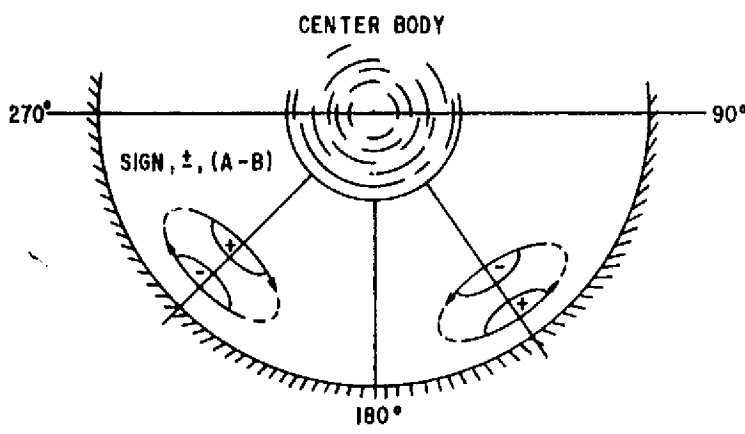
The mean axial velocities from both X-probes were much higher than the circumferential velocities during inlet turbulence measurements. Therefore, a dc suppression arrangement was made with a pair of Tektronix AM2 differential amplifiers to reduce the dc level of these axial velocity measurements. The dc suppression system was designed to preserve the low frequency signals in the hot-film measurements as opposed to a regular ac coupled system. The dc suppressed axial and the circumferential velocity components, measured by the fixed and rotating X-probes, were recorded on magnetic tape for off-line data reduction. A "no flow" and a one-volt calibration signal for each

probe were recorded on each reel of instrumentation tape containing hot-film data. At each recorded hot-film data point, $A + B$ (axial) and $A - B$ (circumferential) dc-suppressed rms signals were recorded for both probes simultaneously at 30 in./s for approximately 3-1/2 minutes. The Sangamo Sabre IV model 4918 tape recorder had 20 kHz capability in the FM mode at 30 in./s.



"X"-ARRAY HOT FILM DIRECTIONALITY

(a)



GROUND VORTEX VISUALIZATION VIA
CIRCUMFERENTIAL VELOCITY MEASUREMENTS

(b)

Figure 12. Interpretation of X-Probe Hot-Film Velocity Measurements

Four types of information were obtained from the data reduction system: 1) mean velocities, 2) turbulent velocities, 3) integrated turbulence length scales, and 4) turbulence power spectra. The first two quantities were usually obtained on-line, using dc voltmeters and rms meters. The outputs from the dc voltmeter and rms meter represented the mean and turbulent velocities, respectively. These were plotted on an X-Y, Y plotter (Moseley model 136A X-Y, Y recorder), with X representing the hot-film circumferential position. A pair of low-pass filters set at 5 kHz cutoff frequency were used at the inputs to the dc voltmeter and rms meter to reduce the noise on the signal. During production of these on-line velocity plots, a time constant of 0.1 second was used on both meters to keep up with the scanning speed of the moving hot-film probe. During off-line analyses, however, a time constant of 10 seconds was used for turbulent velocity measurements.

GENERAL ELECTRIC

The integrated turbulence length scales were obtained from the auto- and cross-correlation measurements of the fixed and rotating hot films. The correlation measurements were performed by means of a Saicor model 43A Correlator. The turbulence length scales were obtained on the basis of the usual assumption that the autocorrelation function was an exponential function with respect to delay time. Space-time cross-correlation measurements were performed only on the $Z/D = 0.9$ ground plane configuration. Turbulence power spectra were measured in the HP5451-A Fourier analyzer. Much attention was given to the signals at low frequencies (below 10 Hz) which were expected to correspond to the inlet disturbances.

An electrostatic calibration of the acoustic data acquisition system was performed prior to starting the test series. In addition, all far-field microphones were calibrated with a piston phone, and the calibrations were recorded on each reel of instrumentation tape containing far-field data. Prior to the test series and whenever an instrument was replaced, microphone serial numbers, amplifier serial numbers, monitor scope numbers, and their respective tape tracks were recorded.

The acoustic data from the far-field microphones were recorded simultaneously at 60 in./s for one minute at each data point. The 28 track Sangamo recorder used (Sabre IV model 4918) had a 40 kHz capability in the FM mode at 60 in./s.

Forward radiated SPL and PWL noise spectra were obtained. Basic microphone acoustic output was 1/3-octave bands from 100 Hz to 80 kHz. The 1/3-octave analyzer was a General Radio model 1927 real-time analyzer whose digital output was put on a magnetic tape by the HP 2100 computer system. A final step was scaling the data to standard day conditions (59°F , 70% relative humidity), using the CRD 635 computer.

Section 4

TEST RESULTS

HOT FILM RESULTS

An unfortunate but significant aspect of the test setup was discovered during the hot-film mappings of the baseline configuration. Each of the types of inlet disturbances specifically tested (ground vortices and large-scale turbulence), in addition to wakes shed from test-stand supports (Figure 2), is more likely to be present at an outdoor test facility than in a carefully designed indoor test chamber. However, the baseline experiments carried out during this program demonstrated that such anechoic chambers have yet another source of inlet distortions. These disturbances can be classified as those arising from the "upstream" flow along the exterior cowl as ambient air is drawn into the inlet from all directions (Figure 13). Such disturbances may be caused by instrumentation leads, probe supports and actuators, and flanges. These types of distortions may also occur in outdoor test facilities; but during indoor anechoic chamber tests, in the absence of those disturbances occurring outdoors, these distortions can become important to inlet noise generation.

PRECEDING PAGE BLANK NOT FILMED

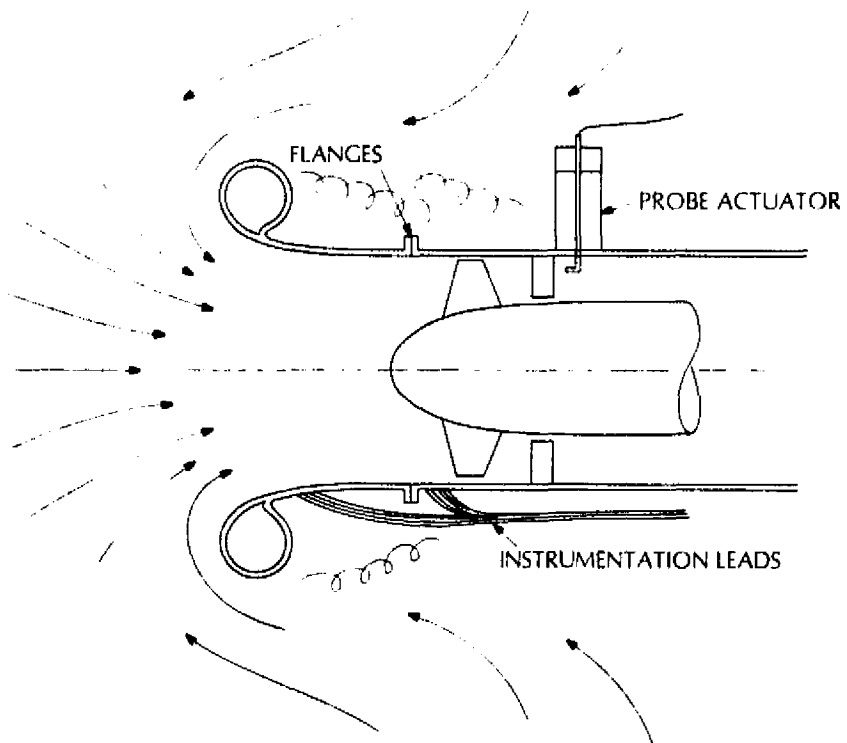


Figure 13. Inlet Disturbances Arising Along the Exterior Cowl as Ambient Air is Drawn into the Inlet

Evidence of such exterior-cowl-related disturbances are shown in Figure 14, where inlet hot-film mappings are shown for the baseline chamber arrangement. The 180° location shown in all such figures as Figure 14 was the bottom center of the inlet. Distortions originating from the circumferential actuator motor support (seen at the top of the photograph in Figure 7, but located near the bottom of the inlet during testing) and

a V-retainer flange coupling bolt are indicated in Figure 14 (a) and (b). A conventional radial actuator was added between these disturbance sources during a second circumferential mapping; the influence of its wake is clearly seen in the data shown in Figure 14(b). (A pair of these radial actuators is seen at 90° and 180° in Figure 4, a photograph taken during an earlier program.) Freely moving tufts were attached to each of these protuberances, and there was clear visual evidence of wakes being shed by them as flow passed upstream over them toward the inlet.

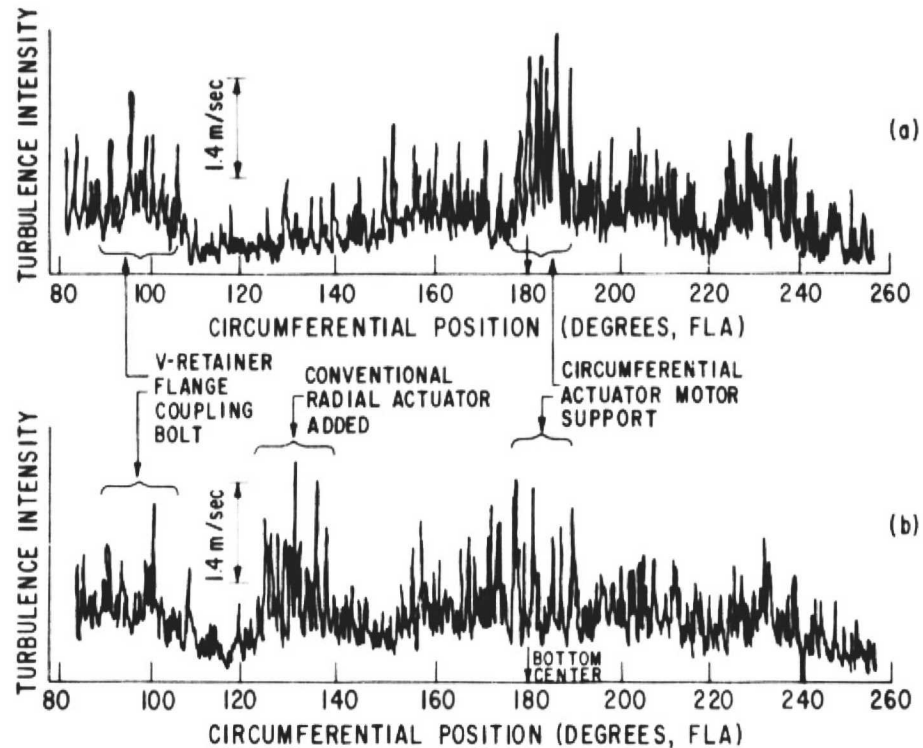


Figure 14. Baseline Configuration Circumferential Hot-Film Mappings Showing Wakes Shed by Several Disturbances on Exterior Cowl (corrected speed, $N/\sqrt{\theta} = 100\%$; mean velocity, $\bar{U} = 145$ m/sec; hot-film probe immersion = 1.27 cm)

One obvious ramification of these results is that, whenever an actuator is used for a hot-film probe during a static test, care must be exercised to assure that the inlet flow fluctuations being measured are not directly attributable to the actuator, its support, or even the probe stem itself. Although these fixtures are outside the inlet, they are directly in line with the upstream flow along the exterior cowl, which passes into the inlet and over the sensor.

Figure 15 (a) and (b) show scanning plots of the on-line circumferential mean and turbulent velocities, respectively, at the $Z/D = 0.9$ ground plane location for 69% speed. The abscissa is the angular location, θ , of the rotating hot-film probe. Velocity traces were obtained at various radial immersions from the outer wall of the inlet section. The existence of a ground vortex pair can be seen clearly in these two sets of velocity and turbulence traces. First, the mean circumferential velocities at the 0.635 cm (0.25 in.), 1.27 cm (0.50 in.), and 2.54 cm (1.0 in.) immersions were found positive on one side of the bottom center (180°) and negative on the other. Based on the direction interpretation

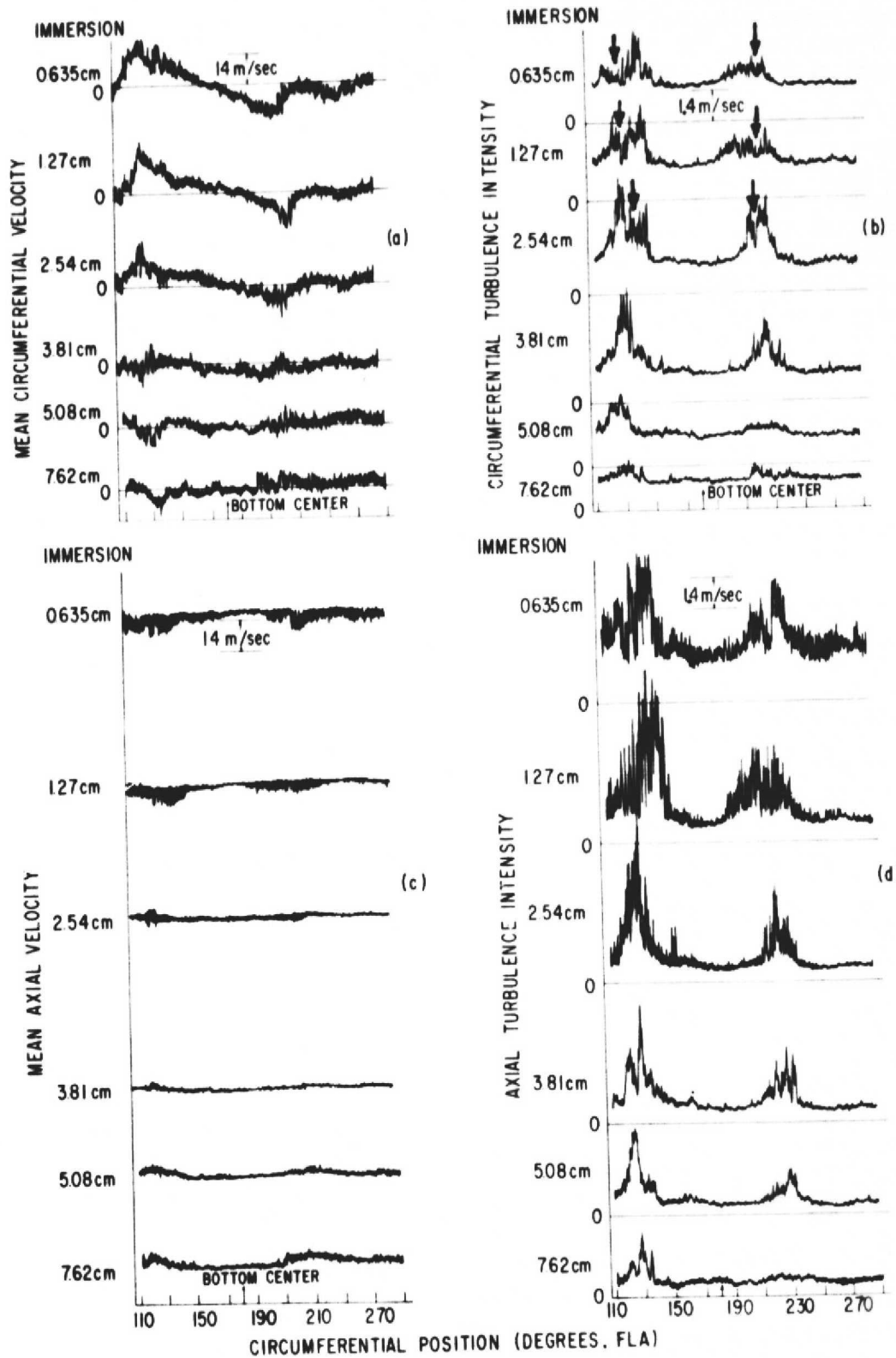


Figure 15. On-Line Inlet Mean and Turbulent Velocity Profiles with Ground Plane at $Z/D = 0.9$; 69% Speed

shown in Figure 12(a), the flow moved in opposite directions on either side of the bottom center. As the hot-film immersion increased from 2.54 cm (1.0 in.), toward inlet centerline, to 7.62 cm (3.0 in.), the transverse velocities reversed their directions. A sketch of this measured velocity orientation observation is shown in Figure 12 (b).

A pair of ground vortices easily fits into the explanation of this observation. Further evidence for the ground vortices can be deduced from the turbulent velocity plots shown in Figure 15(b). High turbulence is observed where the vortices are identified from the mean velocity plots. Slight dips in the turbulent velocity measurements near the middle of the high turbulence areas are indications of the existence of the vortex centers (0.635, 1.27, and 2.54 cm [0.25, 0.50, and 1.0 in.] immersions); these are indicated by the arrows in Figure 15(b). One vortex was centered near 135° FLA, while the other occurred near 225°. The swirl direction of the vortices deduced from the hot-film velocity scans agreed with the observation of tufts on the ground plane. At distances greater than 3.81 cm (1.5 in) from the outer wall, the turbulence and the mean circumferential velocity gradually diminish. The edge of the ground vortices appears to be situated near the 7.62 cm (3 in) immersion location.

The vortices can also be seen from the corresponding axial velocity and turbulence plots shown in Figures 15(c) and (d). At the vortex, the mean axial velocity always showed a decrease except near the vortex center. This can be attributed to the momentum transfer from the axial direction to the radial and circumferential direction due to swirling motion of the vortices. The turbulence maxima of the axial velocity were found at locations similar to those obtained in the corresponding circumferential velocity plots. Again, there were definite minima within the high turbulence regions which were indications of the vortex centers. The amplitudes of the maxima of the axial and circumferential velocity turbulence were found peaked at about 2.54 cm (1 in.) and 3.81 cm (1.5 in.) immersions. The amplitudes of the axial turbulent velocity maxima were about twice those in the circumferential direction. However, the axial velocity measured by (A+B) of the X-probe also contains the radial velocity.

For the inlet flow configuration, both mean and turbulent velocities in the radial direction should be of the same magnitude as those in the circumferential direction. Thus, the mean axial velocity was close to the measured mean sum (A+B) from the X-probe because the mean radial velocity was much smaller than the axial velocity. For the turbulence measurement, the radial turbulent velocity was the same magnitude as the axial turbulent velocity. When the radial component was separated from the sum (A+B) turbulence measurement, the amplitudes of the turbulent velocity maxima were found about the same in axial, radial, and circumferential directions.

At 86% speed and $Z/D = 0.9$, a similar ground vortex pair was observed from on-line hot-film measurements and tuft motion. However, the hot-film measurements at this supersonic tip speed condition contained significant multiple pure tone noise (MPTs). The MPTs were so dominant in the measurements that these data points were not analyzed beyond on-line velocity scanning.

On-line velocity plots were also made at 69% speed when the ground plane was moved to the $Z/D = 1.16$ position. Results were obtained similar to those shown in Figures 15(a) through (d). The turbulence level was found to be weaker than those obtained for the $Z/D = 0.9$ case. A single vortex was found in some cases, because the weaker of the ground vortex pair either disappeared or became too weak to be observed.

Flow velocities for the baseline anechoic chamber condition (no ground plane and with porous walls, etc) are shown in Figure 16. The mean circumferential and turbulent velocities were found to be smaller than those obtained with the ground plane condition. Although no ground vortex pattern was found, a high turbulence region around the bottom center (180°) was obtained at the 1.27 cm (0.5 in.) immersion. This is attributed to a wake shed from the hot-film actuator, which was discussed earlier.

Similar velocity scannings were performed for the nonporous anechoic chamber condition. As discussed in Section 3, under normal test conditions airflow is manifolded to and aspirated through the walls, floor, and ceiling, thus providing a porous-box arrangement. For this test, however, all manifolding to the floor, ceiling, and walls was blocked and the doors leading from the filter house (which are normally closed) were opened to provide the only means of airflow into the chamber (see Figure 3).

The turbulence level during the nonporous chamber tests was found to be higher than that observed for the porous chamber condition. Composite plots of the turbulent velocities at $Z/D = 1.16$ ground plane, porous chamber and nonporous chamber conditions, are shown in Figure 17. Data presented in these plots were obtained off-line from the recorded hot-film signals, with the rms meter at a time constant of 10 seconds. A single vortex was found between $\theta = 100^\circ$ and 140° in the ground plane case. Near 180° , however, high turbulence regions were found in all three cases. These again are attributed to the wake shed from the actuator. The turbulent velocities for the nonporous chamber condition were about 50 to 100% higher than those for the porous chamber condition. Instead of having coherent turbulent regions, as was the case for the vortex in the ground plane condition, the high turbulence was present around the whole inlet.

Integrated turbulence scales were obtained from the autocorrelation measurement of the hot-film signals. Figure 18 shows these computer turbulence scales for the porous and the nonporous chamber conditions at 69% speed and for two immersions (1.27 cm [0.5 in.] and 3.81 cm [1.5 in.]). The length scale in the axial direction was found to be about 10 times longer than that in the circumferential direction. This was an expected observation, as discussed in the Introduction (Section 2), because flow is accelerated into the inlet, causing turbulence disturbances to be stretched in the axial direction. In the case of ground vortices, they theoretically should have infinite length scale along the flow axial direction. The turbulence length scale for the nonporous chamber condition is about 2 to 4 times longer than that at the porous chamber condition. This confirms that the nonporous chamber introduces large-scale turbulence at the inlet compared with that of the porous chamber.

Circumferential velocity space-time cross-correlations were performed between the stationary and the rotating hot films for the 3.81 cm (1.5 in.) immersion at the $Z/D = 0.9$ ground plane condition and 69% speed. The reference point was the location of the fixed probe ($\theta = 150^\circ$). The cross-correlograms are shown in Figure 19. The angular separation between the rotating and the fixed hot film is indicated as $\Delta\theta$, which ranges from -10° to $+20^\circ$ with respect to $\theta = 150^\circ$. The transverse turbulence scale was found smaller than the circumferential arc of $\Delta\theta = 30^\circ$. Between $\theta = 150^\circ$ and 160° the cross-correlation function changed sign, indicating the ground vortex center.

Figure 20 shows typical autopower spectra of a circumferential velocity signal at $\theta = 150^\circ$, 3.81 cm (1.5 in) immersion, 69% speed, and nonporous chamber condition. Most energy in the signal was clearly at frequencies less than 1 Hz. This is only a qualitative indication of the distorted inlet turbulence frequency characteristics. Only

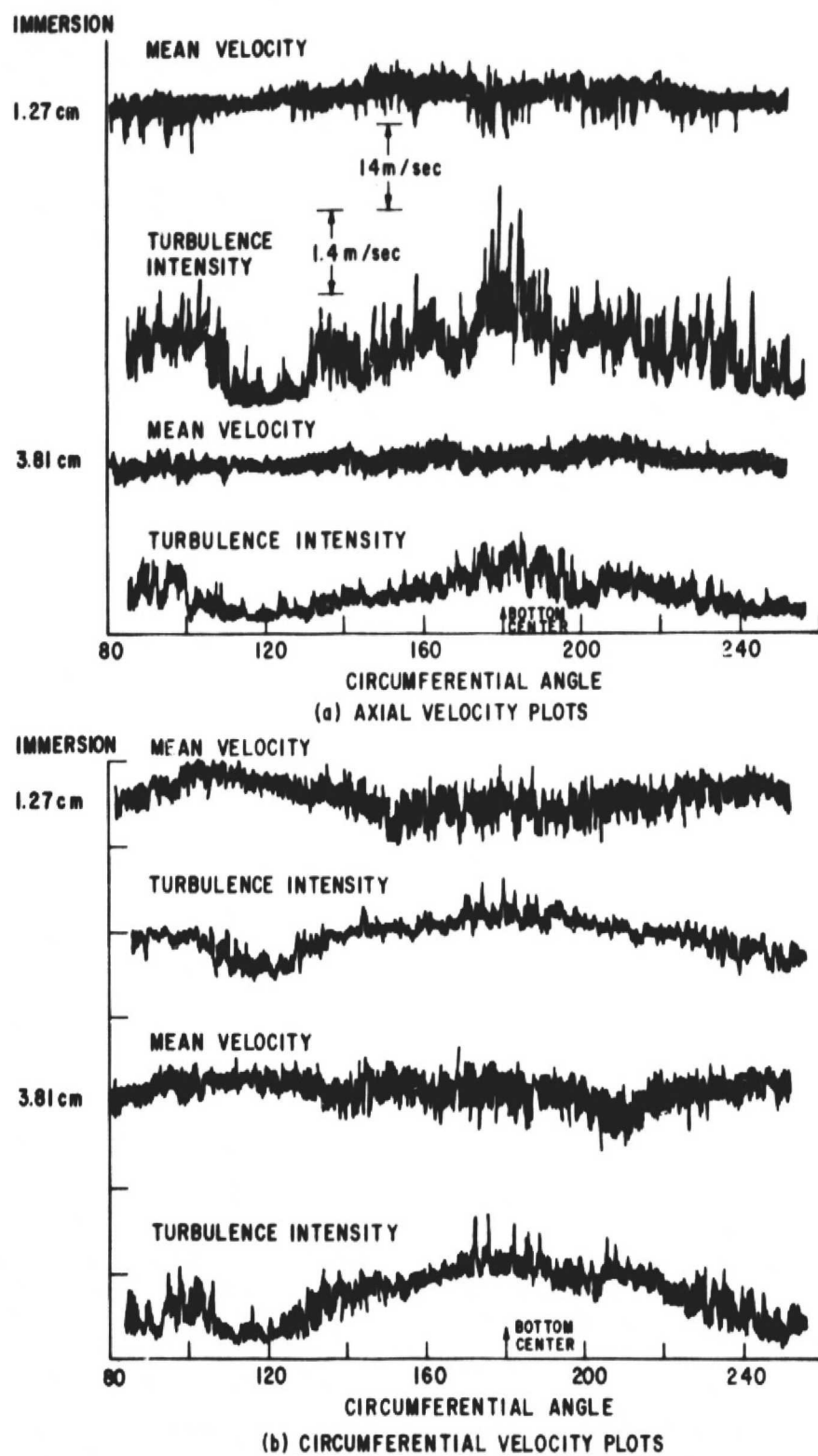


Figure 16. On-Line Inlet Mean and Turbulent Velocity Profiles for the Porous Chamber Configuration (baseline) at 69% Speed

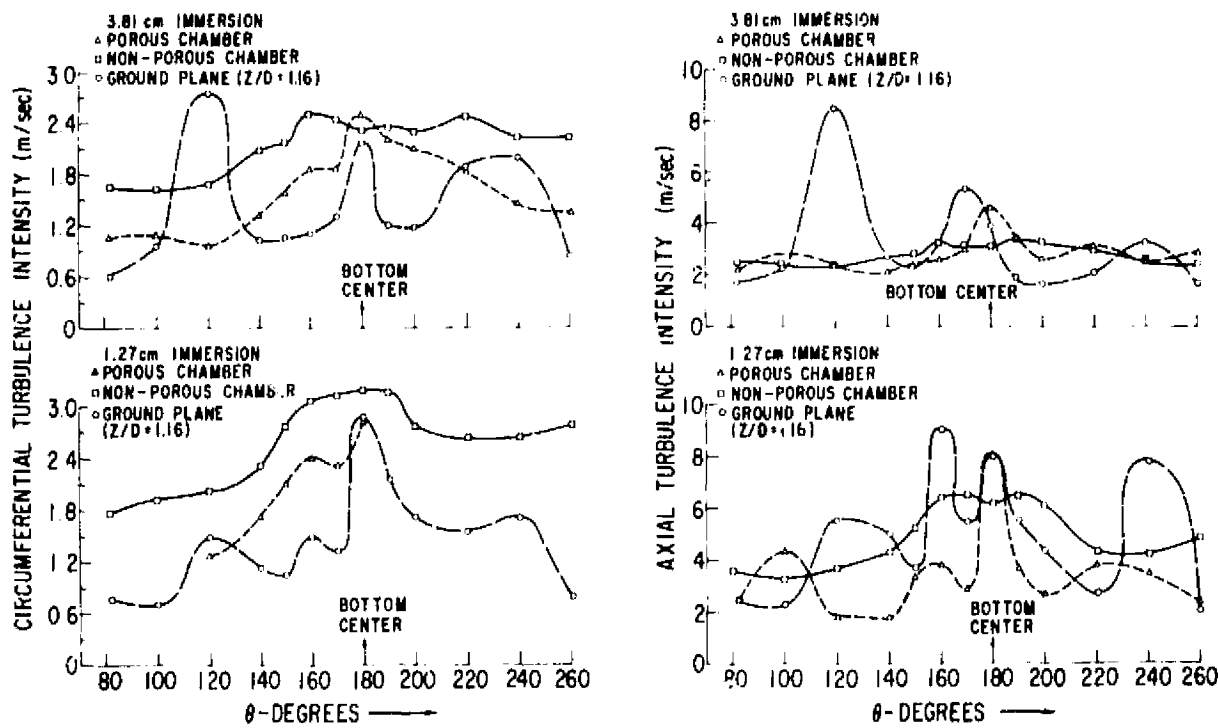


Figure 17. Comparison of Turbulent Velocity Profiles for Ground Plane, Nonporous Chamber and Porous Chamber Configurations at 69% Speed

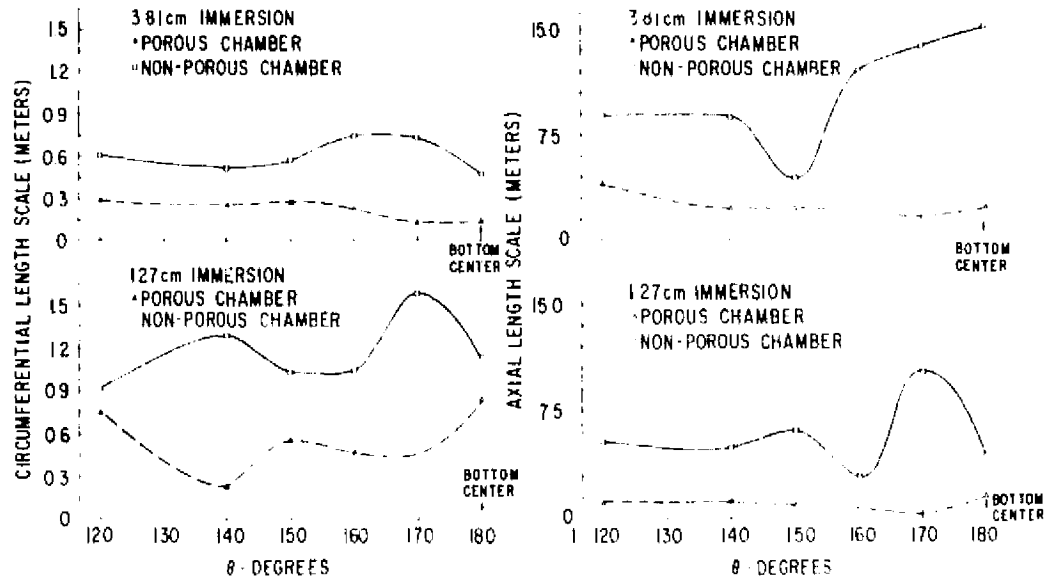


Figure 18. Comparison of Integrated Turbulence Length Scales for the Porous and Nonporous Chamber Configurations at 69% Speed

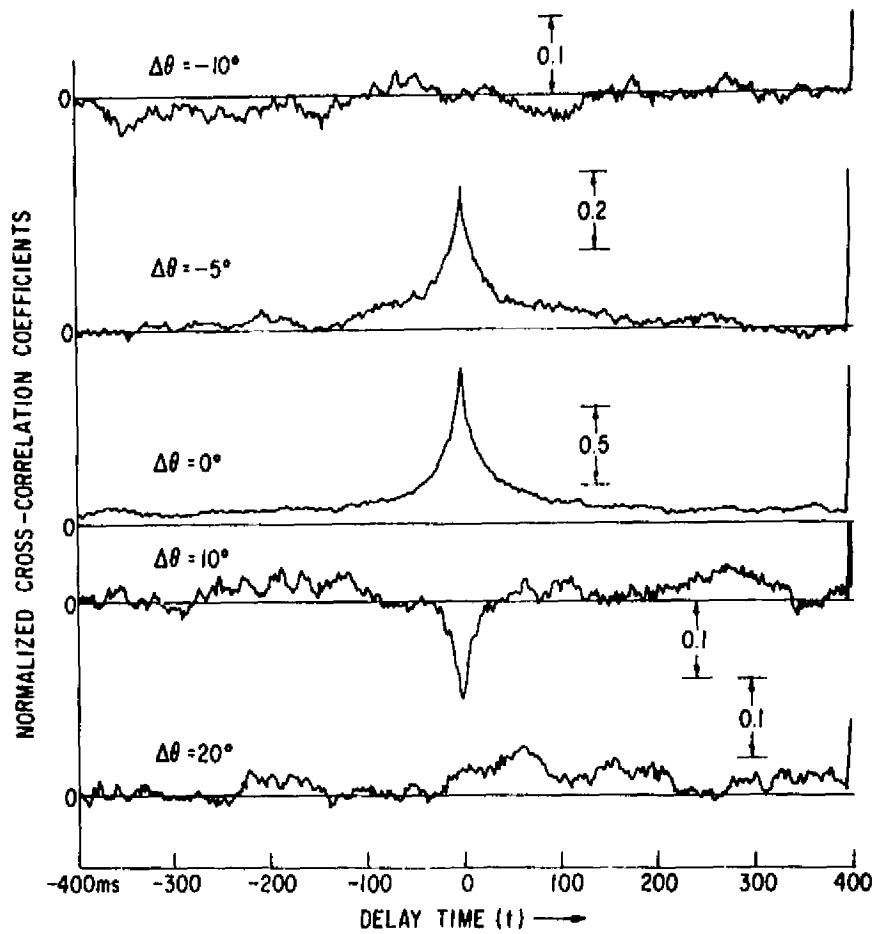


Figure 19. Typical Circumferential Velocity Space-Time Cross-Correlation Measurements with Respect to a Stationary Hot-Film Probe at 150° (3.81 cm immersion; 69% speed; $Z/D = 0.9$ ground plane configuration)

very limited spectral averages were obtained, because of the long sampling time needed to process the data.

In addition to hot-film measurements, flow characteristics in the vicinity of the inlet were investigated by the placement of freely moving tufts. These tuft movements were videotaped. The results showed, as expected, that there was no ground vortex in the baseline (porous) chamber; however, tufts placed on the sunburst arrangement of foam wedges on the plenum wall behind the inlet (see Figure 4) showed moderate activity. Flow over instrumentation leads and probe actuators on the exterior cowl was also clearly in evidence. With the ground plane at $Z/D = 0.9$, flow visualization, consisting of an array of tufts on the ground plane in an area beneath the inlet, indicated that a pair of counter-rotating vortices was present (see Figure 8). These vortices were present at all fan speeds, including idle. The direction of the vortex swirl agreed with the hot-film measurements described earlier. In addition, tufts were placed along the periphery of the ground plane to check for wake flow along the edges. Negligible activity was evidenced by these tufts.

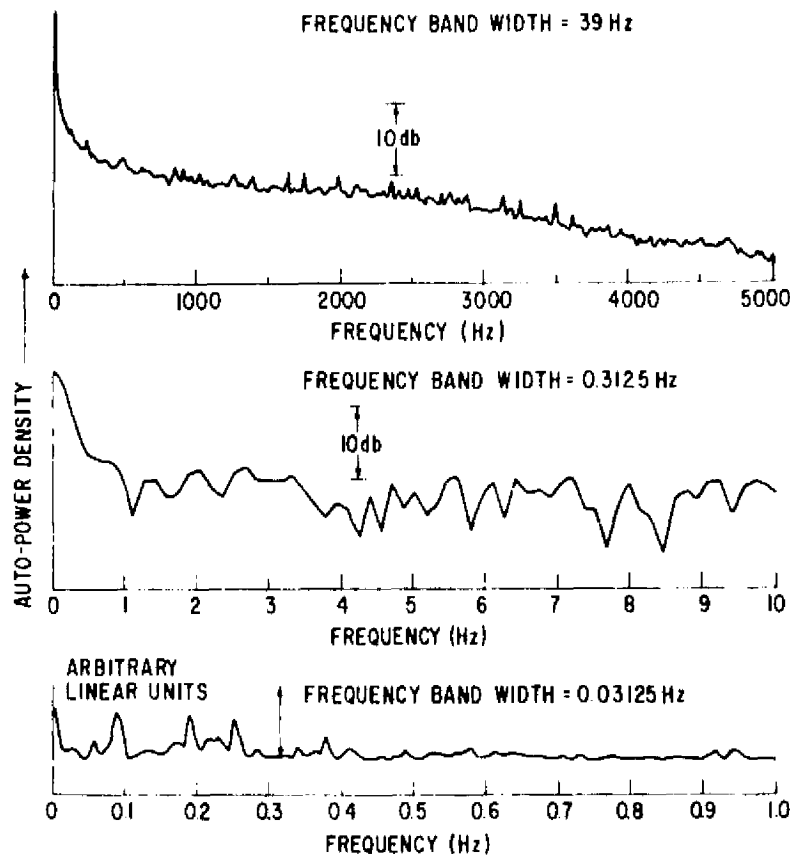


Figure 20. Typical Autopower Spectra of Circumferential Velocity Measurement

ACOUSTIC RESULTS

Far-field acoustic results will be presented for the five speeds tested: 54, 69, 86, 90, and 100%. Rotor 11 is cut-off at the lower two speeds and cut-on at the higher three speeds. Far-field acoustic data repeat points were taken at 69% and 86% and the data were found to be very repeatable. All acoustic data at 69% and 86%, therefore, represent the average of two readings for each configuration. Full information on the 1/3-octave-band acoustic data obtained in this program is given in tabular form in Appendix II. These data include 1/3-octave-band sound-pressure levels (SPL) and calculated overall sound-pressure levels (OASPL), sound-power levels (PWL), and overall sound-power levels (OAPWL).

Analyses of the complete set of the SPLs showed that there was no noticeable evidence of ground plane reflection influencing the measured far-field data. This was investigated further by using a controlled noise source. While the test vehicle was shut down, a whistle was placed in the inlet face at the center of the far-field microphone arc. Acoustic measurements were then taken with the ground plane in its two test locations ($Z/D = 0.9, 1.16$) and with the ground plane completely removed from the chamber. These data showed no clear evidence of ground reflections.

Further analyses of the far-field acoustic data showed that the presence of the ground plane caused no significant redirection of the blade-passage-frequency (BPF)

tone noise. For example, the BPF 1/3-octave-band SPLs for the $Z/D = 0.9$ configuration are shown in the directivity plots of Figures 21 to 25. These data generally do indicate a 1 to 2 dB increase in BPF SPL when the ground plane was present. However, on the basis of past experience, these slight increases in SPL, which seem to be the trend here, cannot be considered too significant. In fact, at isolated angles, the SPL level at a particular speed might show a slight decrease. However, if data from only a particular microphone are examined, even a very slight change in directivity might result in misleading interpretations of the data. Therefore, no attempt at firm conclusions is made based on these plots. Further acoustic comparisons made using PWL spectra obtained by integrating the sound level around the microphone arc are discussed in the following paragraphs.

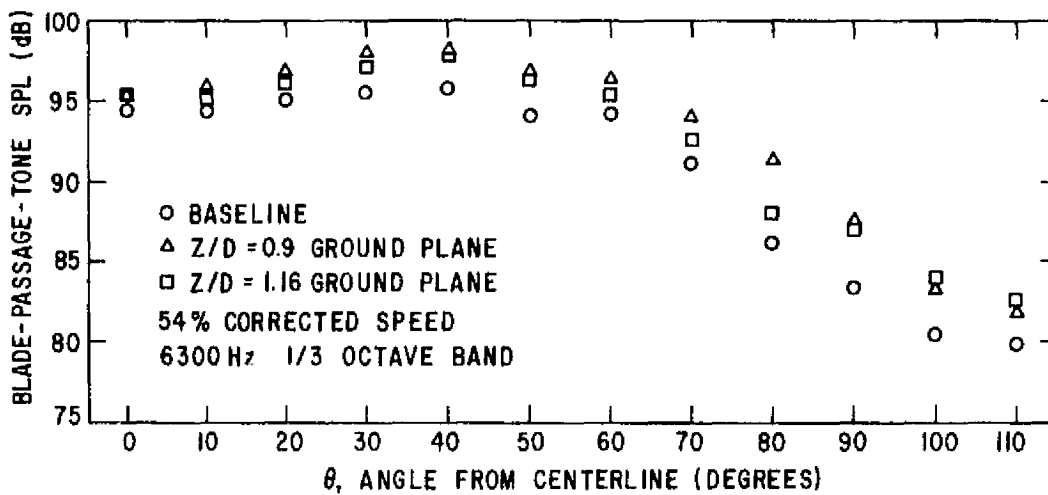


Figure 21. Blade Passing Frequency SPL Directivity; 54% Corrected Speed

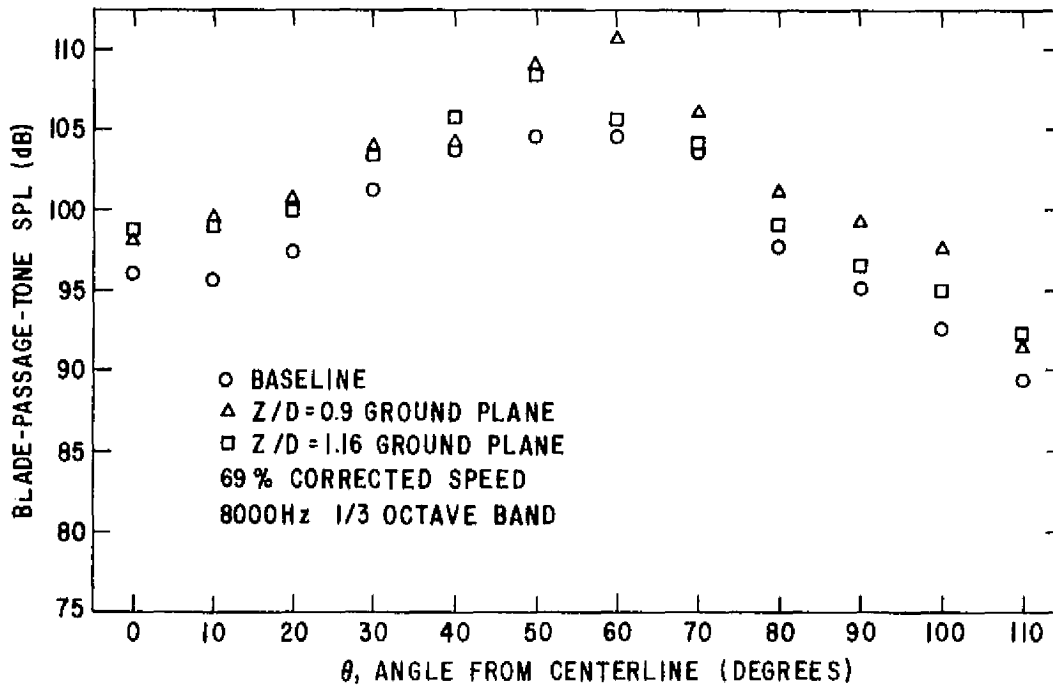


Figure 22. Blade Passing Frequency SPL Directivity; 69% Corrected Speed

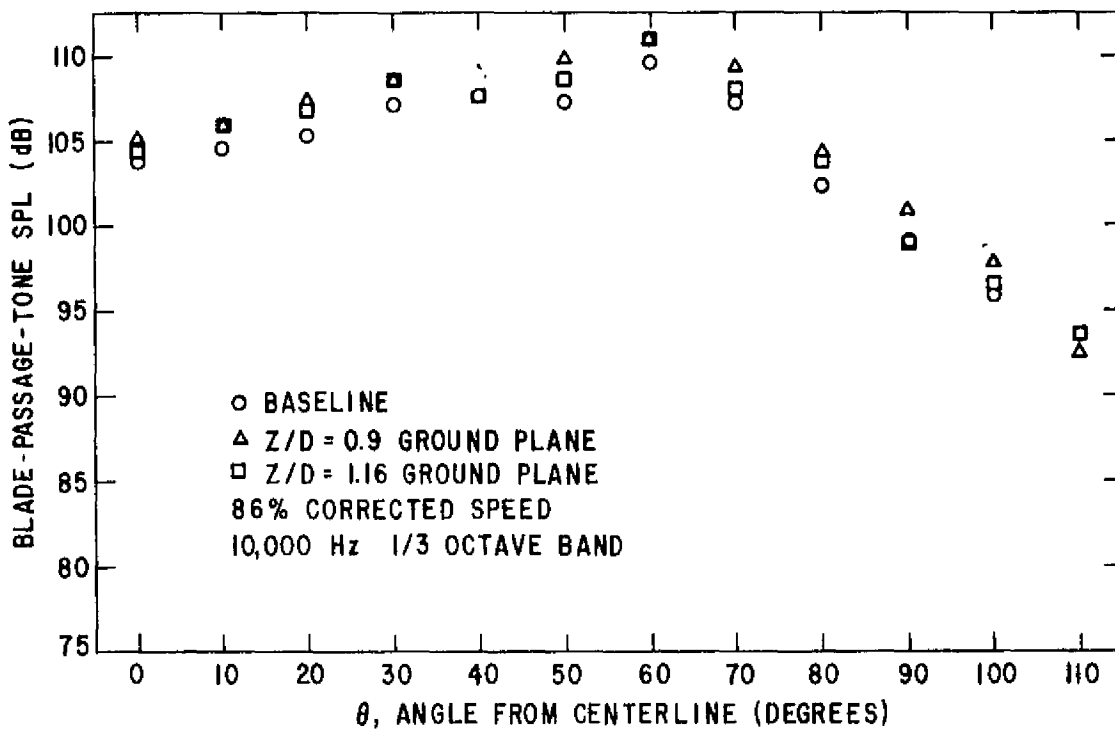


Figure 23. Blade Passing Frequency SPL Directivity; 86% Corrected Speed

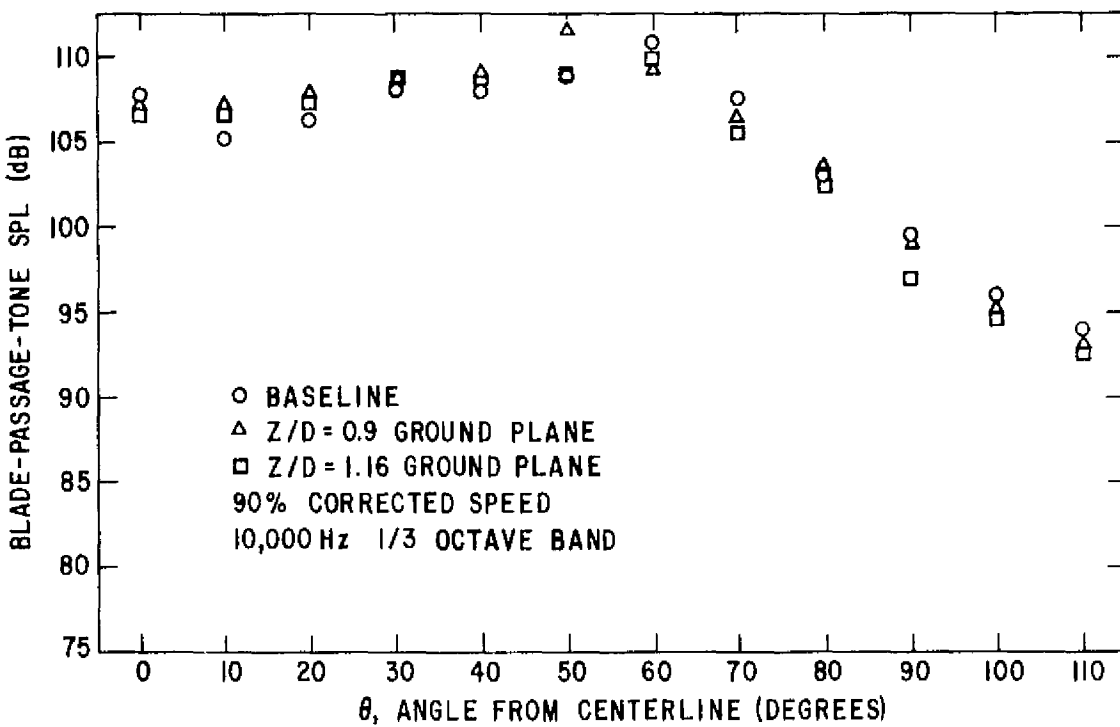


Figure 24. Blade Passing Frequency SPL Directivity; 90% Corrected Speed

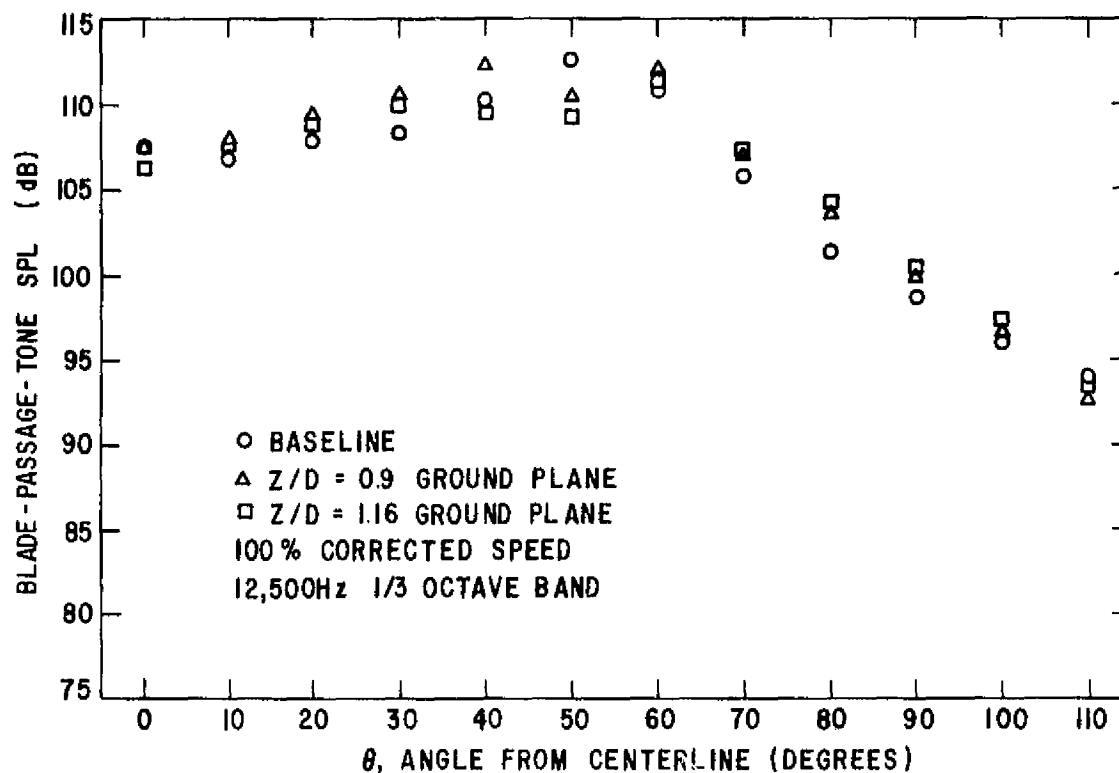


Figure 25. Blade Passing Frequency SPL Directivity; 100% Corrected Speed

Power level spectra for the baseline and the two ground plane configurations ($Z/D = 0.9$ and $Z/D = 1.16$) are shown in Figures 26 to 30 for the five speeds tested. The data for these three configurations are barely distinguishable from one another when plotted in this manner, because of the small changes in PWL (< 5 dB) resulting from the presence of the ground vortices. Therefore, in an attempt to see if any trends are present, the data in Figures 26 to 30 are replotted in Figures 31 to 35 on a Δ PWL basis; i.e., subtracting the appropriate baseline PWL spectra from each ground plane configuration PWL spectra. Thus, a positive Δ PWL represents an increase in noise for the ground plane configuration as compared with the baseline. The blade passage tone 1/3-octave band is indicated for each speed.

It is seen in Figures 31 to 35 that both broadband and tone level increases are less for $Z/D = 1.16$ than for $Z/D = 0.9$.* This result is not surprising, since the ground vortices were weaker and more unsteady when the ground plane was further from the inlet.

*Although the PWL spectra in Figures 26 to 30 are very close together, it can be seen that the acoustic levels in the broadband region below blade passage frequency, as well as the BPF tone level for the $Z/D = 1.16$ ground plane configuration, generally fall between the baseline and the $Z/D = 0.9$ case.

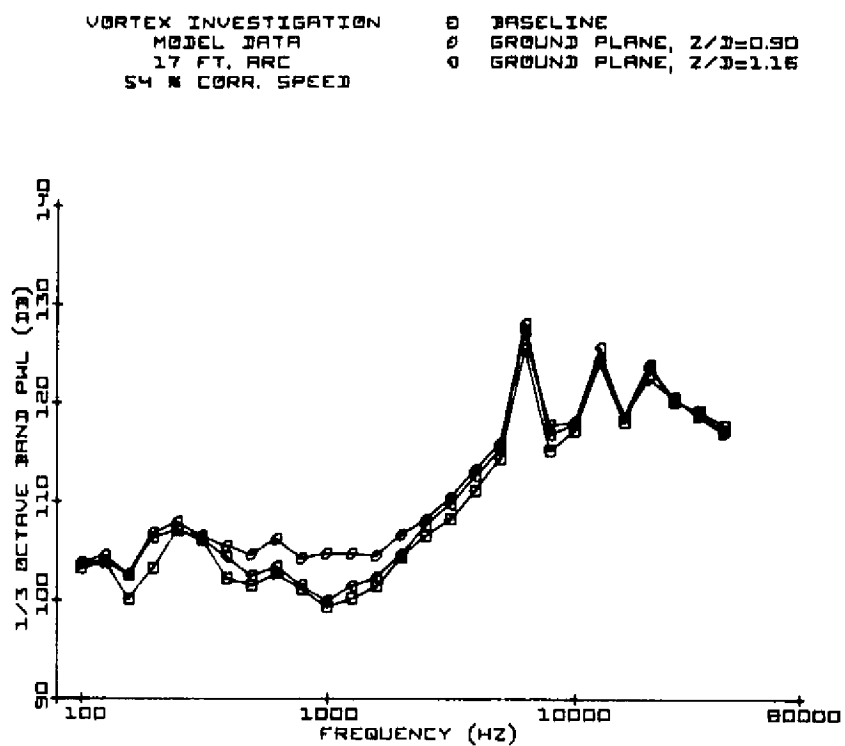


Figure 26. Baseline and Ground Plane PWL Spectra for 54% Corrected Speed

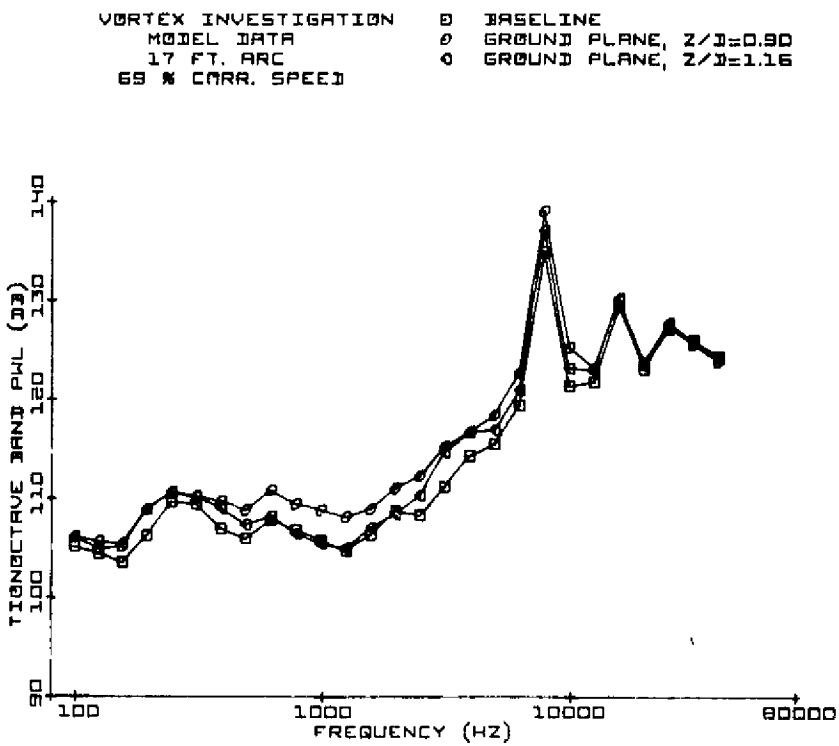


Figure 27. Baseline and Ground Plane PWL Spectra for 69% Corrected Speed

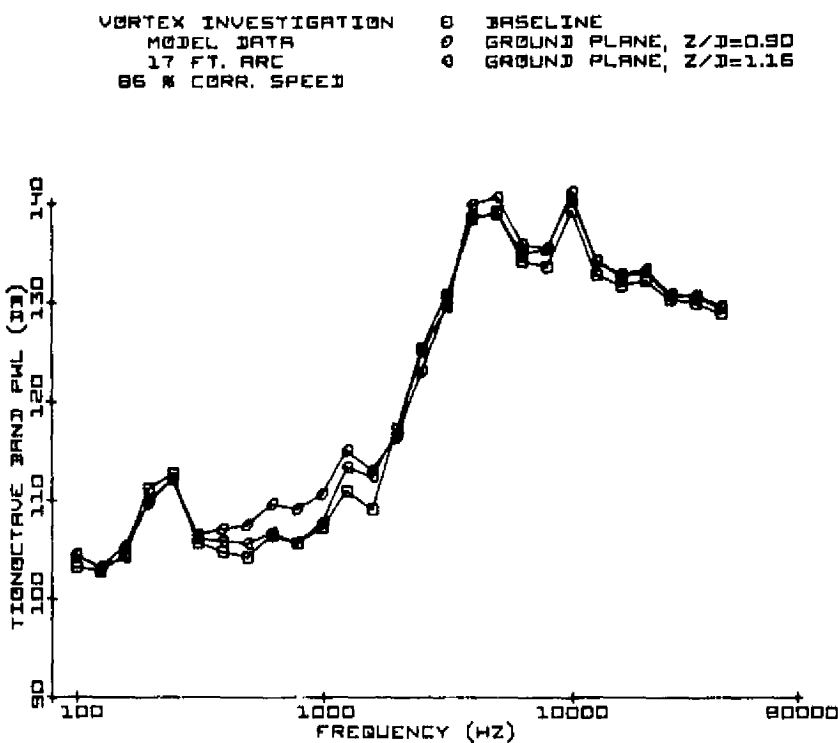


Figure 28. Baseline and Ground Plane PWL Spectra for 86% Corrected Speed

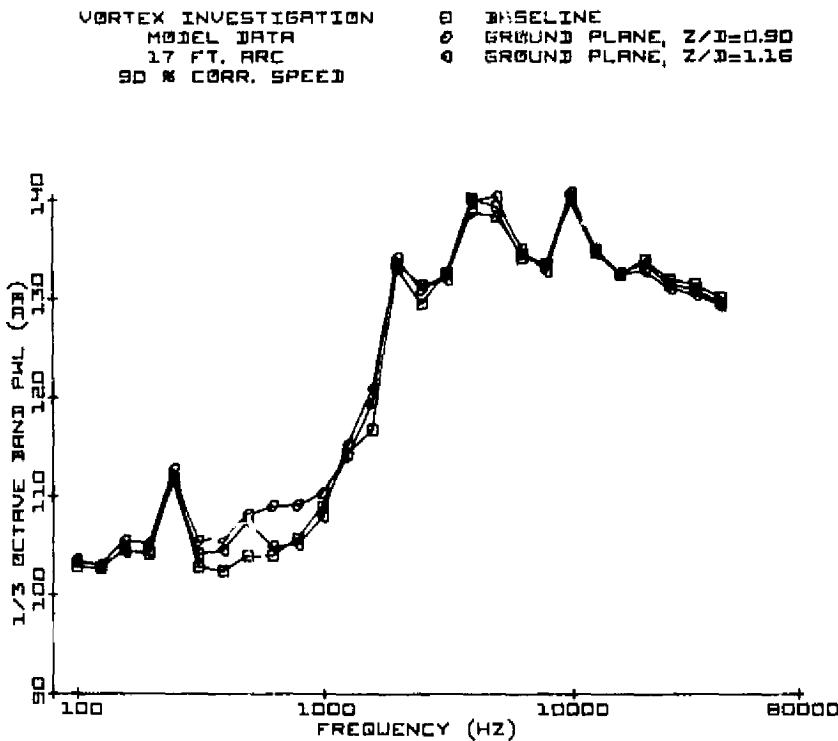


Figure 29. Baseline and Ground Plane PWL Spectra for 90% Corrected Speed

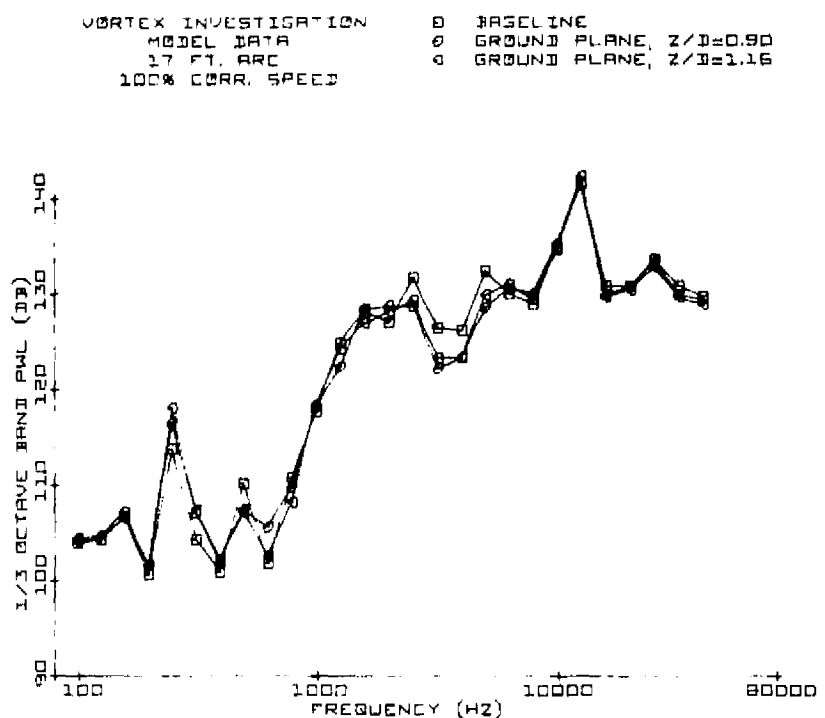


Figure 30. Baseline and Ground Plane PWL Spectra for 100% Corrected Speed

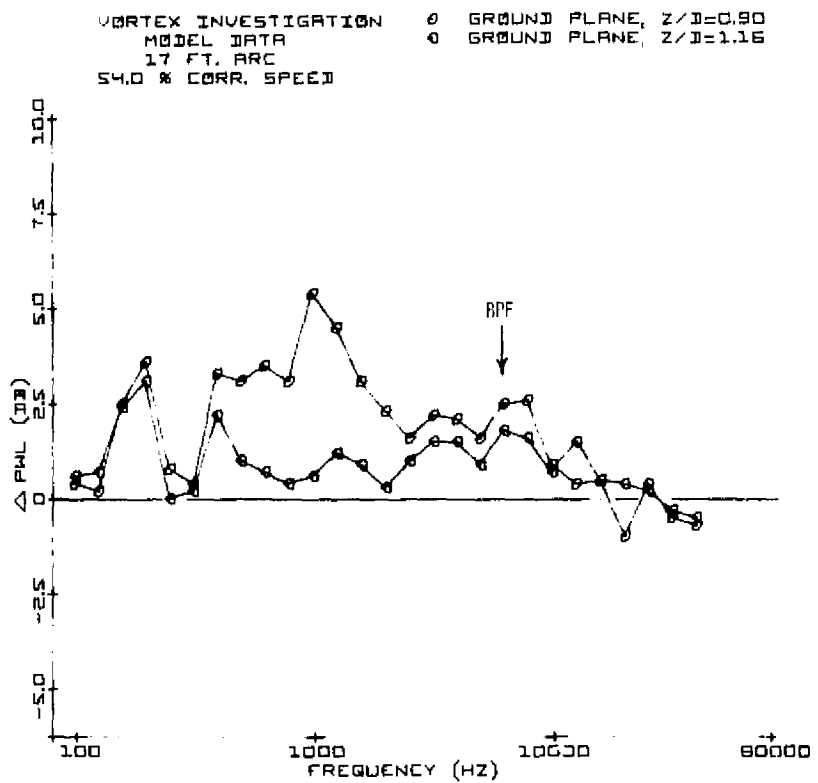


Figure 31. 54% Speed PWL Increase Due to Ground Plane

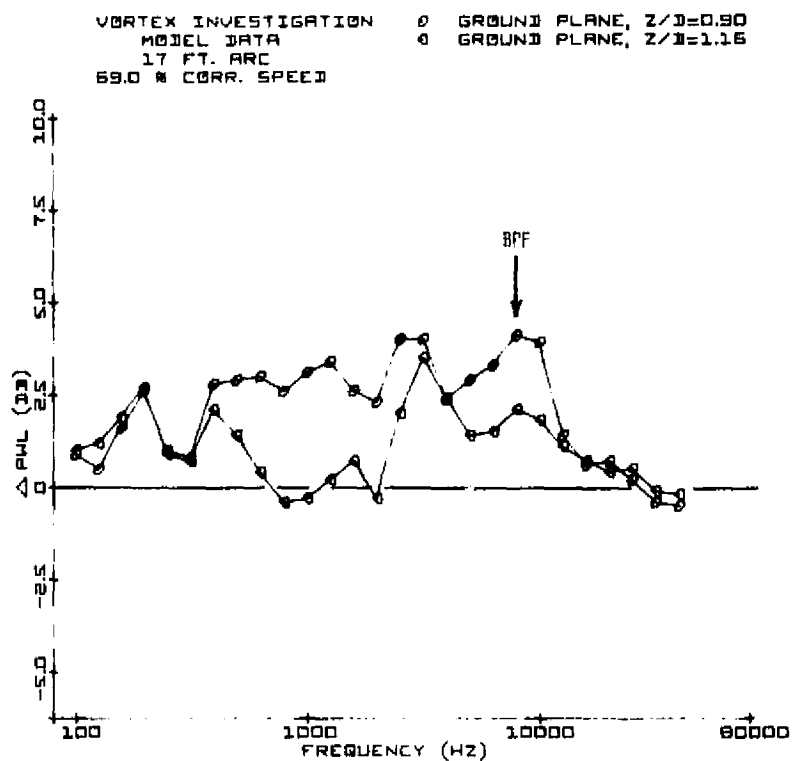


Figure 32. 69% Speed PWL Increase Due to Ground Plane

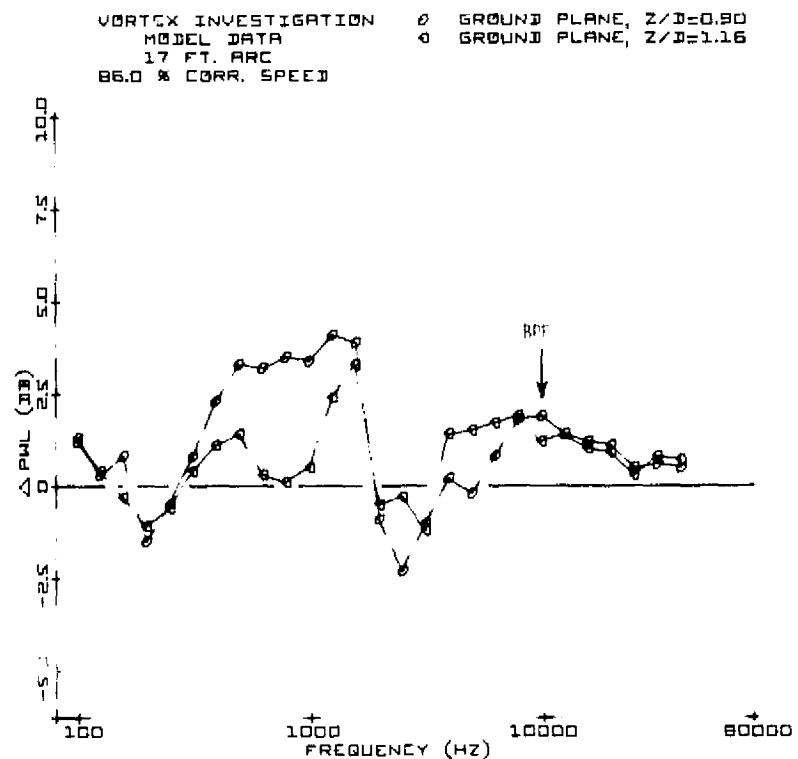


Figure 33. 86% Speed PWL Increase Due to Ground Plane

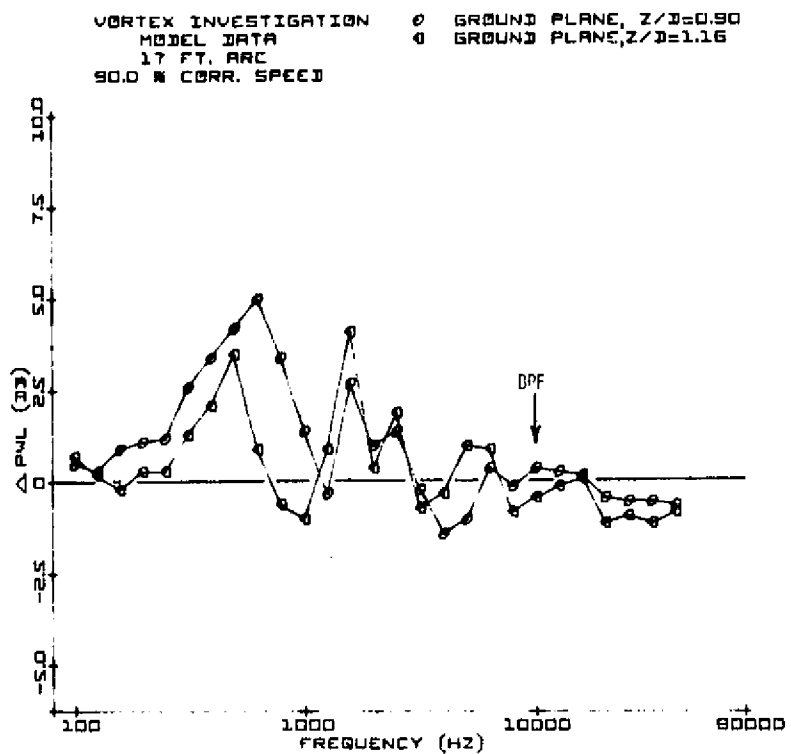


Figure 34. 90% Speed PWL Increase Due to Ground Plane

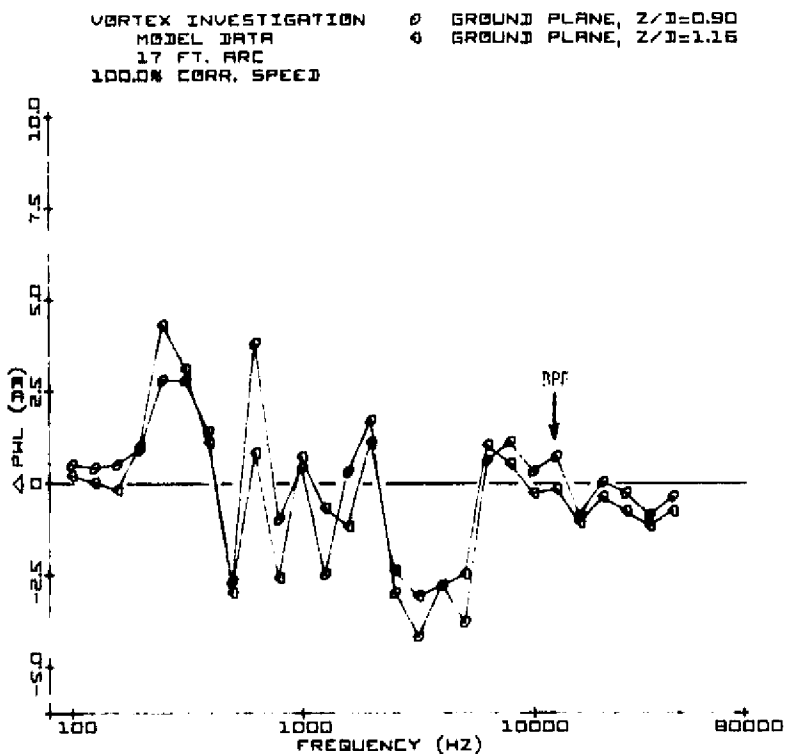


Figure 35. 100% Speed PWL Increase Due to Ground Plane

The Δ PWLs at blade passing frequency are plotted versus corrected fan speed in Figure 36. Of particular interest is the similar trend shown for the two ground plane conditions tested. The increases in blade-passage-frequency PWL were greater for the subsonic relative tip speed (cut-off) data points (54% and 69%) than for the supersonic relative tip speeds (cut-on). In fact, for the $Z/D = 1.16$ ground plane condition, the results at 90% and 100% fan speeds indicated that the BPF PWLs were slightly lower than for the baseline. The lesser increases in BPF tone levels for supersonic speeds was an expected result. At supersonic relative tip speeds, the noise generation mechanisms are dominated by multiple pure tones (buzz-saw noise) which, as a noise source, do not rely heavily on inlet disturbances. Results reported in References 2, 3, and 14 also indicated that inlet-distortion/rotor interaction noise was most noticeable at subsonic relative tip speeds. It was also pointed out in the Introduction (Section 2) that the difference between measured static and actual flight data is generally greater at approach (subsonic tip speed) than during takeoff (supersonic tip speed) operating conditions.

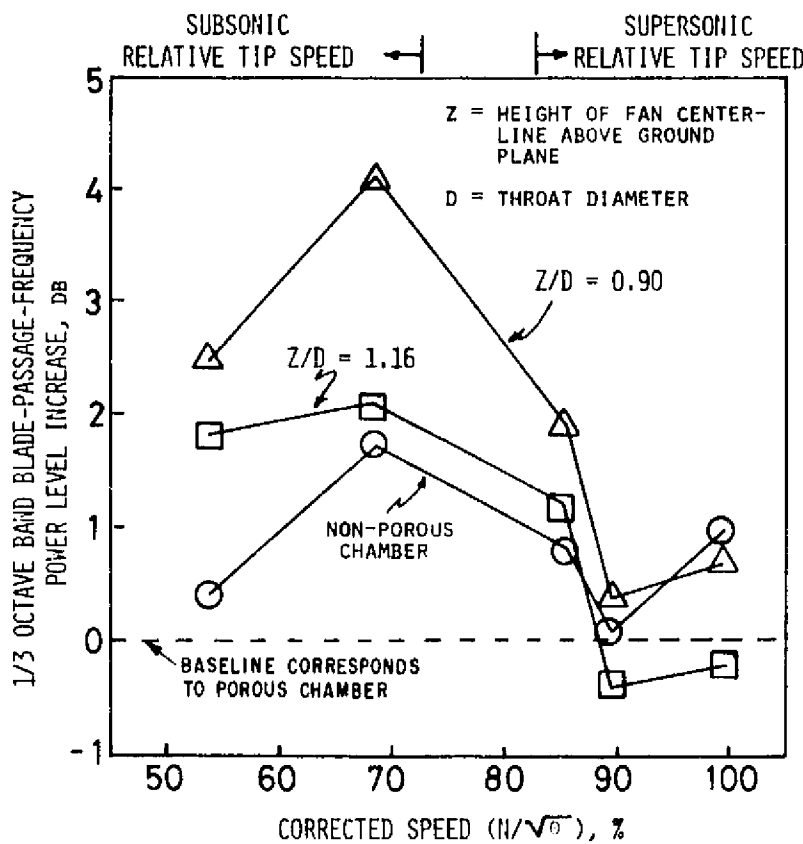


Figure 36. Blade-Passage-Tone PWL Increase for Ground Plane and Nonporous Chamber Configurations Compared with Baseline

Far-field acoustic data were also measured while the anechoic chamber was modified into the nonporous test cell configuration, in order to assess the possible influence such a chamber inflow arrangement might have on the noise generated by the fan. The measured sound power level increase at blade passage frequency for the nonporous test chamber arrangement, compared with the porous (baseline) chamber, is

summarized as a function of fan speed in Figure 36. These BPF tone levels are again presented on a Δ PWL basis such that a positive Δ PWL indicates that the nonporous configuration was noisier than the porous (baseline) chamber. The subsonic/supersonic tip speed regimes were as evident here as they were for the ground plane results. However, the levels of tone increase for the nonporous chamber are generally less than for either of the two ground vortex situations.

Section 5

DISCUSSION OF RESULTS

The fan inlet airflow always has a turbulence field consisting of many eddy cells whose associated characteristic time, τ , can be found by autocorrelating a hot-film signal. This characteristic time is then related to the length scale of the inflow turbulence by $L = \bar{U}\tau$, where \bar{U} is the mean axial flow velocity. As the turbulence cell passes through the rotor, each blade which interacts with it will experience a lift fluctuation. This mechanism can therefore cause noise to be generated at blade passage frequency and higher harmonics. The time it takes the fan to rotate one pitch width is equal to the reciprocal of the blade passage frequency. Therefore, the number of times the characteristic turbulence cell is interacted with as it passes through the rotor is $n = \tau \times (BPF)$. A more thorough analytical investigation of this noise generating mechanism has been presented in References 13 and 15 through 19. The authors only wish to remind the reader here that the number of times the characteristic turbulence cell is "chopped" as it passes through the rotor is a qualitative measure of the efficiency of this noise source mechanism.

The results presented in Figure 18 indicated that, in the nonporous chamber configuration, the characteristic turbulence cell interacted with the rotor considerably more times (factor of 2 to 4) during its passage through the fan than it did for the porous chamber. Apparently the aspirating walls sufficiently reduced the length scale of turbulence to effect the BPF PWL changes indicated in Figure 36 for subsonic tip speeds. This physical description of the noise mechanism also helps explain why both ground planes tested exhibited greater BPF PWL increases than did the nonporous chamber. When a ground vortex is present in the inlet, $\tau \rightarrow \infty$ and the inlet-distortion/rotor interaction noise source mechanism is expected to be most efficient.

It was pointed out earlier that inlet disturbances whose origins were flow over protuberances on the exterior cowl were also present. It is not possible with the data on hand to assess the acoustic impact of these disturbances. However, it is speculated that the influence was substantial, because these disturbances were nearly as high in amplitude as, and steadier than, the distortions generated intentionally. So, in reality, the Δ PWLs presented earlier (Figure 36) were based on a contaminated baseline rather than a baseline with a "pure" undistorted inlet flow. The actual acoustic impact of large-scale inlet turbulence and ground vortices is probably greater than that measured under this effort.

An attempt will be made in the anechoic chamber which was used during this test program to remove the exterior-cowl source of inflow disturbance. The method to be investigated incorporates a partially porous, flared inlet (see Figure 37). The purpose of such an inlet is not only to enclose some of the possible sources of flow contamination but also to remove by suction that portion of the airflow which is most likely to be nonuniform. The cone-shaped inlet fairing will extend from the bellmouth back toward the chamber wall, following the expected streamlines as closely as possible. The fairing will cover the flanges, probe mechanisms, etc., that have been shown to be sources of inflow distortions. In addition, the perforated section will be included on the fairing near the bellmouth so that suction can be applied to the reverse flow to extract any disturbed flow that might still exist.

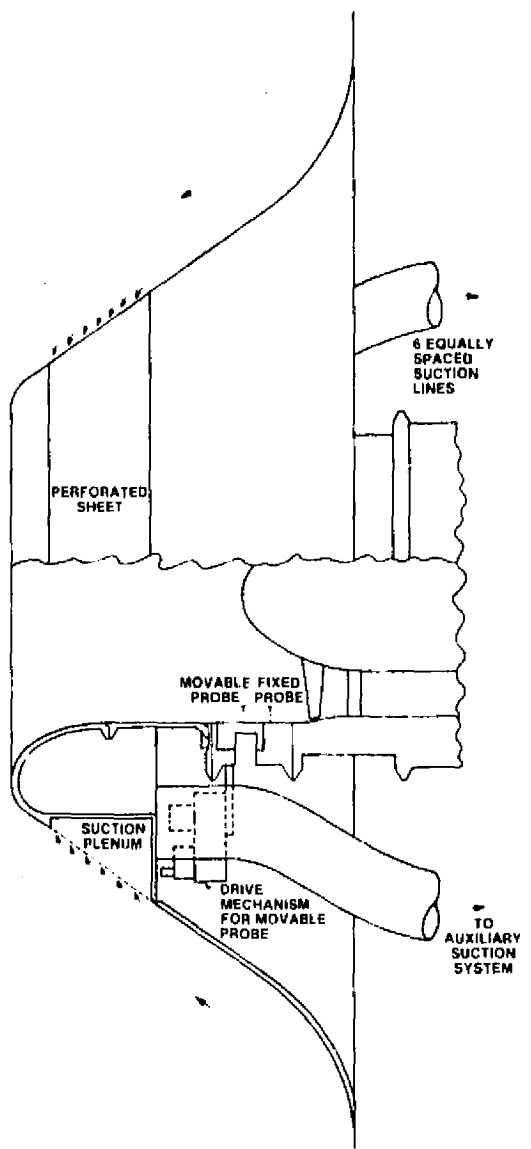


Figure 37. Conceptual Sketch of Flared Inlet with Exterior Cowl Boundary Layer Suction

Section 6

CONCLUSIONS

The hot-film measurements using a rotatable X-probe have successfully provided information on fan inlet disturbances at various inlet conditions. A strong ground vortex pair was detected when a simulated ground plane was located at $Z/D = 0.9$; the strength of the vortices decreased as the ground plane was moved away from the inlet to $Z/D = 1.16$. Although no particular coherent ground vortex type structure was found for the nonporous chamber condition, the turbulence length scale for this condition was measured as 2 to 4 times that for the porous chamber (baseline) condition. This large-scale turbulence was dominated by frequencies less than 1 Hz.

The acoustic results can be separated into subsonic relative tip speed and supersonic relative tip speed regimes, indicating that different noise-generating mechanisms are active in the two regions. At subsonic speeds, modest increases in blade-passage-tone levels (up to 4 dB) were measured while ground vortices or large-scale turbulence were artificially created in the anechoic chamber. For the supersonic tip speed data points, where the noise source mechanisms were dominated by multiple pure tones, there was little significant change in BPF power levels. These results indicated that large-scale inlet flow disturbances, which can occur during static tests, will have a greater acoustic impact on aircraft engines with subsonic relative tip speed fans.

The flow visualization and hot-film measurements indicated that reverse flow was found to occur along the exterior cowl in the anechoic chamber. This appears to be a prime candidate for producing inlet disturbances, in addition to those which were generated intentionally. These disturbances came from flanges, instrumentation probes and leads, and actuator support and drive mechanisms. Such disturbances are likely to occur in all static test facilities, and they provide further explanation for the variance between flight and projected static acoustic data.

Several methods of simulating flight in a static test situation have been attempted by others. These included introducing relative forward motion in a wind tunnel (Ref. 5) or with blowers (Ref. 6) and reducing inlet distortions with large honeycomb or mesh screen structures (Refs. 3, 6, and 14). Each method seems to have its own drawbacks, and to date nothing has been attempted to specifically reduce the inflow distortions arising along the exterior cowl of the inlet duct. Further, such methods as described above are rather difficult to accomplish in an anechoic chamber while retaining its desirable acoustic features. An attempt will be made to eliminate all protuberances in the fan inlet flow in the anechoic chamber, at which time these experiments should be repeated.

Section 7

ACKNOWLEDGMENTS

The authors are indebted to E.M. Birbilis, R.E. Otten, and R.E. Warren of General Electric Corporate Research and Development and to G. Dollinger of Yale University, a summer employee at CRD, for their assistance in carrying out the experiments and data reduction for the tests described in this report. Support of this research by the National Aeronautics and Space Administration under contract NAS 3-17853 (Dr. James H. Dittmar, Project Manager), issued by the V/STOL and Noise Division, NASA Lewis Research Center, Cleveland, Ohio, is gratefully acknowledged.

APPENDIXES

Appendix I

HOT FILM SYSTEM

Figure 11 is the schematic diagram of the hot film and its data acquisition system. The hot-film probes used were TSI model 1240 cross-flow X-probes, each probe having two sensors, at 90° to each other and perpendicular to the probe axis. Such probes are suited for measurements of two turbulence components, correlations, and flow vectors in two-dimensional flows. The signal from each individual sensor was fed into a constant-temperature anemometer with a built-in linearizer (TSI model 1054 A). The output signals from both anemometers were then input to the sum-and-difference module (TSI model 1063). The sum (A + B) and difference (A - B) of the outputs from the X-hot-film sensors are related to the velocity components of the two-dimensional flow when the orientation of the two sensors with respect to flow direction is known. In the work reported here, the two sensors of the X hot film were at + 45° with respect to the main flow direction (the axis of the fan) (see Figure 12). The output (A + B) represented the velocity measured along axial and radial directions: $(A + B) = K(u + w)$ where K = constant obtained via calibration, u = axial velocity component, and w = radial velocity component.

Similarly, the output (A - B) represented the circumferential velocity component, v, in $(A - B) = K'v$ where K' = constant obtained via calibration. For the inlet flow configuration, the mean and the turbulent velocities in the radial direction should be of the same magnitude as those in the circumferential direction. The mean circumferential velocity was found about one order-of-magnitude smaller than the mean axial velocity in the present experiments. Thus, the measured mean sum (A + B) from the X-probe was used to represent the mean axial velocity. For the turbulence measurement, the radial turbulent velocity was the same magnitude as the axial turbulent velocity. The actual axial turbulent velocity should be close to half the value measured from the (A + B) output.

The two sensors on the X-hot-film probe were, at first, calibrated independently in the potential core of the jet from a standard ASME nozzle of 1.78 cm (0.7 in.) diameter perpendicular to the flow direction. The slope and the span of the two linearized sensor outputs were matched to within $\pm 1\%$ of the full-scale value at air jet velocity of 150 m/s (500 ft/sec). The sensors were then rotated to approximately 45° with respect to the flow direction, until the output from the sum (A + B) reached the maximum, and the angular position was recorded as θ_1 . A similar rotation of the sensors was also performed until the output from the "diff" (A - B) reached zero and was recorded as θ_2 . The final angular position of the X hot film was set at the bisector of θ_1 and θ_2 . Flow calibration on the (A + B) output was performed similarly to that for the single sensor. Figure 38 shows a typical calibration curve of flow velocity vs (A + B) output used in the inlet turbulence study.

The mean and turbulence velocities in the axial and the circumferential directions were obtained as the mean and the root-mean-square (rms) values of the outputs from (A + B) and (A - B). A TSI model 1976 dc voltmeter and a TSI model 1060 rms meter were used to obtain the mean and the turbulence velocities, respectively. A time constant of 0.1 sec was used for the on-line X-Y, Y plots and 10 sec was used for the off-line measurements. A pair of Kron-Hite low pass filters at 5 kHz were used before the dc voltmeter and the rms meter to remove the high-frequency noise from the anemometer.

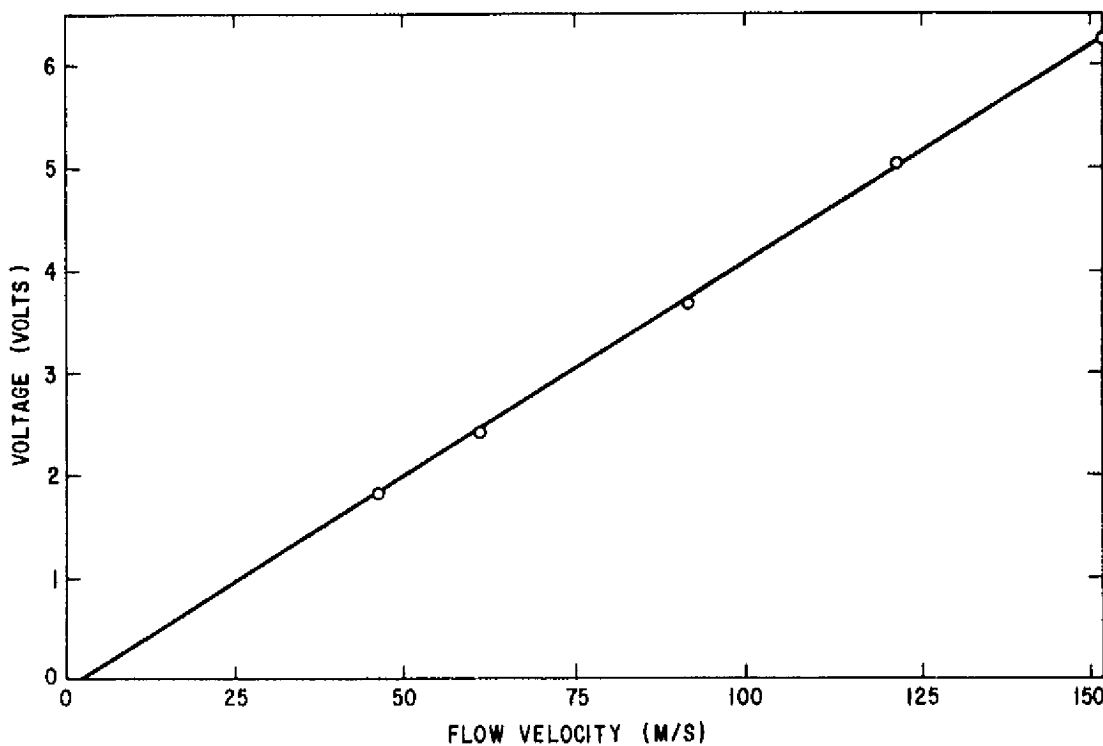


Figure 38. X-Hot-Film Calibration (A + B) Flow at 45° to the Sensors

To record the hot-film signals on magnetic tape for off-line data reduction and to obtain auto- and cross-correlation functions as well as turbulence spectra on-line, the high dc value associated with the hot-film signals had to be removed. Because of the low-frequency nature of the inlet turbulence, usual ac coupling devices for the dc value removal were not satisfactory. A pair of Tektronix 500-AM2 differential amplifiers were used as the dc level suppressors. Low-frequency signals of the order of 0.01 Hz were demonstrated to be preserved after these dc suppressors. However, the dc value could not be suppressed completely during most measurements. The small dc value remaining in the hot-film signal was found to raise the dc offset in the auto-covariance function at long time delay; i.e., $R(t \approx \infty)$. One had to be careful about this dc offset in the turbulent length scale measurements from the auto-covariance functions. Sufficient delay time was needed to identify this dc offset value, and then to remove it before calculating the turbulence length scale value.

Let the instantaneous velocity, $U(t)$, at time, t , be separated into a mean velocity, \bar{U} , and an instantaneous velocity perturbation, $u'(t)$; i.e.:

$$U(t) = \bar{U} + u'(t) \quad (A-1)$$

The correlation function is defined as the expectation of the quantity $[U(t)U(t+\tau)]$ at τ , which is the time separation between the two velocity measurements. This can be expressed as

$$\begin{aligned} R(\tau) &= E[U(t)U(t+\tau)] \\ &= \bar{U}^2 + C(\tau) \end{aligned} \quad (A-2)$$

where $E[\cdot]$ denotes the expectation value and $C(\tau)$ is the covariance function coefficient at delay time τ . Since the value of $C(\tau)$ at infinite time delay is zero, one can obtain the value of \bar{U}^2 as

$$\bar{U}^2 = \lim_{\tau \rightarrow \infty} R(\tau) \quad (A-3)$$

In other words, if one can measure the correlation function for a long enough time delay interval, he can subtract the value of $R(\tau)$ from Equation A-2 to obtain the covariance function

$$C(\tau) = R(\tau) - \lim_{\tau_0 \rightarrow \infty} R(\tau_0) \quad (A-4)$$

In practice, one has to choose a finite time window, T , such that $T \ll \infty$. The estimate of the covariance function coefficient can be obtained from the correlation function measurement as

$$\hat{C}(\tau) = R(\tau) - R(T) \quad (A-5)$$

The accuracy of this covariance estimate depends on how close the value of $R(T)$ is to the value of \bar{U}^2 . In other words, the longer the time window interval one has, the better covariance function estimate he will get. The criteria for determining the length of the delay time window and the accuracy of the covariance function estimates depend on the nature of the covariance function. For a commonly encountered exponential form covariance function,

$$C(\tau) = C(0)e^{-\tau/\tau_I} \quad (A-6)$$

where τ_I = the characteristic time scale at which the value of the covariance function reaches $(1/e)$. The turbulence length scale L can be found by the definition,

$$L = \frac{\bar{U}}{C(0)} \int_0^{\infty} C(\tau) d\tau = \bar{U} \tau_I \quad (A-7)$$

The measured turbulence scale, \hat{L} , based on the measured covariance function estimate $\hat{C}(\tau)$ can be found as

$$\hat{L} = \frac{\bar{U}}{\hat{C}(0)} \int_0^T \hat{C}(\tau) d\tau = \frac{\bar{U} \tau_I}{1 - e^{-T/\tau_I}} \left[1 - e^{-T/\tau_I} \left(1 + \frac{T}{\tau_I} \right) \right] \quad (A-8)$$

Substituting Equation A-7 into Equation A-8 and rearranging some of the terms, one obtains

$$\frac{\hat{L}}{L} = 1 - \left(\frac{T}{\tau_I} \right) \left[\frac{1}{e^{T/\tau_I} - 1} \right] \quad (A-9)$$

A plot of (\hat{L}/L) versus (T/τ_i) is shown in Figure 39. An accuracy of the turbulence length scale estimate above 99% will be obtained if the time delay window interval is of the order of ten times the characteristic time of the covariance function. Two turbulence length scale measurements with delay time window interval of 5 to 10 times difference were used as a validation check for the measurement.

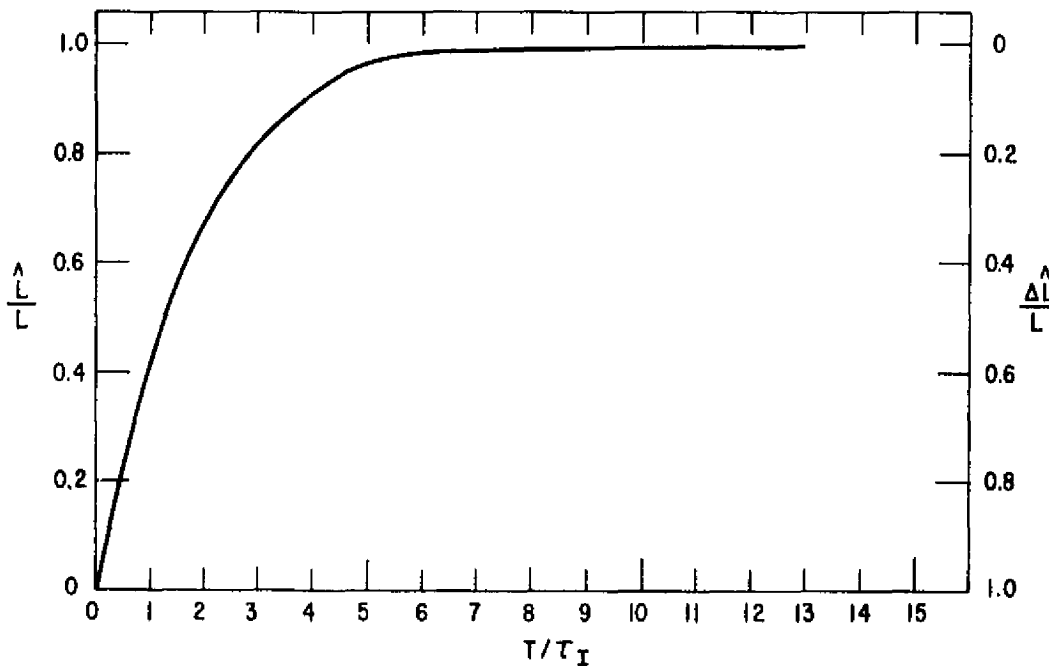


Figure 39. Effect of Time Delay Window Length on the Turbulence Length Scale Measurement for an Exponential Covariance Function

Appendix II

TABULATION OF 1/3 OCTAVE ACOUSTIC DATA

Tables 2 to 36 contain the 1/3-octave noise spectra for all tests carried out during this program. The sound pressure levels (SPL) from 100 Hz to 80 kHz measured at each of the microphone positions from 0° to 110° have been corrected to standard day conditions. Information describing the actual test point conditions is listed in the far-left side of each SPL table. Overall calculated sound pressure levels (OASPL) are compiled under each SPL spectrum. The sound power levels (PWL) for each 1/3-octave band are listed at the right of the SPL spectra, and an overall sound power level (OAPWL) is listed under the column. The nomenclature used in these tables is as follows:

BAR	Barometric Pressure
FREQ	1/3-Octave-Band Center Frequencies
HACT	Actual Humidity
NFA	Actual Fan Speed
NFD	Design Fan Speed
NFK	Corrected Fan Speed
OAPWL	Overall Sound Power Level Calculated by Summation of Power Level Spectra from 100 Hz to 80 kHz
OASPL	Overall Sound Pressure Level Calculated by Summation of Sound Pressure Levels at each 1/3 Octave from 100 Hz to 80 kHz
PWL	Sound Power Level, Re 10^{-13} watts
SPL	Sound Pressure Level, Re 0.0002 dynes/cm ²
TAMB	Ambient Temperature
TWET	Wet Bulb Temperature

Table 2
MODEL SOUND PRESSURE LEVELS (59°F, 70% Relative Humidity, Day)

Angles from Inlet in Degrees (and Radians)

	0°	15°	30°	45°	54°	60°	75°	84°	90°	105°	120°	135°	144°	150°	162°	174°	180°	186°	192°	198°	204°	210°	216°	222°	228°	234°	240°	246°	252°	258°	264°	270°	276°	282°	288°	294°	298°	304°	310°	316°	322°	328°	334°	340°	346°	352°	358°	364°	370°	376°	382°	388°	394°	398°	404°	410°	416°	422°	428°	434°	440°	446°	452°	458°	464°	470°	476°	482°	488°	494°	498°	504°	510°	516°	522°	528°	534°	540°	546°	552°	558°	564°	570°	576°	582°	588°	594°	598°	604°	610°	616°	622°	628°	634°	640°	646°	652°	658°	664°	670°	676°	682°	688°	694°	698°	704°	710°	716°	722°	728°	734°	740°	746°	752°	758°	764°	770°	776°	782°	788°	794°	798°	804°	810°	816°	822°	828°	834°	840°	846°	852°	858°	864°	870°	876°	882°	888°	894°	898°	904°	910°	916°	922°	928°	934°	940°	946°	952°	958°	964°	970°	976°	982°	988°	994°	998°	1004°	1010°	1016°	1022°	1028°	1034°	1040°	1046°	1052°	1058°	1064°	1070°	1076°	1082°	1088°	1094°	1098°	1104°	1110°	1116°	1122°	1128°	1134°	1140°	1146°	1152°	1158°	1164°	1170°	1176°	1182°	1188°	1194°	1198°	1204°	1210°	1216°	1222°	1228°	1234°	1240°	1246°	1252°	1258°	1264°	1270°	1276°	1282°	1288°	1294°	1298°	1304°	1310°	1316°	1322°	1328°	1334°	1340°	1346°	1352°	1358°	1364°	1370°	1376°	1382°	1388°	1394°	1398°	1404°	1410°	1416°	1422°	1428°	1434°	1440°	1446°	1452°	1458°	1464°	1470°	1476°	1482°	1488°	1494°	1498°	1504°	1510°	1516°	1522°	1528°	1534°	1540°	1546°	1552°	1558°	1564°	1570°	1576°	1582°	1588°	1594°	1598°	1604°	1610°	1616°	1622°	1628°	1634°	1640°	1646°	1652°	1658°	1664°	1670°	1676°	1682°	1688°	1694°	1698°	1704°	1710°	1716°	1722°	1728°	1734°	1740°	1746°	1752°	1758°	1764°	1770°	1776°	1782°	1788°	1794°	1798°	1804°	1810°	1816°	1822°	1828°	1834°	1840°	1846°	1852°	1858°	1864°	1870°	1876°	1882°	1888°	1894°	1898°	1904°	1910°	1916°	1922°	1928°	1934°	1940°	1946°	1952°	1958°	1964°	1970°	1976°	1982°	1988°	1994°	1998°	2004°	2010°	2016°	2022°	2028°	2034°	2040°	2046°	2052°	2058°	2064°	2070°	2076°	2082°	2088°	2094°	2098°	2104°	2110°	2116°	2122°	2128°	2134°	2140°	2146°	2152°	2158°	2164°	2170°	2176°	2182°	2188°	2194°	2198°	2204°	2210°	2216°	2222°	2228°	2234°	2240°	2246°	2252°	2258°	2264°	2270°	2276°	2282°	2288°	2294°	2298°	2304°	2310°	2316°	2322°	2328°	2334°	2340°	2346°	2352°	2358°	2364°	2370°	2376°	2382°	2388°	2394°	2398°	2404°	2410°	2416°	2422°	2428°	2434°	2440°	2446°	2452°	2458°	2464°	2470°	2476°	2482°	2488°	2494°	2498°	2504°	2510°	2516°	2522°	2528°	2534°	2540°	2546°	2552°	2558°	2564°	2570°	2576°	2582°	2588°	2594°	2598°	2604°	2610°	2616°	2622°	2628°	2634°	2640°	2646°	2652°	2658°	2664°	2670°	2676°	2682°	2688°	2694°	2698°	2704°	2710°	2716°	2722°	2728°	2734°	2740°	2746°	2752°	2758°	2764°	2770°	2776°	2782°	2788°	2794°	2798°	2804°	2810°	2816°	2822°	2828°	2834°	2840°	2846°	2852°	2858°	2864°	2870°	2876°	2882°	2888°	2894°	2898°	2904°	2910°	2916°	2922°	2928°	2934°	2940°	2946°	2952°	2958°	2964°	2970°	2976°	2982°	2988°	2994°	2998°	3004°	3010°	3016°	3022°	3028°	3034°	3040°	3046°	3052°	3058°	3064°	3070°	3076°	3082°	3088°	3094°	3098°	3104°	3110°	3116°	3122°	3128°	3134°	3140°	3146°	3152°	3158°	3164°	3170°	3176°	3182°	3188°	3194°	3198°	3204°	3210°	3216°	3222°	3228°	3234°	3240°	3246°	3252°	3258°	3264°	3270°	3276°	3282°	3288°	3294°	3298°	3304°	3310°	3316°	3322°	3328°	3334°	3340°	3346°	3352°	3358°	3364°	3370°	3376°	3382°	3388°	3394°	3398°	3404°	3410°	3416°	3422°	3428°	3434°	3440°	3446°	3452°	3458°	3464°	3470°	3476°	3482°	3488°	3494°	3498°	3504°	3510°	3516°	3522°	3528°	3534°	3540°	3546°	3552°	3558°	3564°	3570°	3576°	3582°	3588°	3594°	3598°	3604°	3610°	3616°	3622°	3628°	3634°	3640°	3646°	3652°	3658°	3664°	3670°	3676°	3682°	3688°	3694°	3698°	3704°	3710°	3716°	3722°	3728°	3734°	3740°	3746°	3752°	3758°	3764°	3770°	3776°	3782°	3788°	3794°	3798°	3804°	3810°	3816°	3822°	3828°	3834°	3840°	3846°	3852°	3858°	3864°	3870°	3876°	3882°	3888°	3894°	3898°	3904°	3910°	3916°	3922°	3928°	3934°	3940°	3946°	3952°	3958°	3964°	3970°	3976°	3982°	3988°	3994°	3998°	4004°	4010°	4016°	4022°	4028°	4034°	4040°	4046°	4052°	4058°	4064°	4070°	4076°	4082°	4088°	4094°	4098°	4104°	4110°	4116°	4122°	4128°	4134°	4140°	4146°	4152°	4158°	4164°	4170°	4176°	4182°	4188°	4194°	4198°	4204°	4210°	4216°	4222°	4228°	4234°	4240°	4246°	4252°	4258°	4264°	4270°	4276°	4282°	4288°	4294°	4298°	4304°	4310°	4316°	4322°	4328°	4334°	4340°	4346°	4352°	4358°	4364°	4370°	4376°	4382°	4388°	4394°	4398°	4404°	4410°	4416°	4422°	4428°	4434°	4440°	4446°	4452°	4458°	4464°	4470°	4476°	4482°	4488°	4494°	4498°	4504°	4510°	4516°	4522°	4528°	4534°	4540°	4546°	4552°	4558°	4564°	4570°	4576°	4582°	4588°	4594°	4598°	4604°	4610°	4616°	4622°	4628°	4634°	4640°	4646°	4652°	4658°	4664°	4670°	4676°	4682°	4688°	4694°	4698°	4704°	4710°	4716°	4722°	4728°	4734°	4740°	4746°	4752°	4758°	4764°	4770°	4776°	4782°	4788°	4794°	4798°	4804°	4810°	4816°	4822°	4828°	4834°	4840°	4846°	4852°	4858°	4864°	4870°	4876°	4882°	4888°	4894°	4898°	4904°	4910°	4916°	4922°	4928°	4934°	4940°	4946°	4952°	4958°	4964°	4970°	4976°	4982°	4988°	4994°	4998°	5004°	5010°	5016°	5022°	5028°	5034°	5040°	5046°	5052°	5058°	5064°	5070°	5076°	5082°	5088°	5094°	5098°	5104°	5110°	5116°	5122°	5128°	5134°	5140°	5146°	5152°	5158°	5164°	5170°	5176°	5182°	5188°	5194°	5198°	5204°	5210°	5216°	5222°	5228°	5234°	5240°	5246°	5252°	5258°	5264°	5270°	5276°	5282°	5288°	5294°	5298°	5304°	5310°	5316°	5322°	5328°	5334°	5340°	5346°	5352°	5358°	5364°	5370°	5376°	5382°	5388°	5394°	5398°	5404°	5410°	5416°	5422°	5428°	5434°	5440°	5446°	5452°	5458°	5464°	5470°	5476°	5482°	5488°	5494°	5498°	5504°	5510°	5516°	5522°	5528°	5534°	5540°	5546°	5552°	5558°	5564°	5570°	5576°	5582°	5588°	5594°	5598°	5604°	5610°	5616°	5622°	5628°	5634°	5640°	5646°	5652°	5658°	5664°	5670°	5676°	5682°	5688°	5694°	5698°	5704°	5710°	5716°	5722°	5728°	5734°	5740°	5746°	5752°	5758°	5764°	5770°	5776°	5782°	5788°	5794°	5798°	5804°	5810°	5816°	5822°	5828°	5834°	5840°	5846°	5852°	5858°	5864°	5870°	5876°	5882°	5888°	5894°	5898°	5904°	5910°	5916°	5922°	5928°	5934°	5940°	5946°	5952°	5958°	5964°	5970°	5976°	5982°	5988°	5994°	5998°	6004°	6010°	6016°	6022°	6028°	6034°	6040°	6046°	6052°	6058°	6064°	6070°	6076°	6082°	6088°	6094°	6098°	6104°	6110°	6116°	6122°	6128°	6134°	6140°	6146°	6152°	6158°	6164°	6170°	6176°	6182°	6188°	6194°	6198°	6204°	6210°	6216°	6222°	6228°	6234°	6240°	6246°	6252°	6258°	6264°	6270°	6276°	6282°	6288°	6294°	6298°	6304°	6310°	6316°	6322°	6328°	6334°	6340°	6346°	6352°	6358°	6364°	6370°	6376°	6382°	6388°	6394°	6398°	6404°	6410°	6416°	6422°	6428°	6434°	6440°	6446°	6452°	6458°	6464°	6470°	6476°	6482°	6488°	6494°	6498°	6504°	6510°	6516°	6522°	6528°	6534°	6540°	6546°	6552°	6558°	6564°</

Table 3

MODEL SOUND PRESSURE LEVELS (59°F, 70% Relative Humidity, Day)

Angles from Inlet in Degrees (and Radians)

	0°	10°	20°	30°	40°	50°	60°	70°	80°	90°	100°	110°	120°
	P <small>RE</small> ₁₀₀ (0.0) (0.17) (0.35) (0.52) (0.7) (0.9) (1.05) (1.22) (1.4) (1.5) (1.65) (1.8) (2.0)												
BASELINE CLEAN CHAMBER													
CORRECTED SPEED = 69%													
PA													
RADIAL 17° F1	94												
(5. 7)	100	73.3	73.3	73.0	71.8	69.0	71.0	72.0	72.0	74.7	72.1	72.4	76.0
VEHICLE R-11	120	74.0	73.8	72.0	70.0	71.1	70.5	71.0	71.4	71.3	70.8	69.3	104.0
CONF16 CT 0	100	72.0	71.0	71.0	70.0	71.0	70.0	71.0	70.0	69.0	69.0	69.0	103.9
LOC SCHENECTARY	200	77.0	76.0	77.0	75.0	74.5	74.0	71.7	71.0	72.0	71.7	71.7	109.7
DATE 3/19/76	200	82.0	81.0	80.0	81.1	79.3	77.0	75.0	74.0	72.0	73.0	71.0	69.0
RWD 875	315	81.0	81.0	80.5	80.0	79.1	77.0	75.0	74.0	71.7	72.1	69.8	109.4
TAPE	400	79.0	78.0	77.0	77.0	76.1	74.0	73.0	72.0	69.0	70.0	69.4	64.0
BAR 49.9 RG (30973. N/M2)	300	76.0	75.3	75.0	75.0	75.1	74.0	73.0	71.5	71.4	70.0	69.0	106.1
TAMB 43. DEG F (279. DEG K)	600	72.0	72.0	72.0	72.0	70.0	74.0	73.0	73.0	72.5	70.0	69.0	107.0
REF 40. DEG F (27.0. DEG K)	1000	74.0	74.5	75.0	75.0	75.1	73.0	71.0	70.0	69.1	74.0	69.6	69.0
REF 40. DEG F (27.0. DEG K)	1200	75.0	74.0	74.5	74.0	73.0	72.0	70.0	69.0	69.4	71.0	69.2	64.0
REF 5.65 GM/MJ (0.00565 RG/M3)	1000	75.0	75.0	75.0	75.0	75.1	74.0	73.0	73.0	74.0	69.1	69.4	105.5
NFA 10951. RPM (1147. RAD/SEC)	3150	81.0	82.0	81.0	82.0	81.0	80.0	78.0	76.0	75.0	74.0	73.0	107.0
NFA 10951. RPM (1147. RAD/SEC)	4000	83.0	84.0	84.0	84.0	84.0	83.0	83.0	83.0	83.0	84.0	83.0	108.0
NFA 11124. RPM (1105. RAD/SEC)	5000	83.0	84.0	84.0	84.0	84.0	83.0	83.0	83.0	83.0	84.0	83.0	111.4
NFA 10951. RPM (1147. RAD/SEC)	6000	85.0	86.0	85.0	86.0	85.0	84.0	82.0	81.0	80.0	81.0	80.0	114.0
NFA 10951. RPM (1147. RAD/SEC)	7000	87.0	88.0	87.0	88.0	87.0	86.0	84.0	83.0	82.0	83.0	82.0	114.0
NFA 10951. RPM (1147. RAD/SEC)	8000	88.0	89.0	88.0	89.0	88.0	87.0	85.0	84.0	83.0	84.0	83.0	115.0
NFA 10951. RPM (1147. RAD/SEC)	9000	89.0	90.0	89.0	90.0	89.0	88.0	86.0	85.0	84.0	85.0	84.0	116.0
NFA 10951. RPM (1147. RAD/SEC)	10000	90.0	91.0	90.0	91.0	90.0	89.0	87.0	86.0	85.0	86.0	85.0	117.0
NFA 10951. RPM (1147. RAD/SEC)	12000	92.0	93.0	92.0	93.0	92.0	91.0	90.0	89.0	88.0	89.0	88.0	121.0
NFA 10951. RPM (1147. RAD/SEC)	14000	94.0	95.0	94.0	95.0	94.0	93.0	92.0	91.0	90.0	91.0	90.0	121.0
NFA 10951. RPM (1147. RAD/SEC)	16000	96.0	97.0	96.0	97.0	96.0	95.0	94.0	93.0	92.0	93.0	92.0	121.0
NFA 10951. RPM (1147. RAD/SEC)	18000	98.0	99.0	98.0	99.0	98.0	97.0	96.0	95.0	94.0	95.0	94.0	121.0
NFA 10951. RPM (1147. RAD/SEC)	20000	100.0	101.0	100.0	101.0	100.0	99.0	98.0	97.0	96.0	97.0	96.0	121.0
NFA 10951. RPM (1147. RAD/SEC)	22000	102.0	103.0	102.0	103.0	102.0	101.0	100.0	99.0	98.0	99.0	98.0	121.0
NFA 10951. RPM (1147. RAD/SEC)	24000	104.0	105.0	104.0	105.0	104.0	103.0	102.0	101.0	100.0	101.0	100.0	121.0
NFA 10951. RPM (1147. RAD/SEC)	26000	106.0	107.0	106.0	107.0	106.0	105.0	104.0	103.0	102.0	103.0	102.0	121.0
NFA 10951. RPM (1147. RAD/SEC)	28000	108.0	109.0	108.0	109.0	108.0	107.0	106.0	105.0	104.0	105.0	104.0	121.0
NFA 10951. RPM (1147. RAD/SEC)	30000	110.0	111.0	110.0	111.0	110.0	109.0	108.0	107.0	106.0	107.0	106.0	121.0
NFA 10951. RPM (1147. RAD/SEC)	32000	112.0	113.0	112.0	113.0	112.0	111.0	110.0	109.0	108.0	109.0	108.0	121.0
NFA 10951. RPM (1147. RAD/SEC)	34000	114.0	115.0	114.0	115.0	114.0	113.0	112.0	111.0	110.0	111.0	110.0	121.0
NFA 10951. RPM (1147. RAD/SEC)	36000	116.0	117.0	116.0	117.0	116.0	115.0	114.0	113.0	112.0	113.0	112.0	121.0
NFA 10951. RPM (1147. RAD/SEC)	38000	118.0	119.0	118.0	119.0	118.0	117.0	116.0	115.0	114.0	115.0	114.0	121.0
NFA 10951. RPM (1147. RAD/SEC)	40000	120.0	121.0	120.0	121.0	120.0	119.0	118.0	117.0	116.0	117.0	116.0	121.0
OVERALL CALCULATED 100.4 100.7 102.4 103.0 106.0 107.0 107.0 109.0 99.2 96.0 94.0 91.0 138.0													

Table 4
MODEL SOUND PRESSURE LEVELS (59° F, 70% Relative Humidity, Day)

Angles from Inlet in Degrees (and Radians)

	40°	100°	200°	300°	40°	50°	60°	70°	80°	90°	100°	110°	120°	130°	140°	150°	160°	170°	180°	190°	195°
	θ ₄₀	θ ₁₀₀	θ ₂₀₀	θ ₃₀₀	θ ₄₀	θ ₅₀	θ ₆₀	θ ₇₀	θ ₈₀	θ ₉₀	θ ₁₀₀	θ ₁₁₀	θ ₁₂₀	θ ₁₃₀	θ ₁₄₀	θ ₁₅₀	θ ₁₆₀	θ ₁₇₀	θ ₁₈₀	θ ₁₉₀	
PNEUM (U.) (0.17) (0.35) (0.52) (0.7) (0.87) (1.05) (1.22) (1.4) (1.57) (1.75) (1.94)																					
θ ₄₀ θ ₅₀																					
BASELINE CLEAN CHAMBER																					
CORRECTED SPEED = 86%																					
RADIAL - 17.5 FT. (5. M)	100	07.1	07.3	67.0	07.1	65.3	70.7	70.2	71.7	71.0	79.3	70.0	74.1	106.0							
VEHICLE R-11	100	08.0	09.0	09.3	09.8	07.3	72.2	70.2	71.0	70.0	84.0	98.0	74.1	107.0							
CONFIG OF 0	100	09.1	07.0	07.0	09.8	00.1	73.0	72.0	70.0	09.0	81.0	100.0	75.0	108.0							
LOC SCHENECTADY	200	02.0	02.0	01.0	03.0	02.1	79.2	70.2	70.5	120.0	83.0	74.0	72.0	113.2							
DATE 3/19/76	200	04.0	04.0	03.0	05.1	83.0	80.0	77.1	77.2	70.0	83.0	73.0	70.0	114.2							
RUN 8/6	312	20.0	25.0	12.0	2.1	73.0	64.2	71.4	71.7	90.0	84.0	92.0	20.0	111.0							
TAPE	400	75.3	74.3	74.0	74.0	72.0	79.3	71.1	70.5	07.6	85.0	94.0	70.0	111.0							
BAR 24.4 MG (00973, N/M2)	300	75.0	73.0	73.0	74.0	73.0	75.1	71.7	72.0	92.0	88.0	90.0	76.0	111.0							
TAMB 43. DEG F (279. DEG K)	1000	70.0	70.0	70.0	70.0	75.0	74.0	72.0	70.0	07.0	87.0	97.0	70.0	113.0							
WET 39. DEG F (277. DEG K)	1000	70.0	70.0	70.0	70.0	75.0	75.1	75.7	74.0	70.0	74.0	80.0	80.0	61.0	113.0						
RAD 5.12 GM/M3 (0.00512 AG/M3)	2000	81.0	84.1	81.1	86.1	85.1	88.7	80.0	83.0	81.7	87.0	77.0	84.0	118.0							
NFB 13649. RPM (1429. RAD/SEC)	3150	86.0	88.1	87.0	87.0	93.0	98.2	100.2	101.5	92.0	93.0	90.0	90.0	130.0							
NFB 13665. RPM (1452. RAD/SEC)	5000	91.3	92.0	93.0	99.4	100.5	106.1	109.4	108.5	103.4	100.0	101.0	97.0	130.0							
NFB 13665. RPM (1452. RAD/SEC)	5000	97.1	98.7	98.9	98.4	107.3	114.0	118.7	140.0	101.0	99.0	98.0	98.0	134.0							
NFB 16100. RPM (1686. RAD/SEC)	8000	94.0	94.0	95.0	94.0	97.4	100.0	102.3	103.0	95.0	95.0	92.0	92.0	133.0							
NO. OF BLAIDS 44 12540 FAN TIP SPEED	10000	94.0	93.0	95.0	97.3	97.9	99.1	101.0	100.0	90.0	92.0	97.0	94.0	134.0							
1182. FT/SEC	20000	96.1	96.0	97.0	98.4	99.8	99.9	101.0	99.0	94.0	94.0	91.0	92.0	132.0							
	25000	93.3	93.4	94.0	95.0	96.0	97.4	98.0	97.0	92.0	92.0	88.0	90.0	130.0							
	31500	93.2	92.2	94.1	95.5	95.0	96.5	97.1	95.1	94.0	94.0	87.0	91.0	130.0							
	40000	90.3	89.9	91.3	93.2	93.2	94.0	95.0	93.5	87.0	85.0	70.0	70.0	129.0							
	50000	98.9	98.0	98.0	91.0	91.7	91.9	93.0	91.0	90.0	90.0	84.0	72.0	129.0							
	53000	95.0	95.7	95.0	95.7	95.7	89.7	90.0	89.0	84.0	84.0	51.0	51.0	129.0							
	60000	77.0	77.0	77.0	77.0	84.1	86.0	83.2	84.0	82.0	82.0	74.0	74.0	129.0							
OVERALL CALCULATIONS 107.0 107.4 100.3 110.4 110.9 113.4 116.3 115.3 111.2 402.8 403.0 403.0 140.2																					

Table 5

MODEL SOUND PRESSURE LEVELS (59°F, 70% Relative Humidity, Day)

Angles from Inlet in Degrees (and Radians)

OVERALL CALCULATED 105.3 400.1 109.2 111.4 113.1 110.3 117.0 115.2 116.9 117.0 105.9 105.5 147.3

Table 6

MODEL SOUND PRESSURE LEVELS (59° F, 70% Relative Humidity, Day)

Angles from Inlet in Degrees (and Radians)

OVERALL CALCULATED 109.7 109.4 110.2 111.3 113.2 115.5 114.4 111.6 109.9 109.9 109.7 109.7 109.3

Table 7

MODEL SOUND PRESSURE LEVELS (59° F, 70% Relative Humidity, Day)

Angles from Inlet in Degrees (and Radians)

	0°	15°	30°	45°	50°	60°	70°	80°	90°	100°	110°	120°	130°	140°	PAL
	0°	0°	0°	0°	0°	0°	0°	0°	0°	0°	0°	0°	0°	0°	
FREQUENCY (Hz)															
0.0000 (0.0) (0.017) (0.035) (0.052) (0.070) (0.089) (0.107) (0.125) (0.143) (0.161) (0.179) (0.197) (0.215) (0.233)															
ANGLE FROM INLET (DEGREES)															
ANGLE FROM INLET (RADIAN)															
ANGLE FROM INLET (DEGREES)															
ANGLE FROM INLET (RADIAN)															
ANGLE FROM INLET (DEGREES)															
ANGLE FROM INLET (RADIAN)															
ANGLE FROM INLET (DEGREES)															
ANGLE FROM INLET (RADIAN)															
ANGLE FROM INLET (DEGREES)															
ANGLE FROM INLET (RADIAN)															
ANGLE FROM INLET (DEGREES)															
ANGLE FROM INLET (RADIAN)															
ANGLE FROM INLET (DEGREES)															
ANGLE FROM INLET (RADIAN)															
ANGLE FROM INLET (DEGREES)															
ANGLE FROM INLET (RADIAN)															
ANGLE FROM INLET (DEGREES)															
ANGLE FROM INLET (RADIAN)															
ANGLE FROM INLET (DEGREES)															
ANGLE FROM INLET (RADIAN)															
ANGLE FROM INLET (DEGREES)															
ANGLE FROM INLET (RADIAN)															
ANGLE FROM INLET (DEGREES)															
ANGLE FROM INLET (RADIAN)															
ANGLE FROM INLET (DEGREES)															
ANGLE FROM INLET (RADIAN)															
ANGLE FROM INLET (DEGREES)															
ANGLE FROM INLET (RADIAN)															
ANGLE FROM INLET (DEGREES)															
ANGLE FROM INLET (RADIAN)															
ANGLE FROM INLET (DEGREES)															
ANGLE FROM INLET (RADIAN)															
ANGLE FROM INLET (DEGREES)															
ANGLE FROM INLET (RADIAN)															
ANGLE FROM INLET (DEGREES)															
ANGLE FROM INLET (RADIAN)															
ANGLE FROM INLET (DEGREES)															
ANGLE FROM INLET (RADIAN)															
ANGLE FROM INLET (DEGREES)															
ANGLE FROM INLET (RADIAN)															
ANGLE FROM INLET (DEGREES)															
ANGLE FROM INLET (RADIAN)															
ANGLE FROM INLET (DEGREES)															
ANGLE FROM INLET (RADIAN)															
ANGLE FROM INLET (DEGREES)															
ANGLE FROM INLET (RADIAN)															
ANGLE FROM INLET (DEGREES)															
ANGLE FROM INLET (RADIAN)															
ANGLE FROM INLET (DEGREES)															
ANGLE FROM INLET (RADIAN)															
ANGLE FROM INLET (DEGREES)															
ANGLE FROM INLET (RADIAN)															
ANGLE FROM INLET (DEGREES)															
ANGLE FROM INLET (RADIAN)															
ANGLE FROM INLET (DEGREES)															
ANGLE FROM INLET (RADIAN)															
ANGLE FROM INLET (DEGREES)															
ANGLE FROM INLET (RADIAN)															
ANGLE FROM INLET (DEGREES)															
ANGLE FROM INLET (RADIAN)															
ANGLE FROM INLET (DEGREES)															
ANGLE FROM INLET (RADIAN)															
ANGLE FROM INLET (DEGREES)															
ANGLE FROM INLET (RADIAN)															

Table 8

MODEL SOUND PRESSURE LEVELS (59° F, 70% Relative Humidity, Day)

Angles from Inlet in Degrees (and Radians)

	U.	10.	20.	30.	40.	50.	60.	70.	80.	90.	100.	110.	120.
FRW = (U.) (U.17) (U.05) (U.02) (0.74) (0.87) (1.05) (1.22) (1.40) (1.57) (1.75) (1.94) (1.94)													
BASELINE CLEAN CHAMBER													
CORRECTED SPEED = 69% (REPEAT)													
RADIAL 12. FT.	84												
(0. m)	100	72.0	73.0	72.0	71.4	69.3	70.3	72.0	70.0	71.7	75.0	74.7	70.0
VEHICLE R-11	120	74.0	75.0	74.0	74.4	70.0	70.0	70.0	70.0	74.7	70.0	74.7	70.0
CONFIG OF 6	100	73.0	71.0	71.0	70.0	71.0	71.5	71.0	70.0	70.0	70.0	70.0	70.0
LOC SCHENECTADY	200	75.0	77.0	76.0	75.0	74.1	74.0	71.0	71.0	71.0	74.0	74.0	75.0
DATE 3/19/76	200	82.0	81.0	80.0	80.0	79.0	77.0	75.0	74.0	74.0	71.0	70.0	70.0
RUN 8/10	315	82.3	81.0	81.0	80.8	79.1	77.0	75.0	75.0	74.2	74.1	74.0	74.0
TAPE	400	79.0	78.0	77.0	77.0	76.0	75.5	75.0	74.0	74.0	70.0	70.0	70.0
BAR 24.9 KG	500	76.0	76.0	76.0	76.0	75.0	74.0	72.0	73.0	73.0	70.0	70.0	70.0
(00973, NYM2)	600	75.0	76.0	76.0	76.0	77.0	75.0	74.0	75.0	75.0	71.0	70.0	70.0
ITEM 44. DEG F	800	78.0	77.0	77.0	78.0	76.0	74.0	72.0	75.0	75.0	64.0	64.0	64.0
(280. DEG R)	1000	74.0	74.0	74.0	75.0	74.0	73.0	70.0	74.0	74.0	67.0	70.0	70.0
FACT 40. DEG F	1200	73.0	74.0	75.0	74.0	73.0	74.0	70.0	72.0	72.0	51.0	52.0	52.0
(278. DEG R)	1600	75.0	75.0	75.0	75.0	75.0	75.0	71.0	68.0	68.0	79.0	79.0	79.0
MACT 5.35 GYM/10	2000	77.0	77.0	77.0	78.0	77.0	76.0	73.0	71.0	71.0	80.0	80.0	80.0
(.00535 KG/M3)	2500	78.0	78.0	78.0	79.0	78.0	77.0	75.0	74.0	74.0	84.0	84.0	84.0
NFA 10461. RPM	3150	81.0	81.0	81.0	81.0	81.0	80.0	78.0	78.0	78.0	78.0	78.0	78.0
(1148. RAD/SEC)	4000	83.0	84.0	84.0	84.0	84.0	83.0	82.0	79.0	78.0	70.0	70.0	70.0
BFR 11123. RPM	5000	83.0	83.0	83.0	83.0	83.0	85.0	83.0	84.0	84.0	77.0	78.0	78.0
(11165. RAD/SEC)	6300	85.0	87.0	87.0	88.0	88.0	88.0	86.0	86.0	86.0	80.0	76.0	76.0
NFO 16100. RPM	8000	96.0	96.0	97.0	101.0	103.0	104.0	104.0	104.0	104.0	98.0	98.0	98.0
(16686. RAD/SEC)	10000	87.0	87.0	88.0	90.0	91.0	90.0	90.0	88.0	88.0	82.0	77.0	74.0
NO. OF BLADES 44	12500	87.0	88.0	89.0	91.0	91.0	91.0	94.0	88.0	88.0	78.0	78.0	78.0
FAN TIP SPEED	15000	92.0	92.0	94.0	97.0	98.0	99.0	98.0	95.0	95.0	80.0	82.0	79.0
244. FT/SEC	20000	82.0	82.0	84.0	86.0	82.0	81.0	80.0	80.0	80.0	74.0	74.0	74.0
	25000	85.0	91.0	93.0	95.0	95.0	95.0	94.0	91.0	95.0	81.0	70.0	74.0
	31000	87.0	91.0	96.0	92.0	93.0	92.0	92.0	94.0	94.0	92.0	74.0	74.0
	40000	83.0	91.0	97.0	98.0	90.0	90.0	89.0	88.0	88.0	79.0	77.0	74.0
	50000	92.0	93.0	93.0	93.0	93.0	93.0	93.0	93.0	93.0	94.0	94.0	94.0
	60000	93.0	93.0	93.0	94.0	94.0	95.0	95.0	95.0	95.0	93.0	93.0	93.0
	65000	74.0	95.0	95.0	95.0	97.0	78.0	78.0	78.0	78.0	95.0	95.0	95.0
OVERALL CALCULATED	1000.0	452.0	452.0	452.0	452.0	452.0	452.0	452.0	452.0	452.0	97.0	93.0	93.0
	1000.0	452.0	452.0	452.0	452.0	452.0	452.0	452.0	452.0	452.0	97.0	93.0	93.0

Table 9

MODEL SOUND PRESSURE LEVELS (59° F, 70% Relative Humidity, Day)

Angles from Inlet in Degrees (and Radians)

	0.	10.	20.	30.	40.	50.	60.	70.	80.	90.	100.	110.		
	0.0	0.17	0.35	0.52	0.70	0.87	1.05	1.22	1.40	1.57	1.75	1.92	PWL	
50 deg														
GROUND PLANE, Z/D = 0.90														
CORRECTED SPEED = 54%														
RADIAL 17. FT. (5. M)	100	73.6	73.5	72.5	71.4	68.6	69.3	71.3	71.5	70.3	70.6	69.7	68.6	104.0
VEHICLE R=11	125	76.1	75.9	75.3	71.6	71.3	70.5	70.8	72.0	70.6	69.5	68.6	69.3	104.4
CONFIG CF 6	150	73.3	71.5	72.0	73.4	71.3	70.0	69.0	68.8	67.8	65.5	67.4	68.3	103.0
LOC SCHENECTADY	200	77.8	79.0	78.3	76.9	75.6	75.0	73.0	72.8	71.3	69.0	67.4	66.5	106.4
DATE 3/31/76	250	79.5	79.0	78.3	78.4	77.1	75.9	74.2	73.3	72.3	72.7	70.1	68.3	108.1
RLN 10/2	310	79.8	79.0	77.5	77.0	76.1	74.3	72.5	71.5	69.5	68.0	67.4	68.3	106.6
TAPE	400	77.5	77.5	76.8	76.8	74.6	73.3	72.0	70.5	66.6	67.7	64.7	62.6	105.6
BAR 26.9 KG (01106. N/M2)	500	76.0	75.5	75.3	75.1	74.1	73.0	72.0	70.3	68.5	66.8	64.2	61.6	104.7
TAMB 50. DEG F (283. DEG K)	630	76.8	76.5	76.8	77.8	75.0	74.8	72.5	71.5	69.5	68.4	66.5	63.6	106.3
TAPE 50. DEG F (283. DEG K)	800	76.3	76.0	75.5	75.8	73.6	73.5	69.5	68.0	66.5	65.4	64.5	61.6	104.3
TAPE 47. DEG F (281. DEG K)	1000	75.8	74.3	75.5	76.5	74.3	75.2	70.7	68.0	65.7	63.9	62.5	61.2	104.8
TAPE 47. DEG F (281. DEG K)	1250	77.0	76.8	77.0	76.1	73.8	72.7	71.4	68.4	66.8	66.0	63.4	61.5	104.4
TAPE 47. DEG F (281. DEG K)	1600	76.8	76.1	74.5	74.6	74.3	74.0	72.0	69.5	66.5	66.1	64.9	61.6	104.6
HACT 7.55 GM/M3 (0.00755. KG/M3)	2000	76.5	76.8	77.0	77.6	76.6	75.7	73.9	71.3	68.5	66.1	64.4	62.7	106.6
NFA 6631. RPM (504. RAD/SEC)	2500	78.3	78.1	78.0	78.6	78.6	77.5	76.2	72.8	70.3	67.9	65.4	64.8	108.2
NFA 6631. RPM (504. RAD/SEC)	3150	79.8	79.8	80.3	80.4	79.8	80.2	78.8	75.8	72.5	69.6	67.7	66.4	110.6
NFA 6707. RPM (5000. RAD/SEC)	4000	82.0	82.7	82.7	83.1	82.2	82.6	81.8	78.9	75.5	73.5	70.9	69.6	113.2
NFA 6707. RPM (5000. RAD/SEC)	5000	85.2	86.2	86.9	87.0	85.6	84.8	83.7	80.1	76.7	73.9	72.7	71.4	116.0
NFA 6707. RPM (5000. RAD/SEC)	6400	85.3	90.0	90.0	90.0	98.2	96.7	96.5	94.1	91.5	87.4	85.7	82.6	128.1
NFA 16100. RPM (8000. RAD/SEC)	8000	85.4	85.9	87.1	88.1	87.5	87.2	85.8	83.0	80.8	75.0	73.4	71.4	117.6
NFA 16100. RPM (8000. RAD/SEC)	10000	86.7	86.1	87.8	88.2	87.8	87.7	86.1	82.3	77.3	73.7	72.3	71.1	118.1
NO. OF BLADES 44 (25000. RPM)	12500	89.3	93.4	94.0	94.0	93.3	93.1	93.0	89.8	84.6	80.5	76.4	76.0	124.0
FAN TIP SPEED 747. FT/SEC (24000. RPM)	16000	85.4	85.8	87.2	89.0	87.9	87.1	86.2	83.1	77.2	73.2	71.0	69.2	118.6
FAN TIP SPEED 747. FT/SEC (24000. RPM)	24000	86.0	87.4	86.9	91.2	90.7	91.1	90.4	84.6	81.3	77.4	75.2	74.4	122.5
FAN TIP SPEED 747. FT/SEC (25000. RPM)	25000	82.0	83.7	86.5	88.0	88.3	90.3	87.6	83.7	76.4	71.0	68.6	66.4	120.7
FAN TIP SPEED 747. FT/SEC (31500. RPM)	31500	80.4	81.4	84.0	86.2	85.7	86.0	85.0	81.3	72.7	70.4	64.3	62.5	118.7
FAN TIP SPEED 747. FT/SEC (40000. RPM)	40000	77.3	76.4	81.3	83.3	83.1	83.2	81.7	77.7	69.5	66.0	64.6	62.6	117.0
FAN TIP SPEED 747. FT/SEC (50000. RPM)	50000	77.3	77.3	79.0	82.3	81.3	81.5	79.7	75.4	67.0	60.7	63.7	60.6	117.2
FAN TIP SPEED 747. FT/SEC (63000. RPM)	63000	75.4	76.9	70.7	74.7	79.5	79.5	77.7	72.5	65.1	64.0	64.0	60.7	117.8
FAN TIP SPEED 747. FT/SEC (65000. RPM)	65000	72.4	72.1	74.3	74.7	75.7	74.1	73.0	66.0	59.8	58.0	57.0	57.0	116.6
OVERALL CALCULATED 101.9 99.9 101.0 101.8 101.5 101.0 100.3 97.5 93.7 90.0 87.0 85.0 132.0														

Table 10
MODEL SOUND PRESSURE LEVELS (59° F, 70% Relative Humidity, Day)
Angles from Inlet in Degrees (and Radians)

Table 11
MODEL SOUND PRESSURE LEVELS (59°F, 70% Relative Humidity, Day)
Angles from Inlet in Degrees (and Radians)

	0°	10°	20°	30°	40°	50°	60°	70°	80°	90°	100°	110°	PNL	
FREQ. (0.1) (0.17) (0.35) (0.52) (0.70) (0.87) (1.05) (1.22) (1.40) (1.57) (1.75) (1.92)	50	50	50	50	50	50	50	50	50	50	50	50	50	
GROUND PLANE, Z/D = 0.90														
CORRECTED SPEED = 86%														
RADIAL 17. FT. (5. M)	100	70.1	76.0	79.0	69.1	69.5	89.5	71.3	73.0	72.5	75.5	71.3	70.0	113.5
VEHICLE R-11	125	72.0	71.0	71.0	66.9	69.0	86.0	70.4	71.5	69.3	74.0	69.3	70.0	110.5
CONFIG CF 6	100	71.8	70.3	70.3	71.1	73.2	85.5	73.2	73.2	70.0	76.5	72.0	72.0	110.7
LOC SCHENECTADY	200	77.3	76.8	78.0	77.9	78.0	86.7	75.2	77.2	76.0	79.5	76.5	74.0	113.1
DATE 3/31/76	250	79.0	79.8	79.5	81.1	80.2	86.5	77.2	79.5	79.5	81.0	76.0	77.0	114.3
RUN 10/4	315	79.0	78.5	77.3	77.3	76.0	89.2	73.0	72.2	65.7	70.4	67.4	69.0	113.0
TAPE	400	79.0	79.0	76.0	76.3	76.2	87.5	74.0	73.0	70.2	80.5	67.1	69.0	112.9
BAR 29.9 HG (01100. N/M2)	500	78.5	77.8	77.0	77.0	76.5	87.0	75.0	74.2	71.2	81.0	66.0	72.0	112.6
TAMB 50. DEG F (283. DEG K)	600	81.0	80.3	80.0	80.0	79.0	91.2	76.2	77.0	73.2	81.3	69.0	67.0	116.0
TNET -47. DEG F (261. DEG K)	1000	81.8	81.6	81.0	82.3	81.0	92.9	76.2	78.0	72.2	81.7	72.0	70.0	117.5
TNET -47. DEG F (261. DEG K)	1250	83.5	82.0	82.8	85.0	84.5	93.2	82.2	81.5	75.4	80.0	72.4	73.0	118.9
HAUT 7.55 GM/M3 (.00755 KG/M3)	2000	88.0	86.1	85.0	85.6	87.5	92.9	82.7	81.8	79.7	80.4	70.0	75.0	119.0
NFA 13743. RPM (1439. RAD/SEC)	2500	88.3	87.1	87.3	87.9	92.0	94.2	92.2	90.0	86.0	84.4	82.0	82.0	123.2
NFA 13864. RPM (1452. RAD/SEC)	3150	91.0	90.1	91.0	94.0	91.2	98.9	96.0	100.0	97.7	91.9	90.0	86.4	129.0
NFA 13864. RPM (1452. RAD/SEC)	4000	99.2	100.5	101.4	99.8	101.1	107.3	109.1	108.9	105.4	102.5	100.3	97.0	138.9
NFA 13864. RPM (1452. RAD/SEC)	5000	99.2	100.9	100.6	102.0	100.8	108.7	110.2	107.9	105.3	102.7	100.0	97.0	139.3
NFA 16100. RPM (1686. RAD/SEC)	6000	96.5	95.5	97.0	97.6	96.3	104.9	106.2	104.4	99.9	98.5	94.0	90.7	135.3
NFA 16100. RPM (1686. RAD/SEC)	8000	97.7	97.0	96.0	100.6	101.9	105.4	106.1	104.5	100.5	96.9	92.3	90.7	135.6
NO. OF BLADES 44	12500	96.0	96.9	96.3	100.2	100.5	104.0	104.9	102.0	98.1	93.5	90.4	87.0	134.0
FAN TIP SPEED 1190. FT/SEC	16000	95.1	95.3	96.9	99.0	99.8	103.8	102.7	100.0	96.8	91.7	87.7	84.7	133.6
16000	97.0	97.2	96.7	100.6	100.9	104.4	101.6	100.5	95.5	91.4	86.0	82.4	134.1	
20000	93.0	94.2	95.0	96.6	97.0	102.5	99.1	96.7	92.0	87.9	82.0	78.1	132.0	
31500	93.1	92.9	94.0	96.2	95.9	99.9	97.7	96.1	90.4	86.7	86.0	76.0	131.3	
40000	70.0	96.9	92.0	93.0	93.8	103.7	95.5	93.0	87.9	84.9	70.0	73.0	133.2	
50000	89.0	69.0	96.0	92.0	92.5	101.0	94.0	92.4	86.7	85.0	74.0	74.0	132.9	
63000	87.4	87.2	88.0	89.7	90.1	105.2	92.0	90.7	85.4	83.0	72.0	75.0	138.1	
80000	86.1	79.0	81.0	82.7	84.4	104.1	87.7	85.0	80.2	77.0	76.0	74.0	140.4	
CALCULATED 109.2 116.0 111.0 114.1 112.0 117.2 116.9 115.4 111.0 108.0 105.0 102.0 148.5														

Table 12
MODEL SOUND PRESSURE LEVELS (59° F, 70% Relative Humidity, Day)

Angles from Inlet in Degrees (and Radians)														
	0°	10°	20°	30°	40°	50°	60°	70°	80°	90°	100°	110°	PNL	
FREQUENCIES (Hz) (0.17) (0.35) (0.52) (0.70) (0.87) (1.05) (1.24) (1.40) (1.57) (1.75) (1.92)														
50														
60														
RADIAL 17. FT. (5. M)														
VEHICLE R-11	100	67.0	67.0	67.0	66.9	69.5	70.0	70.2	71.5	71.3	75.0	76.0	66.0	104.4
CONFIG CF 6	125	72.0	70.0	70.3	67.1	70.5	70.2	70.2	71.5	69.5	76.0	69.3	70.1	105.0
LOC SCHENECTADY	100	72.1	69.3	69.5	70.4	72.7	72.7	73.5	73.2	70.8	77.0	73.0	73.3	107.3
DATE 3/31/76	200	74.0	74.5	73.8	74.0	73.0	72.7	71.7	72.7	72.2	77.8	69.5	67.0	106.8
RUN 10/5	250	78.0	76.3	76.3	76.4	77.0	75.0	75.5	80.0	83.0	81.0	86.0	75.0	112.9
TAPE	315	78.0	76.5	76.0	75.6	74.7	73.7	72.2	71.5	69.2	80.0	87.5	86.0	108.1
BAR 29.9 HG (01106. N/M2)	500	78.0	78.0	78.0	78.0	77.0	76.7	77.2	76.0	74.7	74.2	77.0	66.0	109.1
TAMB 50. UFG F (283. UFG K)	600	61.0	79.3	79.3	80.3	78.7	77.0	76.0	74.7	72.7	83.0	69.5	66.3	111.6
TWET 47. UFG F (281. UFG K)	1000	82.0	80.0	80.0	81.0	86.2	75.4	77.7	75.0	72.7	77.2	71.1	67.0	110.8
HAET 7.55 GM/M3 (.00755 KG/M3)	1200	85.3	84.1	84.0	85.1	82.5	80.7	81.9	81.2	79.2	83.0	70.4	73.0	114.6
NFA 14372. RPM (1505. RAD/SEC)	1600	86.0	86.3	86.0	84.8	85.7	88.7	89.4	88.6	85.5	83.7	79.7	80.7	119.7
NFK 14468. RPM (1518. RAD/SEC)	2000	93.0	90.1	89.0	90.1	100.0	103.9	103.4	103.0	99.5	97.4	93.2	94.2	134.2
NFD 16100. RPM (1686. RAD/SEC)	2500	87.0	88.1	89.3	81.4	95.7	100.4	102.4	102.1	102.0	97.5	93.4	93.1	132.4
NO. OF BLADES 44	31500	90.5	92.0	93.5	93.1	98.9	102.4	102.1	102.0	97.5	93.4	93.1	94.4	138.7
FAN TIP SPEED 1245. FT/SEC	40000	96.0	97.2	97.9	98.8	106.3	110.3	109.3	105.4	102.6	98.8	97.0	94.3	130.4
	50000	96.2	100.1	101.5	107.0	109.7	109.2	104.1	100.8	98.5	95.0	95.0	94.0	134.0
	60000	96.5	97.8	98.0	101.6	106.2	105.2	101.0	96.2	95.4	90.0	90.0	90.0	134.0
	70000	97.4	97.4	98.9	101.0	101.4	103.9	103.4	99.0	98.0	93.9	98.0	98.0	133.4
	80000	107.0	107.1	107.8	108.0	109.0	111.6	109.4	100.5	103.5	98.0	95.2	92.9	140.7
	90000	99.0	100.0	100.0	102.2	102.3	105.0	104.9	100.0	97.3	92.0	99.4	98.9	135.0
	100000	95.9	96.0	97.7	99.0	100.3	102.5	101.7	98.0	94.0	89.5	86.5	83.7	132.6
	120000	94.9	95.2	96.0	97.0	98.0	100.0	99.8	96.2	91.0	86.0	84.0	81.0	133.6
	150000	94.1	93.8	95.0	96.7	96.9	99.2	98.0	94.0	89.2	85.0	81.0	78.0	131.4
	200000	91.3	91.1	92.0	93.8	94.3	96.2	95.5	91.4	86.4	83.4	74.0	73.4	129.6
	300000	89.5	90.1	90.8	93.0	93.5	95.0	94.7	90.4	85.7	83.0	73.0	73.0	130.5
	400000	87.4	87.9	88.5	90.0	91.1	94.0	93.1	88.5	83.7	81.1	71.0	75.7	131.4
	500000	86.4	79.0	82.3	83.4	85.4	86.6	87.4	83.5	78.2	73.0	76.0	73.0	129.7
OVERALL CALCULATED 110.4 110.3 111.2 112.6 114.5 117.5 119.7 113.3 109.8 106.5 103.5 101.5 147.1														

GROUND PLANE, Z/D = 0.90
CORRECTED SPEED = 90%

Table 13
MODEL SOUND PRESSURE LEVELS (59°F, 70% Relative Humidity, Day)

Angles from Inlet in Degrees (and Radians)

	0°	10°	20°	30°	40°	50°	60°	70°	80°	90°	100°	110°	PAL	
FREQU. (0.1) (0.17) (0.33) (0.52) (0.71) (0.87) (1.03) (1.22) (1.41) (1.57) (1.75) (1.92)	50	60	70	80	90	100	110	120	130	140	150	160		
VEHICLE	100	64.0	65.6	65.5	65.1	69.5	70.0	70.7	72.7	73.0	75.0	72.0	105.5	
VEHICLE R-11	125	66.1	68.0	69.3	66.9	69.7	70.0	70.5	72.0	72.3	74.0	73.0	105.8	
VEHICLE R-11 (5.0 M)	100	72.1	69.8	69.0	69.6	72.2	72.5	73.5	74.5	74.0	76.0	73.0	108.3	
VEHICLE R-11 (5.0 M) (0.17)	200	68.3	68.3	67.0	67.4	71.0	70.7	70.2	70.0	65.2	75.0	64.0	103.8	
VEHICLE R-11 (5.0 M) (0.33)	300	61.0	60.3	61.0	63.4	65.2	64.7	66.2	63.0	65.0	77.0	70.0	116.5	
VEHICLE R-11 (5.0 M) (0.52)	400	72.0	71.3	70.0	71.3	71.2	70.5	70.2	70.0	66.7	76.0	65.0	107.0	
VEHICLE R-11 (5.0 M) (0.71)	500	73.0	71.6	72.3	70.8	76.5	74.7	76.2	73.5	76.5	75.0	68.0	104.0	
VEHICLE R-11 (5.0 M) (0.87)	600	75.0	74.0	74.0	75.0	75.2	74.0	73.2	72.7	70.0	79.0	66.0	109.4	
VEHICLE R-11 (5.0 M) (1.03)	700	78.0	77.5	75.8	78.3	77.5	78.7	77.2	75.5	76.7	81.5	74.0	111.1	
VEHICLE R-11 (5.0 M) (1.22)	800	79.5	77.0	77.0	79.5	84.2	84.7	86.7	87.0	87.4	84.0	81.0	110.2	
VEHICLE R-11 (5.0 M) (1.41)	900	81.0	80.1	86.0	85.1	91.0	91.0	91.7	91.7	87.9	88.0	83.7	122.0	
VEHICLE R-11 (5.0 M) (1.57)	1000	84.5	85.6	84.0	94.3	96.7	98.4	97.7	96.0	94.5	91.0	91.0	120.3	
VEHICLE R-11 (5.0 M) (1.75)	1100	83.0	66.1	90.8	93.1	98.7	98.9	97.9	98.0	92.0	93.2	90.0	126.0	
VEHICLE R-11 (5.0 M) (1.92)	1200	88.0	88.3	86.6	92.0	92.4	97.0	99.4	98.7	97.3	91.0	91.0	126.0	
VEHICLE R-11 (5.0 M) (2.00)	1300	85.0	84.6	86.8	86.6	90.2	93.6	90.0	90.5	86.2	87.0	84.3	122.0	
VEHICLE R-11 (5.0 M) (2.17)	1400	88.2	89.3	90.4	90.1	92.3	94.8	92.6	89.4	86.4	87.0	86.0	123.7	
VEHICLE R-11 (5.0 M) (2.33)	1500	95.4	95.7	97.4	95.0	98.0	99.5	98.5	91.9	89.0	90.7	84.5	128.0	
VEHICLE R-11 (5.0 M) (2.50)	1600	94.0	93.7	95.0	97.3	101.6	101.2	98.5	96.9	94.2	92.0	89.3	87.0	
VEHICLE R-11 (5.0 M) (2.67)	1700	95.0	95.2	95.0	96.0	98.4	98.0	98.1	100.2	95.0	90.0	87.0	130.1	
VEHICLE R-11 (5.0 M) (2.83)	1800	102.0	103.1	103.3	104.5	105.2	103.6	104.0	100.3	96.0	92.0	89.0	87.0	
VEHICLE R-11 (5.0 M) (3.00)	1900	107.0	107.9	105.3	114.5	112.3	110.5	116.4	107.1	103.0	98.0	96.0	92.0	
VEHICLE R-11 (5.0 M) (3.17)	2000	95.0	96.0	90.0	90.0	98.3	98.0	98.7	95.0	92.0	88.0	84.0	129.0	
VEHICLE R-11 (5.0 M) (3.33)	2100	96.0	96.5	97.7	99.5	98.9	98.0	94.1	95.7	91.0	86.0	82.0	130.0	
VEHICLE R-11 (5.0 M) (3.50)	2200	96.4	97.5	99.0	100.5	100.0	101.0	101.0	97.2	93.0	88.0	83.0	133.0	
VEHICLE R-11 (5.0 M) (3.67)	2300	93.0	94.0	95.0	96.5	96.4	97.4	96.7	92.0	88.7	86.7	78.0	130.0	
VEHICLE R-11 (5.0 M) (3.83)	2400	91.0	91.4	92.0	94.3	95.1	95.2	95.0	90.9	86.7	82.0	75.0	129.4	
VEHICLE R-11 (5.0 M) (4.00)	2500	90.0	90.1	91.0	93.0	93.7	94.2	94.0	89.0	85.5	82.0	73.0	130.1	
VEHICLE R-11 (5.0 M) (4.17)	2600	87.0	87.9	89.2	90.7	91.4	92.5	92.1	87.5	83.7	79.1	71.0	130.7	
VEHICLE R-11 (5.0 M) (4.33)	2700	89.0	89.3	88.0	89.4	85.4	86.3	86.0	82.0	77.0	73.0	73.0	128.0	
VEHICLE R-11 (5.0 M) (4.50)	2800	116.3	116.6	111.8	113.0	114.6	113.8	114.5	110.5	106.9	103.7	100.0	97.0	145.5
VEHICLE R-11 (5.0 M) (4.67)	2900	116.3	116.6	111.8	113.0	114.6	113.8	114.5	110.5	106.9	103.7	100.0	97.0	145.5
VEHICLE R-11 (5.0 M) (4.83)	3000	116.3	116.6	111.8	113.0	114.6	113.8	114.5	110.5	106.9	103.7	100.0	97.0	145.5
VEHICLE R-11 (5.0 M) (5.00)	3100	116.3	116.6	111.8	113.0	114.6	113.8	114.5	110.5	106.9	103.7	100.0	97.0	145.5
VEHICLE R-11 (5.0 M) (5.17)	3200	116.3	116.6	111.8	113.0	114.6	113.8	114.5	110.5	106.9	103.7	100.0	97.0	145.5
VEHICLE R-11 (5.0 M) (5.33)	3300	116.3	116.6	111.8	113.0	114.6	113.8	114.5	110.5	106.9	103.7	100.0	97.0	145.5
VEHICLE R-11 (5.0 M) (5.50)	3400	116.3	116.6	111.8	113.0	114.6	113.8	114.5	110.5	106.9	103.7	100.0	97.0	145.5
VEHICLE R-11 (5.0 M) (5.67)	3500	116.3	116.6	111.8	113.0	114.6	113.8	114.5	110.5	106.9	103.7	100.0	97.0	145.5
VEHICLE R-11 (5.0 M) (5.83)	3600	116.3	116.6	111.8	113.0	114.6	113.8	114.5	110.5	106.9	103.7	100.0	97.0	145.5
VEHICLE R-11 (5.0 M) (6.00)	3700	116.3	116.6	111.8	113.0	114.6	113.8	114.5	110.5	106.9	103.7	100.0	97.0	145.5
VEHICLE R-11 (5.0 M) (6.17)	3800	116.3	116.6	111.8	113.0	114.6	113.8	114.5	110.5	106.9	103.7	100.0	97.0	145.5
VEHICLE R-11 (5.0 M) (6.33)	3900	116.3	116.6	111.8	113.0	114.6	113.8	114.5	110.5	106.9	103.7	100.0	97.0	145.5
VEHICLE R-11 (5.0 M) (6.50)	4000	116.3	116.6	111.8	113.0	114.6	113.8	114.5	110.5	106.9	103.7	100.0	97.0	145.5
VEHICLE R-11 (5.0 M) (6.67)	4100	116.3	116.6	111.8	113.0	114.6	113.8	114.5	110.5	106.9	103.7	100.0	97.0	145.5
VEHICLE R-11 (5.0 M) (6.83)	4200	116.3	116.6	111.8	113.0	114.6	113.8	114.5	110.5	106.9	103.7	100.0	97.0	145.5
VEHICLE R-11 (5.0 M) (7.00)	4300	116.3	116.6	111.8	113.0	114.6	113.8	114.5	110.5	106.9	103.7	100.0	97.0	145.5
VEHICLE R-11 (5.0 M) (7.17)	4400	116.3	116.6	111.8	113.0	114.6	113.8	114.5	110.5	106.9	103.7	100.0	97.0	145.5
VEHICLE R-11 (5.0 M) (7.33)	4500	116.3	116.6	111.8	113.0	114.6	113.8	114.5	110.5	106.9	103.7	100.0	97.0	145.5
VEHICLE R-11 (5.0 M) (7.50)	4600	116.3	116.6	111.8	113.0	114.6	113.8	114.5	110.5	106.9	103.7	100.0	97.0	145.5
VEHICLE R-11 (5.0 M) (7.67)	4700	116.3	116.6	111.8	113.0	114.6	113.8	114.5	110.5	106.9	103.7	100.0	97.0	145.5
VEHICLE R-11 (5.0 M) (7.83)	4800	116.3	116.6	111.8	113.0	114.6	113.8	114.5	110.5	106.9	103.7	100.0	97.0	145.5
VEHICLE R-11 (5.0 M) (8.00)	4900	116.3	116.6	111.8	113.0	114.6	113.8	114.5	110.5	106.9	103.7	100.0	97.0	145.5
VEHICLE R-11 (5.0 M) (8.17)	5000	116.3	116.6	111.8	113.0	114.6	113.8	114.5	110.5	106.9	103.7	100.0	97.0	145.5
VEHICLE R-11 (5.0 M) (8.33)	5100	116.3	116.6	111.8	113.0	114.6	113.8	114.5	110.5	106.9	103.7	100.0	97.0	145.5
VEHICLE R-11 (5.0 M) (8.50)	5200	116.3	116.6	111.8	113.0	114.6	113.8	114.5	110.5	106.9	103.7	100.0	97.0	145.5
VEHICLE R-11 (5.0 M) (8.67)	5300	116.3	116.6	111.8	113.0	114.6	113.8	114.5	110.5	106.9	103.7	100.0	97.0	145.5
VEHICLE R-11 (5.0 M) (8.83)	5400	116.3	116.6	111.8	113.0	114.6	113.8	114.5	110.5	106.9	103.7	100.0	97.0	145.5
VEHICLE R-11 (5.0 M) (9.00)	5500	116.3	116.6	111.8	113.0	114.6	113.8	114.5	110.5	106.9	103.7	100.0	97.0	145.5
VEHICLE R-11 (5.0 M) (9.17)	5600	116.3	116.6	111.8	113.0	114.6	113.8	114.5	110.5	106.9	103.7	100.0	97.0	145.5
VEHICLE R-11 (5.0 M) (9.33)	5700	116.3	116.6	111.8	113.0	114.6	113.8	114.5	110.5	106.9	103.7	100.0	97.0	145.5
VEHICLE R-11 (5.0 M) (9.50)	5800	116.3	116.6	111.8	113.0	114.6	113.8	114.5	110.5	106.9	103.7	100.0	97.0	145.5
VEHICLE R-11 (5.0 M) (9.67)	5900	116.3	116.6	111.8	113.0	114.6	113.8	114.5	110.5	106.9	103.7	100.0	97.0	145.5
VEHICLE R-11 (5.0 M) (9.83)	6000	116.3	116.6	111.8	113.0	114.6	113.8	114.5	110.5	106.9	103.7	100.0	97.0	145.5
VEHICLE R-11 (5.0 M) (10.00)	6100	116.3	116.6	111.8	113.0	114.6	113.8	114.5	110.5	106.9	103.7	100.0	97.0	145.5
VEHICLE R-11 (5.0 M) (10.17)	6200	116.3	116.6	111.8	113.0	114.6	113.8	114.5	110.5	106.9	103.7	100.0	97.0	145.5
VEHICLE R-11 (5.0 M) (10.33)	6300	116.3	116.6	111.8	113.0	114.6	113.8	114.5	110.5	106.9	103.7	100.0	97.0	145.5
VEHICLE R-11 (5.0 M) (10.50)	6400	116.3	116.6	111.8	113.0	114.6	113.8	114.5	110.5	106.9	103.7	100.0	97.0	145.5
VEHICLE R-11 (5.0 M) (10.67)	6500	116.3	1											

Table 14
MODEL SOUND PRESSURE LEVELS (59° F, 70% Relative Humidity, Day)

Angles from Inlet in Degrees (and Radians)

	0°	10°	20°	30°	40°	50°	60°	70°	80°	90°	100°	110°	PNL	
FR _{REV} (U. 1) (0.17) (0.35) (0.52) (0.70) (0.87) (1.05) (1.22) (1.40) (1.57) (1.75) (1.94)	30°	60°	90°	120°	150°	180°	210°	240°	270°	300°	330°	360°		
GROUND PLANE, Z/D = 0.90														
CORRECTED SPEED = 86% (REPEAT)														
RADIAL 17. FT.	0°													
(5. M)	100	70.0	70.8	70.3	66.9	69.5	70.0	71.5	74.0	72.5	76.0	71.0	69.1	105.0
VEHICLE R-11	120	72.0	72.8	71.3	69.6	69.7	70.2	70.5	72.2	69.0	74.0	69.3	70.1	104.0
CONFIG CF 6	150	72.1	72.6	70.5	71.0	73.2	73.2	73.2	73.5	70.5	76.0	72.0	72.3	106.0
LOC SCHENECTALY	200	78.0	79.3	78.4	78.6	78.3	78.5	79.5	77.5	76.2	79.0	75.0	75.0	110.0
DATE 3/31/76	250	79.0	80.0	80.0	81.4	81.0	78.5	77.5	79.7	79.2	82.0	76.0	76.0	113.4
RUN 1047	310	79.0	79.0	77.0	77.3	75.0	74.5	73.2	71.7	69.5	80.0	67.0	66.5	108.7
TAPE	400	79.0	79.0	78.3	77.8	76.5	75.5	74.5	73.0	70.5	80.0	66.0	65.0	109.0
BAR 28.9 KG (01106. N/M2)	500	78.0	78.3	77.8	77.8	77.2	76.5	75.5	73.5	71.2	86.0	66.0	64.0	109.0
TAMB 30. DEG F (26.3. DEG K)	600	82.0	81.3	80.8	80.3	79.2	75.7	74.5	72.7	70.7	80.7	66.4	65.0	110.3
TWF 42. DEG F (28.1. DEG K)	1000	81.0	80.6	81.5	82.3	81.0	77.9	75.9	74.5	72.2	79.7	72.4	66.0	111.3
TWF 42. DEG F (28.1. DEG K)	1250	82.0	82.1	83.3	85.1	85.0	85.4	84.7	81.0	70.7	85.0	77.4	74.0	116.2
HACT 7.55 GM/M3 (.00755 KG/M3)	1600	82.0	81.6	81.3	83.8	83.0	83.2	81.4	78.8	76.2	86.0	71.4	70.0	115.1
NFA 13742. RPM (1439. RAD/SEC)	2000	88.0	85.8	85.3	85.4	88.5	84.2	82.9	81.5	80.2	87.7	77.0	77.0	117.0
NFA 13742. RPM (1439. RAD/SEC)	2500	88.0	87.3	88.3	87.9	92.2	93.4	92.9	91.0	88.2	86.2	82.0	63.0	123.0
NFA 13863. RPM (1451. RAD/SEC)	3150	91.0	90.3	89.5	94.0	92.4	96.6	99.1	101.2	98.2	93.1	89.0	66.0	130.2
NFA 13863. RPM (1451. RAD/SEC)	4000	90.0	101.0	101.2	99.1	100.0	107.1	109.1	108.9	105.1	102.3	100.3	97.0	138.0
NFA 13863. RPM (1451. RAD/SEC)	5000	100.4	101.2	101.0	101.5	100.8	107.2	110.0	108.9	105.0	102.2	100.0	97.0	139.2
NFA 16100. RPM (1666. RAD/SEC)	6300	96.3	95.2	97.8	98.0	98.3	103.7	106.5	105.1	100.4	99.0	94.0	91.0	135.0
NFA 16100. RPM (1666. RAD/SEC)	8000	95.9	97.0	99.1	100.4	101.9	103.4	105.9	104.7	100.5	97.4	91.0	89.7	135.4
NFA 16100. RPM (1666. RAD/SEC)	10000	105.0	105.6	107.3	106.7	109.0	109.6	111.1	109.5	104.0	99.0	97.4	92.0	141.2
W.D. OF BLAUGS 44	12500	96.0	98.9	98.5	100.0	101.3	101.8	103.0	102.0	97.0	92.0	89.0	66.0	134.0
FAN TIP SPEED 1190. FT/SEC	16000	95.4	95.5	97.2	99.2	100.0	101.5	101.9	100.8	96.1	91.5	88.0	64.0	132.0
FAN TIP SPEED 1190. FT/SEC	20000	97.0	97.5	98.4	104.5	100.0	101.6	101.4	100.7	94.7	90.7	85.0	81.0	133.4
	25000	93.9	93.7	95.3	97.0	97.5	97.8	94.1	97.2	92.3	87.4	83.1	77.0	130.0
	31500	93.1	93.2	94.5	96.5	95.9	96.9	97.5	96.3	94.2	86.0	80.0	75.0	130.5
	40000	90.0	91.9	92.0	93.0	93.3	94.9	95.0	93.4	87.9	85.1	78.0	73.0	129.4
	50000	89.3	89.3	91.1	92.5	92.0	93.7	93.7	92.9	86.7	85.0	74.0	73.0	130.2
	63000	87.0	86.9	86.2	89.7	90.4	92.0	92.4	91.0	85.2	83.0	72.0	75.0	131.1
	80000	80.1	79.3	82.0	84.9	84.2	86.3	87.4	85.3	79.7	75.0	70.0	73.0	129.3
OVERALL CALCULATED	109.2	109.8	111.0	114.2	112.6	114.9	116.6	115.8	111.0	106.0	105.4	104.0	147.0	

Table 15
MODEL SOUND PRESSURE LEVELS (59° F, 70% Relative Humidity, Day)

Angles from Inlet in Degrees (and Radians)

	0.	10.	20.	30.	40.	50.	60.	70.	80.	90.	100.	110.			
	0.	(0.171)	(0.351)	(0.521)	(0.701)	(0.87)	(1.05)	(1.22)	(1.40)	(1.57)	(1.75)	(1.92)			
GROUND PLANE, Z/D = 0.90															
CORRECTED SPEED - 69% (REPEAT)															
RADIAL 17. FT. (0. M)	100	75.0	75.5	74.5	70.4	70.8	71.3	73.3	74.0	73.2	72.0	71.0	69.7	106.3	
VEHICLE R-11	125	77.3	75.8	74.5	72.0	72.0	72.3	71.5	74.5	71.2	70.1	69.0	69.4	105.2	
CONFIG CF 6	100	75.0	74.5	74.0	70.1	74.1	72.6	71.0	70.8	69.7	70.0	69.0	69.4	105.0	
LOC SCHENECTADY	200	83.0	81.3	80.5	79.5	77.6	77.0	75.5	75.3	74.9	74.0	74.0	71.1	109.3	
DATE 3/31/76	250	82.0	81.0	81.3	81.4	79.8	79.3	77.4	76.0	74.7	75.0	72.0	74.0	110.6	
RUN 10/8	310	83.3	82.2	81.0	81.3	79.0	79.3	76.0	74.0	72.8	72.0	76.4	66.0	110.4	
TAPE 400	82.0	82.0	81.0	80.8	79.1	78.5	76.2	74.0	72.0	72.0	66.0	66.0	66.0	110.0	
BAR 24.9 MG	500	79.0	79.3	79.0	79.0	78.0	78.0	76.4	74.0	72.1	71.1	67.0	65.0	109.2	
(01106. V/M2)	600	81.0	81.3	81.0	81.0	80.0	79.0	77.0	75.5	74.1	74.0	70.1	67.0	110.4	
TAPE 50. DEG F	600	81.0	81.0	81.0	81.0	81.0	79.6	76.7	75.0	73.0	70.6	71.0	66.0	66.1	109.5
(203. DEG K)	1000	80.0	79.3	79.5	80.5	79.0	77.7	75.5	73.0	70.0	71.0	66.0	67.1	109.2	
TAPE 47. DEG F	1250	80.0	80.0	80.0	79.0	76.0	76.2	75.0	72.5	70.1	71.0	66.0	65.0	108.4	
(201. DEG K)	1500	80.0	80.1	79.8	76.8	76.0	77.7	76.7	74.3	71.0	70.0	67.0	66.5	109.4	
FACT 7.55 GM/M3	2000	81.0	81.1	81.8	81.9	80.6	79.7	77.9	76.3	72.0	75.0	66.0	69.0	111.2	
(.00755 KG/M3)	2500	82.0	81.0	82.0	83.1	82.0	82.0	80.2	77.0	73.0	72.0	66.0	67.0	112.3	
NFA 11025. RPM	3150	83.0	83.0	84.0	85.1	84.3	84.2	82.9	80.5	77.0	74.0	72.0	71.0	114.0	
(1154. RAD/SEC)	4000	85.2	85.7	85.9	86.1	86.7	85.8	85.8	83.7	79.1	75.0	74.0	74.4	117.0	
NFA 41122. RPM	5000	86.4	86.7	87.1	88.3	88.4	87.6	86.5	83.9	79.5	76.0	74.0	73.0	118.1	
(1164. RAD/SEC)	6300	88.5	89.2	90.0	91.3	90.9	92.7	92.7	88.7	84.0	81.0	79.0	70.0	122.0	
NFA 16100. RPM	8000	98.7	99.6	100.4	104.1	104.0	109.2	111.2	108.0	101.1	99.0	97.0	91.0	139.2	
(1686. RAD/SEC)	10000	90.2	90.3	91.0	93.5	93.3	95.2	95.0	91.0	86.4	83.0	82.0	78.0	125.4	
NJ. UF BLADES 44	12500	89.0	89.9	91.5	92.7	92.6	92.3	91.7	88.1	83.2	79.0	70.0	74.0	123.2	
FAN TIP SPEED	16000	93.4	94.6	95.4	98.2	98.1	100.3	98.2	96.4	90.3	85.0	83.0	80.0	130.1	
V55. F1/SEG	20000	88.3	89.6	89.4	90.0	92.7	92.9	91.4	88.3	81.4	77.0	73.0	71.2	123.0	
	25000	89.0	90.0	90.5	95.3	95.1	95.5	95.3	91.5	84.7	79.0	75.0	73.0	127.4	
	31500	87.0	88.2	89.2	92.5	92.7	93.0	92.3	88.3	81.3	76.0	70.0	66.0	125.0	
	40000	85.0	85.0	87.5	89.6	89.9	90.2	89.0	85.9	76.1	72.0	66.0	65.5	124.0	
	50000	83.0	83.8	86.1	88.0	88.3	89.0	88.0	84.4	70.0	72.0	65.0	66.0	124.0	
	63000	81.0	81.7	84.2	85.5	85.7	86.0	85.7	81.5	74.9	70.1	66.0	73.0	124.0	
	80000	75.0	75.0	77.0	79.2	79.2	80.1	79.2	75.1	67.0	63.0	64.0	65.0	122.0	

Table 16

MODEL SOUND PRESSURE LEVELS (59°F, 70% Relative Humidity, Day)

Angles from Inlet in Degrees (and Radians)

	0.	10.	20.	30.	40.	50.	60.	70.	80.	90.	100.	110.		
	(0.1)	(0.17)	(0.35)	(0.52)	(0.70)	(0.87)	(1.05)	(1.22)	(1.40)	(1.57)	(1.75)	(1.92)	PWL	
	50	63	80											
GROUND PLANE, Z/D = 1.16														
CORRECTED SPEED - 54%														
RADIAL 17° FT. (5.1)	100	74.7	74.3	72.6	71.8	68.1	69.4	71.4	71.5	70.2	70.5	69.7	68.5	104.1
VEHICLE P-11	125	75.5	75.3	74.3	71.3	72.8	71.1	70.7	71.8	70.7	69.2	70.7	70.5	105.0
CONFIG OF 6	150	72.2	72.0	72.1	72.3	71.1	69.4	68.7	69.8	68.9	66.5	66.4	66.3	103.0
LOC SCHENECTADY	200	77.5	78.8	77.6	75.5	75.0	74.4	72.7	72.5	70.4	69.2	67.4	66.0	106.4
DATE 4/27/76	250	79.0	78.8	77.8	76.3	74.9	72.9	72.0	70.7	71.5	69.4	67.0	67.0	107.2
RUN 14/4	315	79.5	79.3	78.1	77.0	75.8	74.4	72.1	71.0	68.4	67.2	65.9	64.6	106.4
TAPE	400	76.2	76.5	76.3	75.3	73.8	72.6	70.6	68.8	66.6	66.2	63.4	60.8	104.5
BAR 29.0 HG (99983. N/42)	500	73.2	73.8	74.1	73.3	72.3	70.3	68.6	67.3	65.6	64.7	61.7	59.0	102.5
TAMB 50° DFG F (243. DEG K)	630	75.5	76.0	75.6	75.2	73.1	70.8	68.4	67.0	65.4	65.2	62.7	59.5	103.5
TWET 47° DFG F (1281. DEG K)	800	73.4	73.5	73.1	72.7	71.3	69.8	67.6	65.3	63.1	63.2	62.2	59.5	101.0
TAET 47° DFG F (1281. DEG K)	1000	71.4	71.0	71.3	71.2	69.8	68.3	66.1	64.5	61.8	59.7	59.0	58.5	100.0
TAET 47° DFG F (1281. DEG K)	1200	71.7	72.0	72.6	72.5	71.3	69.8	67.9	66.0	63.4	62.4	60.5	59.0	101.4
TAET 47° DFG F (1281. DEG K)	1600	72.2	73.6	72.3	72.3	72.5	72.1	69.1	67.0	63.0	62.9	60.1	59.0	102.4
TAET 7.56 GM/M3 (-0.00756. KG/M3)	2000	74.5	75.3	74.8	73.3	74.3	72.1	69.3	65.9	64.4	61.9	61.7	104.7	
TAET 7.56 GM/M3 (-0.00756. KG/M3)	2500	78.2	78.3	77.6	77.8	77.3	77.0	75.3	72.0	68.9	66.9	64.7	63.4	107.5
NFA 8620° RPM (903. RAD/SEC)	3150	81.7	81.1	79.3	79.8	80.0	79.3	77.6	74.0	70.1	68.1	65.7	65.1	109.7
NFA 8696° RPM (910. RAD/SEC)	4000	83.1	84.0	83.7	83.0	82.4	82.2	79.7	76.2	72.6	71.0	68.4	67.0	112.6
NFA 8696° RPM (910. RAD/SEC)	5000	85.3	85.9	85.9	85.7	85.3	84.6	82.7	78.9	74.8	73.4	71.2	70.5	115.2
NFA 8696° RPM (910. RAD/SEC)	6300	95.4	95.2	96.1	97.2	97.9	96.5	95.4	92.6	88.1	87.1	84.0	82.7	127.4
NFD 16100° RPM (1686. RAD/SEC)	3000	84.1	84.6	86.2	86.8	87.0	87.0	84.3	81.0	76.1	74.1	71.9	71.1	116.8
NFD 16100° RPM (1686. RAD/SEC)	10000	85.7	85.8	86.9	87.2	87.8	87.8	86.3	82.5	76.2	74.0	71.5	70.8	117.9
NO. OF BLADES 44	12500	94.2	92.6	96.1	94.2	93.8	94.2	94.9	90.9	85.2	81.7	79.0	77.6	125.6
FAN TIP SPEED 747. FT/SEC	15000	83.8	85.5	87.5	88.4	87.8	87.4	86.1	83.4	76.5	73.4	70.9	69.2	119.6
FAN TIP SPEED 747. FT/SEC	20000	85.7	87.0	88.5	92.1	92.9	93.2	91.3	89.0	81.9	76.9	74.0	71.7	123.9
FAN TIP SPEED 747. FT/SEC	25000	82.1	84.0	86.6	87.7	88.3	89.1	88.0	83.9	76.0	71.3	68.0	66.9	120.4
FAN TIP SPEED 747. FT/SEC	31500	79.8	81.2	84.0	86.1	86.0	86.0	86.2	81.3	73.1	68.2	64.3	63.0	118.9
FAN TIP SPEED 747. FT/SEC	40000	77.9	78.5	81.5	82.8	83.4	83.6	82.1	78.1	69.6	64.5	60.7	60.1	117.2
FAN TIP SPEED 747. FT/SEC	50000	76.4	78.0	80.1	81.2	81.8	81.6	80.1	76.1	67.4	63.2	60.6	59.0	117.3
FAN TIP SPEED 747. FT/SEC	63000	75.0	76.2	78.8	79.4	79.4	79.3	78.1	72.7	66.4	62.0	60.5	60.0	117.0
FAN TIP SPEED 747. FT/SEC	80000	70.3	70.3	73.6	73.1	73.5	72.9	71.1	66.0	63.1	57.0	57.0	60.0	115.6
OVERALL CALCULATED	99.6	99.4	101.0	101.4	101.7	101.3	100.4	97.1	91.7	89.7	86.9	85.7	132.6	

Table 17

MODEL SOUND PRESSURE LEVELS (59°F, 70% Relative Humidity, Day)

Angles from Inlet in Degrees (and Radians)

	0.	10.	20.	30.	40.	50.	60.	70.	80.	90.	100.	110.	
	50	60	70	80	90	100	110	120	130	140	150	160	PHL
FREE. (0.)	(0.17)	(0.35)	(0.52)	(0.70)	(0.87)	(1.05)	(1.22)	(1.40)	(1.57)	(1.75)	(1.92)		
RADIAl 17. FT.	50	60	70	80	90	100	110	120	130	140	150	160	
(5. MI	100	75.8	75.8	74.3	72.9	70.8	71.3	73.5	73.6	73.2	72.8	72.7	71.4
VEHICLE R-11	125	77.0	76.8	75.0	73.4	74.0	72.0	72.0	72.6	71.7	70.3	71.7	70.5
CONFIG CF 6	100	75.1	75.0	75.0	76.1	74.3	72.3	71.8	70.3	69.9	69.6	70.2	70.0
LOC SCHENECTADY	200	79.5	81.0	79.8	78.4	77.1	76.5	75.0	74.3	72.9	72.1	70.4	72.0
DATE 4/27/76	250	82.8	82.0	81.3	81.6	80.3	78.0	76.2	75.3	74.4	74.8	73.1	71.0
RUN 14/5	315	73.0	83.5	81.8	81.3	79.8	77.8	76.2	74.3	71.9	70.8	69.2	68.5
TAPE	400	81.3	81.5	80.3	80.3	78.3	77.0	74.5	73.3	71.4	70.1	67.4	65.3
BAR 29.5 KG	500	73.5	78.8	78.3	78.8	77.1	75.3	74.0	71.8	70.4	68.3	66.0	64.0
(99089. N/M2)	630	79.8	80.0	79.8	80.3	78.1	75.8	73.2	72.0	70.6	69.3	67.5	64.8
TAMS 50. DEG F	810	77.8	78.3	77.5	78.0	76.3	74.5	72.7	70.3	67.9	67.5	67.2	65.2
(283. DEG K)	1000	74.8	75.5	75.8	76.0	74.3	74.0	73.0	70.3	70.1	67.8	66.2	64.2
INLET 47. DEG F	1250	75.5	75.6	75.0	75.8	74.6	73.7	72.2	69.8	67.9	66.5	64.0	62.5
(281. DEG K)	1600	75.8	76.3	76.0	77.3	77.3	76.2	74.0	71.8	69.1	67.5	65.1	64.2
HACI 7.54 GM/M3	2000	78.0	78.8	78.3	79.5	79.6	77.7	75.9	73.3	69.6	68.0	66.4	63.9
(.00756. KG/M3)	2500	80.0	80.1	79.8	81.6	80.3	79.7	78.2	75.3	72.4	70.2	67.2	65.9
NFA 11000. RPM	3150	84.3	84.3	83.5	84.6	84.0	84.4	84.1	81.5	78.1	75.4	73.5	71.6
(1153. RAD/SEC)	4000	86.2	87.0	85.9	86.6	86.7	86.6	85.1	82.2	77.6	76.8	73.4	73.3
NFK 11105. RPM	5000	85.9	86.2	86.4	87.8	86.9	86.5	85.5	82.1	78.3	76.0	73.9	73.0
(1153. RAD/SEC)	5300	87.3	88.0	88.5	90.0	90.9	91.4	89.2	87.2	82.6	79.6	78.3	76.4
NFD 16100. RPM	8000	97.7	99.4	100.1	103.6	105.7	108.7	104.9	105.0	99.6	96.5	95.7	92.0
(1696. RAD/SEC)	10000	88.7	89.3	90.1	92.5	92.6	93.4	91.4	90.1	84.4	80.8	80.5	77.0
NO. OF BLADES 44	12500	85.0	89.4	90.5	92.5	92.3	92.3	92.0	88.6	83.0	79.3	77.3	75.6
FAN TIP SPEED	16000	93.6	94.3	95.4	98.0	98.9	100.6	98.4	96.9	90.5	86.3	83.4	81.7
953. FT/SEC	20000	87.8	89.2	90.7	92.7	92.5	92.4	90.9	88.5	81.9	76.8	74.0	72.2
	25000	88.0	90.2	92.8	95.0	95.3	96.0	95.8	91.9	86.0	80.7	77.2	74.0
	31500	47.3	88.4	90.5	93.0	93.2	92.7	93.2	89.6	82.6	76.3	72.1	69.0
	40000	34.8	85.6	87.5	89.8	89.6	90.2	89.2	86.7	78.6	72.4	67.7	65.1
	50000	53.0	84.0	86.1	88.3	88.6	89.0	88.0	84.7	77.1	69.6	65.0	63.3
	63000	80.9	81.4	83.5	85.2	86.7	86.8	85.9	82.5	75.2	67.4	63.3	62.4
	80000	75.4	75.6	78.0	78.7	79.7	79.9	79.5	75.6	68.9	61.9	58.2	62.0
OVERALL CALCULATED	101.8	102.9	103.8	106.6	107.9	110.1	107.2	106.4	100.9	97.5	96.5	93.7	139.7

Table 18
MODEL SOUND PRESSURE LEVELS (59° F, 70% Relative Humidity, Day)

Angles from Inlet in Degrees (and Radians)

	0.	10.	20.	30.	40.	50.	60.	70.	80.	90.	100.	110.	PWL
FREQU. (Hz.)	(0.17)	(0.35)	(0.52)	(0.70)	(0.87)	(1.05)	(1.22)	(1.40)	(1.57)	(1.75)	(1.92)		
	50												
	63												
RADIAL 17. FT.	50												
(5. M)	100	73.6	79.3	89.8	98.4	70.0	70.7	71.7	72.2	72.5	72.6	71.0	69.1
VEHICLE R-11	125	71.8	71.8	71.0	67.6	71.7	70.7	70.7	70.5	69.0	68.0	69.8	69.8
CONFIG CF 6	150	77.8	69.8	69.5	70.4	71.5	71.2	71.0	70.7	69.0	70.5	72.3	71.6
LOC SCHNEIDER TADY	200	77.8	79.3	78.3	78.4	78.0	76.2	76.0	77.0	75.2	76.8	71.0	75.0
DATE 4/27/76	250	79.5	80.3	79.8	81.1	79.7	78.0	78.0	78.7	77.7	79.3	72.6	77.0
RUN 11/4	315	79.5	78.3	76.8	76.8	75.5	73.7	73.0	71.2	68.2	67.5	66.5	65.0
TAPE	400	78.0	77.5	76.0	76.6	75.0	74.7	72.7	71.7	68.5	68.0	66.1	64.5
BAR 29.6 KG	500	75.8	76.5	76.0	76.6	74.7	74.0	72.5	71.0	68.0	66.3	63.0	63.0
(99989, N/M2)	630	81.3	73.8	78.0	77.8	76.2	74.5	72.2	72.7	70.5	69.0	65.6	64.0
TAM 69, DFG F	800	75.8	75.8	75.8	76.5	75.5	74.2	72.7	71.5	68.2	68.2	67.4	65.0
(1283, DEG K)	1000	78.5	77.3	77.5	77.5	76.7	74.9	74.4	73.7	71.4	72.4	71.1	69.6
INLET 47. DEG F	1250	83.3	81.6	78.8	79.3	83.0	83.2	82.2	80.2	76.9	76.0	74.7	72.3
(281, DFG K)	1600	82.0	81.8	79.3	79.8	81.5	82.2	80.2	79.8	75.2	73.2	74.0	70.0
HACT 7.86 GM/M3	2000	86.3	86.6	86.0	85.1	84.5	83.4	87.4	81.0	81.2	77.7	77.3	75.4
(0.00786 KG/M3)	2500	86.0	84.3	83.5	86.4	91.2	93.9	97.2	93.0	89.0	88.4	84.5	83.9
NFA 13721. RPM	3150	88.0	89.1	86.5	89.9	91.2	97.1	99.1	99.7	97.2	94.9	91.3	88.7
(1437. RAD/SEC)	4000	99.2	98.5	95.4	100.1	99.6	107.8	111.0	109.7	106.1	102.0	103.3	97.8
NFK 13655. RPM	5000	99.7	98.2	98.4	101.3	100.3	108.2	111.7	110.3	107.8	104.4	103.3	98.0
(1451. RAD/SEC)	6300	95.0	94.2	97.3	99.0	98.3	104.1	107.2	105.4	100.4	98.2	94.6	91.0
NFD 16100. RPM	8000	95.6	96.9	98.3	100.3	99.4	105.4	106.1	103.7	99.2	96.1	92.3	90.1
(1686. RAD/SEC)	10000	104.5	105.5	106.8	108.7	107.7	108.6	110.8	108.0	104.0	99.0	96.6	93.6
NO. OF BLADES 44	12500	95.5	96.6	97.7	100.2	100.2	101.5	104.7	102.6	98.5	94.2	90.6	87.8
FAN TIP SPEED 16000	95.1	95.2	96.4	98.7	99.2	100.2	102.4	100.5	95.5	91.7	87.4	84.2	132.6
t188. FT/SEC 20000	96.5	97.2	97.9	100.2	99.3	101.3	102.1	99.9	94.7	89.9	85.5	82.9	133.1
- 25000	92.8	93.6	94.7	96.9	96.7	97.9	99.0	97.1	92.0	86.0	81.5	79.1	130.6
31500	93.0	93.1	94.4	96.4	95.6	97.1	98.1	95.7	90.1	84.4	79.6	75.9	130.5
40000	91.6	90.5	91.6	93.7	93.4	94.6	95.8	93.7	87.6	81.7	75.7	72.8	129.6
50000	88.9	89.4	90.6	92.1	92.1	93.5	94.5	92.2	86.0	79.8	74.3	72.9	130.1
63000	86.8	86.9	88.7	89.4	90.1	91.7	92.8	91.1	84.7	77.8	72.8	73.6	131.0
80000	79.8	79.7	81.9	82.3	84.3	86.0	87.9	85.4	79.4	72.0	71.0	72.4	129.4
OVERALL CALCULATED	108.4	109.0	109.9	112.1	111.4	115.1	117.7	115.9	112.3	108.6	107.5	102.9	147.4

Table 19
MODEL SOUND PRESSURE LEVELS (59° F, 70% Relative Humidity, Day)

Angles from Inlet in Degrees (and Radians)

	10°	20°	30°	40°	50°	60°	70°	80°	90°	100°	110°
PRE4. (0.) (0.17) (0.35) (0.52) (0.70) (0.87) (1.05) (1.22) (1.40) (1.57) (1.75) (1.92)	5°	10°	20°	30°	40°	50°	60°	70°	80°	90°	100°
VEHICLE	5. M	100	57.1	67.3	56.8	66.6	70.0	70.7	70.7	71.3	71.0
VEHICLE	R-11	120	59.1	70.0	70.5	65.1	71.2	70.7	70.7	68.5	68.3
CONFIG	DF 6	100	69.8	69.0	68.8	69.1	70.7	70.7	70.7	70.3	70.0
LUP	SCHENECTARY	200	73.0	74.3	73.0	71.6	72.0	71.7	71.5	72.2	70.7
DAIF	4/27/76	250	73.3	77.1	78.8	77.1	75.5	74.5	75.7	80.5	81.0
RUN	14/7	315	75.3	75.3	74.0	74.1	73.5	72.0	71.5	70.5	67.0
TAPE		400	75.0	75.1	74.3	74.6	73.5	73.5	71.7	70.5	67.7
BAR	29.6 HQ	500	74.8	77.3	76.5	76.6	77.0	77.5	76.0	73.5	70.5
	(199939. NM2)	630	77.0	76.5	75.8	75.6	75.0	72.7	71.2	70.5	67.2
TAMB	50°, DFG F	800	74.8	74.0	73.8	75.0	75.2	73.7	72.7	70.7	68.7
	(283. DFG K)	1000	74.5	75.8	74.5	77.3	75.5	77.2	76.4	74.2	72.4
TWET	47°, DFG F	1250	83.5	82.6	81.5	82.1	82.7	83.4	83.7	82.7	81.7
	(281. DFG K)	1600	83.8	84.8	85.3	84.8	84.2	90.4	91.7	89.3	87.0
HACI	7.56 GM/M3	2000	87.5	92.3	90.8	94.4	97.7	102.9	103.9	103.5	100.0
	(-0.0756 KG/M3)	2500	88.3	86.6	86.8	89.4	96.0	100.4	102.4	100.8	97.0
NFA	14371. RPM	3150	87.3	88.3	91.5	95.9	97.7	103.1	102.1	100.2	96.7
	(1505. RAD/SEC)	4000	97.7	97.2	96.2	101.3	104.6	110.8	111.1	107.4	104.6
NFA	14492. RPM	5000	98.4	97.9	99.6	102.0	102.3	110.7	111.7	108.6	104.3
	(1518. RAD/SEC)	6300	94.8	95.5	97.3	100.0	97.8	104.7	106.5	103.6	98.4
NFD	16100. RPM	8000	95.4	96.1	97.6	101.1	99.7	101.9	103.4	100.2	95.0
	(1685. RAD/SEC)	10000	106.7	105.6	107.3	108.5	108.5	108.9	109.9	105.5	102.5
NO. OF BLADES	44	12500	98.3	98.6	100.3	101.7	102.8	103.5	104.2	101.6	97.8
FAN TIP SPEED		16000	95.1	96.0	97.7	99.5	99.5	100.5	102.7	99.1	95.3
	1245. FT/SEC	20000	96.8	97.7	98.7	100.7	100.9	101.1	101.6	98.0	93.2
		25000	93.9	94.7	95.8	97.5	97.8	98.7	99.5	96.2	90.8
		31500	93.1	92.9	94.7	97.0	96.4	97.4	98.0	94.0	88.2
		40000	93.7	90.8	91.7	93.8	94.0	94.9	95.4	92.1	85.9
		50000	89.8	89.3	90.8	92.3	92.5	94.2	94.2	90.6	84.4
		63000	86.4	86.9	88.7	89.7	90.6	92.0	92.6	89.2	83.2
		80000	79.1	79.6	81.8	82.4	84.7	86.3	87.7	84.0	77.7

Table 20

MODEL SOUND PRESSURE LEVELS (59°F, 70% Relative Humidity, Day)

Angles from Inlet in Degrees (and Radians)

	0.	10.	20.	30.	40.	50.	60.	70.	80.	90.	100.	110.		
	0.0	0.17	0.35	0.52	0.70	0.87	1.05	1.22	1.40	1.57	1.75	1.92		
PRE ₀₀ (0.0)	50													
	63													
RADIAL 17. FT.	80													
(5. M)	100	64.6	64.3	65.5	64.4	70.0	70.7	71.0	72.2	72.0	72.0	71.5	71.1	104.0
VEHICLE R-11	125	65.8	68.3	69.3	63.4	70.2	70.7	70.7	71.5	71.5	71.0	73.3	73.1	105.1
CONFIG CF 6	150	77.8	69.8	66.5	68.6	70.7	71.2	71.5	73.5	73.8	75.0	76.5	76.1	107.5
LOC SCHEMECTAY	200	66.3	67.0	67.3	66.6	70.5	70.7	70.7	70.5	65.7	64.0	63.8	65.0	101.6
DATE 4/27/76	250	80.5	85.0	86.5	87.1	89.0	86.0	86.0	81.2	86.2	77.8	76.0	81.8	118.3
RUN 1474	315	72.0	74.5	75.5	76.3	77.5	75.5	75.5	72.0	74.7	70.3	68.5	70.0	107.7
TAPE	400	58.8	64.5	68.3	69.6	70.2	70.7	70.7	70.5	65.7	66.3	65.1	64.0	102.2
BAR 27.5 KG	500	59.5	68.5	74.3	78.3	76.5	73.7	75.5	75.7	68.2	73.0	64.3	69.5	107.4
(99989. 4/2)	630	71.3	70.8	71.0	72.1	71.5	70.7	70.7	70.5	66.2	66.0	63.3	64.0	102.7
TAMB 50. DFG F	800	73.3	72.3	71.3	72.3	73.0	76.4	76.5	76.5	76.4	74.7	72.4	69.0	108.3
(1283. JEG K)	1000	75.0	73.3	70.8	76.8	82.7	87.2	88.4	88.0	86.9	78.7	81.4	78.5	118.5
WET 47. DFG F	1250	77.8	79.1	77.0	85.6	93.5	93.9	94.2	93.2	88.9	87.5	82.9	83.0	124.3
(1281. DFG K)	1600	82.8	86.5	88.8	96.3	97.2	94.9	96.7	93.8	90.0	88.0	90.2	89.0	127.1
HACI 7.56 GM/M3	2000	82.5	85.3	87.5	94.6	95.0	97.9	97.7	95.3	93.7	92.2	90.0	88.5	128.2
(-0.0756. KG/M3)	2500	84.0	85.6	90.0	88.4	93.7	100.2	99.9	98.3	92.0	90.9	88.8	82.5	129.3
NFA 15969. RPM	3150	84.3	84.1	86.8	86.5	91.9	94.4	92.6	91.7	87.0	84.1	82.3	81.4	123.4
(15721. RAD/SEC)	4000	80.5	88.7	88.9	89.6	91.8	94.1	94.1	89.4	84.6	83.0	82.5	81.3	123.5
NFA 16109. RPM	5000	94.7	94.4	93.9	97.0	97.5	100.5	100.2	96.6	93.6	89.7	86.5	89.0	130.0
(1687. RAD/SEC)	6300	93.0	93.7	94.0	95.8	101.3	101.2	100.0	98.6	94.2	91.2	89.1	87.0	131.0
NFA 15100. RPM	8000	92.4	93.6	94.4	95.6	96.7	98.2	99.1	98.5	93.2	89.9	87.0	85.7	129.4
(1686. RAD/SEC)	10000	100.5	101.1	102.6	103.7	103.2	102.6	104.4	100.8	97.0	93.8	90.9	87.4	134.6
NO. OF BLADES 44	12500	106.3	107.6	108.8	110.0	109.5	109.3	111.4	107.3	104.1	100.3	97.4	93.6	141.4
FAN TIP SPEED 1383. FT/SEC	16000	94.1	95.0	95.7	97.2	98.0	98.0	98.7	96.6	92.1	87.7	83.5	81.5	129.6
20000	95.0	95.7	97.2	98.5	98.4	98.1	98.6	96.2	91.7	87.0	82.6	79.9	130.4	
25000	96.6	97.5	98.0	99.5	99.5	100.0	101.3	97.7	93.8	88.6	83.0	80.4	132.8	
31500	92.0	93.7	94.2	96.0	95.9	96.4	96.5	93.3	88.7	83.7	77.9	74.8	129.6	
40000	90.0	91.1	92.2	93.3	93.8	94.4	94.9	91.4	86.7	81.1	74.8	72.7	129.0	
50000	89.0	89.3	91.1	92.3	92.7	93.5	93.7	90.9	85.4	79.7	73.0	72.4	129.7	
63000	95.1	87.2	88.2	90.0	90.4	91.2	91.9	88.0	84.0	78.3	71.4	73.4	130.2	
80000	79.4	79.8	81.5	82.2	84.7	85.8	86.7	83.0	77.9	71.1	71.1	72.5	126.5	
OVERALL CALCULATED	109.9	109.9	111.0	112.5	112.7	112.9	114.2	110.9	107.2	103.7	101.2	98.8	144.9	

Table 21
MODEL SOUND PRESSURE LEVELS (59°F, 70% Relative Humidity, Day)

Angles from Inlet in Degrees (and Radians)

RADIAL 17, FT. (5.2)	D. 6.5	ANGLES FROM INLET IN DEGREES (AND RADIANS)											PWL		
		0.	10.	20.	30.	40.	50.	60.	70.	80.	90.	100.			
FREQUENCIES (Hz) (0.17) (0.35) (0.52) (0.70) (0.87) (1.05) (1.22) (1.40) (1.57) (1.75) (1.92)															
GROUND PLANE, Z/D = 1.16															
CORRECTED SPEED = 86% (REPEAT)															
VEHICLE R-11	100	70.0	71.0	70.3	69.1	70.0	70.7	71.5	72.2	72.0	72.3	71.0	69.3	104.8	
CONFID. CF 6	125	72.1	71.5	71.5	67.6	72.0	70.7	70.7	71.0	68.5	58.3	69.0	70.3	103.8	
LOC. SCHENECTADY	150	71.3	71.0	69.9	71.1	71.3	71.7	71.7	71.5	70.0	71.3	72.5	72.1	105.1	
DATE 4/27/78	200	77.3	79.8	78.8	78.9	79.0	77.7	76.2	77.5	76.2	78.0	74.0	76.3	113.9	
RUN 14/9	250	78.3	80.5	80.0	81.4	80.5	79.2	78.0	79.7	78.7	81.0	76.3	78.5	113.0	
TAPE	315	74.5	78.4	77.0	76.8	75.5	74.2	73.0	71.7	68.5	67.0	66.3	65.8	106.3	
RAK 22.6 MG (99000; NYM2)	400	79.3	77.5	77.0	75.8	75.0	74.2	73.0	71.5	68.7	68.3	66.5	64.5	106.1	
FAN 50, DFG F (243, DFG 4)	500	75.8	76.3	74.5	76.8	75.0	74.5	73.0	71.2	68.2	67.0	65.1	63.3	105.9	
TAFT 47, DFG F (281, DFG 4)	1000	78.5	77.5	77.8	77.5	75.5	74.2	73.0	71.2	67.9	68.0	66.6	64.8	105.8	
HAC 7.56 GM/H3 (1.0756 KG/M3)	1200	82.8	81.3	78.3	79.1	82.5	83.7	82.9	80.5	77.4	76.5	74.7	72.0	113.6	
HAC 7.56 GM/H3 (1.0756 KG/M3)	1600	82.3	81.9	79.3	80.1	82.2	82.7	80.7	80.5	75.2	73.2	73.5	69.5	112.7	
NFA 11722, RPM (1437, RAD/SEC)	2000	85.8	86.6	86.8	84.9	83.7	82.4	85.9	81.8	80.7	85.9	75.8	74.2	117.0	
NFA 11722, RPM (1437, RAD/SEC)	2500	85.5	84.1	83.5	86.1	91.2	93.9	96.7	93.0	89.5	87.9	84.1	83.7	125.0	
NFA 11722, RPM (1437, RAD/SEC)	3150	88.8	89.1	86.3	89.9	90.9	97.4	99.6	100.0	97.7	94.9	91.0	88.4	129.9	
NFA 11722, RPM (1437, RAD/SEC)	4000	97.5	98.5	96.2	98.3	99.1	108.1	111.6	109.7	106.1	102.0	102.8	97.6	143.1	
NFA 13843, RPM (1449, RAD/SEC)	5000	99.4	97.7	98.0	100.6	99.5	107.5	111.7	110.6	107.8	103.7	102.8	97.0	140.7	
NFA 13843, RPM (1449, RAD/SEC)	6300	95.0	94.2	97.5	98.6	97.6	103.7	107.7	105.9	100.9	98.2	94.8	90.7	136.1	
NFD 1A100, RPM (1436, RAD/SEC)	8000	95.7	97.1	98.9	100.6	100.2	104.9	106.9	104.0	100.2	96.7	93.3	91.4	135.8	
NO. OF BLADES 44 FAN TIP SPEED	12000	95.0	96.9	98.5	99.7	100.3	100.8	105.7	102.6	97.8	93.8	90.2	88.1	134.4	
184, FT/SEC	15100	94.6	95.5	97.4	99.0	99.3	100.5	102.9	100.8	95.6	91.0	86.7	84.0	132.9	
184, FT/SEC	20100	96.3	97.2	98.4	99.7	99.9	100.6	102.6	99.7	94.5	89.7	84.8	81.9	133.1	
	25200	93.1	94.0	95.3	97.0	96.5	97.5	99.5	97.2	91.8	85.6	81.9	78.4	130.7	
	31500	92.3	93.4	94.7	96.5	95.7	97.7	99.0	96.3	89.7	84.2	79.2	76.3	131.0	
	40000	91.2	91.1	92.2	93.8	93.5	94.7	96.2	93.6	87.2	81.6	75.3	73.2	129.7	
	50000	89.3	89.5	90.8	92.0	91.7	93.5	95.5	92.1	86.7	80.2	73.8	72.4	130.3	
	63000	86.6	87.2	88.5	89.5	90.1	91.7	93.8	90.5	85.0	77.1	72.6	73.4	131.2	
	70000	72.6	79.1	82.0	82.4	84.4	85.6	88.4	85.3	79.2	71.8	71.1	72.1	129.5	
OVERALL CALCULATE, 178.3 179.3 180.3 111.9 111.4 115.0 118.1 116.1 112.4 108.3 107.1 102.0 147.5															

Table 22

MODEL SOUND PRESSURE LEVELS (59° F, 70% Relative Humidity, Day)

Angles from Inlet in Degrees (and Radians)

RADIAL 17, FT. (5.2 M)	60 63	0.	10.	20.	30.	40.	50.	60.	70.	80.	90.	100.	110.	PWL		
		FREQ. (0.)	(0.17)	(0.35)	(0.52)	(0.70)	(0.87)	(1.05)	(1.22)	(1.40)	(1.57)	(1.75)	(1.92)			
		90	53	60	63	60	63	60	63	60	63	60	63			
GROUND PLANE, Z/D = 1.16																
CORRECTED SPEED = 69% (REPEAT)																
VEHICLE P-11	100	80.1	75.6	74.8	73.4	70.8	71.5	73.5	73.8	73.4	73.1	72.5	70.9	106.0		
CONFIG OF 2	125	79.6	77.3	75.3	73.6	73.8	72.8	71.8	72.5	71.7	70.3	70.8	70.1	106.0		
LOC SCHENECTADY	150	79.3	75.9	75.0	76.9	74.3	72.8	71.8	70.8	70.2	69.6	70.3	69.6	105.9		
DATE 4/27/76	200	83.8	81.4	80.5	79.4	77.3	77.8	75.5	75.6	72.9	72.3	70.8	71.3	109.5		
RUN 14/12	250	85.3	82.0	81.3	81.6	79.8	78.3	76.0	74.6	73.9	74.3	72.5	70.1	110.6		
TAPE	315	85.0	83.5	82.0	81.6	79.8	78.0	76.2	74.0	71.9	70.3	68.3	67.0	110.3		
BAR 29.6 HC (99989. N/M2)	400	85.5	81.8	80.5	80.3	78.6	77.3	74.7	73.5	71.9	70.3	67.1	65.1	109.2		
TAMB 50, DFG F (233. DFG X)	500	84.5	79.3	79.0	78.8	76.6	75.3	73.5	72.3	70.1	68.3	65.6	63.8	107.5		
TAET 47, DFG F	600	87.0	83.0	80.0	80.1	78.1	75.5	73.5	72.0	70.9	69.3	68.9	64.1	108.4		
TAET 47, DFG F (231. DFG X)	1000	87.0	75.5	75.5	74.8	74.7	73.0	70.5	70.3	67.5	65.6	64.4	106.0			
TAET 47, DFG F (231. DFG X)	1250	89.3	75.6	75.6	74.3	73.7	72.2	70.0	68.1	66.3	63.2	61.8	105.6			
TAET 7.56 GM/M3 (-0.0756 AG/M3)	1600	89.3	76.6	76.5	77.3	77.6	76.7	74.5	72.0	70.1	57.8	65.2	64.8	107.6		
TAET 7.56 GM/M3 (-0.0756 AG/M3)	2000	90.0	78.8	78.0	79.6	78.6	77.0	74.9	72.5	69.6	67.2	65.3	63.5	108.6		
NFA 11013. RPM (1153. RAD/SEC)	2500	89.5	80.3	79.8	81.4	80.0	79.7	78.2	75.3	72.1	69.5	66.6	66.0	110.6		
NFA 11013. RPM (1153. RAD/SEC)	3150	92.3	84.3	83.3	84.4	83.5	83.4	83.1	80.0	76.9	74.2	72.3	70.2	114.5		
NFK 11110. RPM (1153. RAD/SEC)	4000	92.0	86.5	86.2	86.6	86.9	86.8	84.3	81.2	77.1	75.6	72.3	72.9	116.6		
NFK 11110. RPM (1153. RAD/SEC)	5000	92.2	85.9	85.9	87.3	86.6	86.0	85.0	81.9	78.0	75.6	73.0	72.3	116.6		
NFK 11110. RPM (1153. RAD/SEC)	6300	93.0	88.0	89.3	90.0	90.4	91.2	89.7	86.7	82.1	79.8	77.3	76.0	121.0		
NFD 16170. RPM (1684. RAD/SEC)	8000	92.9	99.1	99.9	103.6	106.0	108.5	106.4	103.5	98.6	97.0	94.6	92.2	137.2		
NO. OF BLADES 44	12500	96.5	89.1	90.1	92.0	92.6	93.4	91.4	89.3	83.9	81.6	78.9	77.4	123.2		
FAN TIP SPEED 954. FT/SEC	15000	96.9	94.5	95.7	97.7	98.4	100.3	98.4	96.1	90.5	85.5	83.5	81.6	130.2		
	20000	95.5	88.7	90.7	92.2	92.2	91.9	90.9	87.5	81.2	76.8	73.1	71.2	123.3		
	25000	95.1	89.7	93.0	95.5	95.1	95.8	95.6	91.7	85.7	79.9	76.1	74.2	127.6		
	31500	93.1	88.2	90.5	93.2	93.2	92.9	92.5	88.3	81.8	75.0	71.2	68.8	125.8		
	40000	92.5	85.3	87.5	89.6	90.1	90.5	89.5	85.2	78.6	71.9	66.3	65.5	124.2		
	50000	91.3	83.5	86.1	88.6	88.1	88.7	87.7	84.2	76.4	69.5	65.0	64.2	124.5		
	63000	94.1	81.7	84.0	87.0	86.0	86.8	86.2	81.5	74.9	66.9	63.6	64.7	125.3		
	80000	94.9	75.6	78.0	81.2	79.2	80.1	79.5	74.3	68.6	61.4	61.3	65.1	123.4		

OVERALL CALCULATED 107.3 102.8 103.8 106.5 107.9 109.9 108.1 105.1 100.1 97.9 95.5 93.3 139.7

Table 23

MODEL SOUND PRESSURE LEVELS (59°F, 70% Relative Humidity, Day)

Angles from Inlet in Degrees (and Radians)

	20.	10.	20.	30.	40.	50.	60.	70.	80.	90.	100.	110.	PWL
FR=4.0 (3.0) (3.17) (3.35) (3.52) (0.70) (0.87) (1.00) (1.22) (1.40) (1.57) (1.75) (1.92)													
NON-POROUS CHAMBER (DOORS TO FILTER HOUSE OPEN) CORRECTED SPEED = 54%													
RADIAL 17° FPT	43	53	53	53	53	53	53	53	53	53	53	53	53
VEHICLE R-11	101	74.3	74.3	69.5	57.5	53.3	56.5	68.9	62.3	67.5	58.0	60.2	66.4
VEHICLE R-11	125	77.7	77.7	75.3	72.3	71.5	72.1	73.7	73.3	72.8	73.0	71.4	59.8
VEHICLE CF 8	151	71.3	71.3	57.1	57.0	59.1	55.5	57.7	72.3	71.1	56.2	71.2	72.1
VEHICLE CF 8	201	74.7	75.3	74.3	72.1	70.5	73.0	69.7	69.3	67.3	65.5	64.2	63.5
DATE 7/1/73	200	73.7	73.3	78.5	77.4	75.3	74.4	72.9	71.3	70.3	72.2	68.9	66.3
RUN 20/1	310	79.3	79.3	78.3	75.1	75.5	74.9	73.2	72.3	69.0	58.7	67.7	66.3
TAPE	434	75.3	75.3	74.8	73.3	71.5	71.4	67.2	67.0	65.0	54.7	61.7	60.0
BAR 24.5 43	503	74.0	72.3	71.0	70.3	69.3	69.4	67.3	66.5	65.0	53.7	51.7	59.3
(39895. 4/12)	533	75.7	74.3	74.1	72.3	71.5	71.4	63.4	67.0	65.3	54.7	63.2	61.3
TAPE 31. 0E3 F	633	73.9	73.3	73.0	72.7	71.1	70.3	63.1	66.0	64.3	54.4	63.2	61.2
(300. 0E3 4)	1030	73.9	71.0	70.3	71.7	69.0	68.3	65.5	64.3	52.0	50.4	59.3	58.4
WET 75. 0E3 F	1200	71.1	72.1	72.3	71.5	71.5	59.1	56.9	64.8	62.0	50.4	59.1	57.5
(297. 0E3 5)	1300	72.7	73.1	72.9	71.8	70.6	70.1	68.4	55.6	63.3	51.7	58.6	57.5
FACT 19.83 54/43	2000	74.7	75.3	75.1	75.1	73.3	73.1	71.4	68.3	65.1	53.9	61.2	60.7
(-01983. 53/43)	2300	73.0	73.0	77.4	75.8	75.5	75.6	74.1	70.8	68.1	56.1	53.4	62.4
WFA 8877. 2P4	3100	81.3	80.3	79.1	79.1	78.7	79.0	77.5	74.3	71.3	58.3	56.3	65.4
(929. RAD/SEC)	4000	81.9	82.5	81.7	82.3	81.7	81.9	81.5	78.4	74.5	72.5	69.7	68.0
WFA 8605. 2P4	5100	83.8	84.9	85.2	85.7	84.1	83.4	81.4	78.1	73.9	71.9	70.2	69.2
(913. RAD/SEC)	5100	94.2	94.4	95.6	95.7	95.1	95.3	94.3	92.4	85.2	85.1	81.9	81.9
WFA 16100. 2P4	9000	84.7	85.3	87.3	87.1	85.9	87.0	84.2	81.7	76.7	75.0	72.3	71.1
(1686. RAD/SEC)	10000	84.5	85.7	85.0	87.3	87.4	87.1	85.4	81.9	76.2	73.3	71.5	70.2
WFA 3F 3LAUGS 44 12500	95.2	95.4	95.3	95.4	92.5	92.2	92.9	90.1	84.9	80.7	78.3	77.1	124.6
WFA TIP SPEED	15000	86.1	85.1	87.8	87.3	86.7	87.0	85.2	83.0	78.5	72.0	70.5	69.3
WFA TIP SPEED	20000	93.3	93.4	87.9	91.3	91.0	91.5	90.0	87.4	80.0	75.0	72.0	70.3
WFA TIP SPEED	25000	90.2	91.2	90.3	90.1	85.2	87.5	87.5	83.1	73.5	59.0	60.7	64.5
WFA TIP SPEED	31000	75.3	75.3	81.6	83.3	83.3	53.2	82.3	78.7	70.8	55.0	61.7	59.9
WFA TIP SPEED	40000	72.9	74.3	77.3	77.3	79.1	79.1	78.1	74.4	55.7	51.0	58.2	58.1
WFA TIP SPEED	50000	59.8	71.1	74.5	75.6	75.9	75.9	74.5	70.8	62.6	59.3	57.8	58.4
WFA TIP SPEED	53000	57.2	67.3	70.5	71.3	71.9	72.2	70.2	66.1	59.9	59.1	58.1	59.0
WFA TIP SPEED	60000	51.6	61.4	54.4	54.0	54.1	54.3	53.2	59.9	56.1	54.6	54.6	50.9
WFA TIP SPEED	70000	49.4	49.5	49.5	49.3	49.3	49.3	49.3	49.3	49.3	49.3	49.3	49.3
WFA TIP SPEED	80000	49.4	49.5	49.5	49.3	49.3	49.3	49.3	49.3	49.3	49.3	49.3	49.3
WFA TIP SPEED	90000	49.4	49.5	49.5	49.3	49.3	49.3	49.3	49.3	49.3	49.3	49.3	49.3
WFA TIP SPEED	100000	49.4	49.5	49.5	49.3	49.3	49.3	49.3	49.3	49.3	49.3	49.3	49.3
WFA TIP SPEED	110000	49.4	49.5	49.5	49.3	49.3	49.3	49.3	49.3	49.3	49.3	49.3	49.3
WFA TIP SPEED	120000	49.4	49.5	49.5	49.3	49.3	49.3	49.3	49.3	49.3	49.3	49.3	49.3
WFA TIP SPEED	130000	49.4	49.5	49.5	49.3	49.3	49.3	49.3	49.3	49.3	49.3	49.3	49.3
WFA TIP SPEED	140000	49.4	49.5	49.5	49.3	49.3	49.3	49.3	49.3	49.3	49.3	49.3	49.3
WFA TIP SPEED	150000	49.4	49.5	49.5	49.3	49.3	49.3	49.3	49.3	49.3	49.3	49.3	49.3
WFA TIP SPEED	160000	49.4	49.5	49.5	49.3	49.3	49.3	49.3	49.3	49.3	49.3	49.3	49.3
WFA TIP SPEED	170000	49.4	49.5	49.5	49.3	49.3	49.3	49.3	49.3	49.3	49.3	49.3	49.3
WFA TIP SPEED	180000	49.4	49.5	49.5	49.3	49.3	49.3	49.3	49.3	49.3	49.3	49.3	49.3
WFA TIP SPEED	190000	49.4	49.5	49.5	49.3	49.3	49.3	49.3	49.3	49.3	49.3	49.3	49.3
WFA TIP SPEED	200000	49.4	49.5	49.5	49.3	49.3	49.3	49.3	49.3	49.3	49.3	49.3	49.3
WFA TIP SPEED	210000	49.4	49.5	49.5	49.3	49.3	49.3	49.3	49.3	49.3	49.3	49.3	49.3
WFA TIP SPEED	220000	49.4	49.5	49.5	49.3	49.3	49.3	49.3	49.3	49.3	49.3	49.3	49.3
WFA TIP SPEED	230000	49.4	49.5	49.5	49.3	49.3	49.3	49.3	49.3	49.3	49.3	49.3	49.3
WFA TIP SPEED	240000	49.4	49.5	49.5	49.3	49.3	49.3	49.3	49.3	49.3	49.3	49.3	49.3
WFA TIP SPEED	250000	49.4	49.5	49.5	49.3	49.3	49.3	49.3	49.3	49.3	49.3	49.3	49.3
WFA TIP SPEED	260000	49.4	49.5	49.5	49.3	49.3	49.3	49.3	49.3	49.3	49.3	49.3	49.3
WFA TIP SPEED	270000	49.4	49.5	49.5	49.3	49.3	49.3	49.3	49.3	49.3	49.3	49.3	49.3
WFA TIP SPEED	280000	49.4	49.5	49.5	49.3	49.3	49.3	49.3	49.3	49.3	49.3	49.3	49.3
WFA TIP SPEED	290000	49.4	49.5	49.5	49.3	49.3	49.3	49.3	49.3	49.3	49.3	49.3	49.3
WFA TIP SPEED	300000	49.4	49.5	49.5	49.3	49.3	49.3	49.3	49.3	49.3	49.3	49.3	49.3
WFA TIP SPEED	310000	49.4	49.5	49.5	49.3	49.3	49.3	49.3	49.3	49.3	49.3	49.3	49.3
WFA TIP SPEED	320000	49.4	49.5	49.5	49.3	49.3	49.3	49.3	49.3	49.3	49.3	49.3	49.3
WFA TIP SPEED	330000	49.4	49.5	49.5	49.3	49.3	49.3	49.3	49.3	49.3	49.3	49.3	49.3
WFA TIP SPEED	340000	49.4	49.5	49.5	49.3	49.3	49.3	49.3	49.3	49.3	49.3	49.3	49.3
WFA TIP SPEED	350000	49.4	49.5	49.5	49.3	49.3	49.3	49.3	49.3	49.3	49.3	49.3	49.3
WFA TIP SPEED	360000	49.4	49.5	49.5	49.3	49.3	49.3	49.3	49.3	49.3	49.3	49.3	49.3
WFA TIP SPEED	370000	49.4	49.5	49.5	49.3	49.3	49.3	49.3	49.3	49.3	49.3	49.3	49.3
WFA TIP SPEED	380000	49.4	49.5	49.5	49.3	49.3	49.3	49.3	49.3	49.3	49.3	49.3	49.3
WFA TIP SPEED	390000	49.4	49.5	49.5	49.3	49.3	49.3	49.3	49.3	49.3	49.3	49.3	49.3
WFA TIP SPEED	400000	49.4	49.5	49.5	49.3	49.3	49.3	49.3	49.3	49.3	49.3	49.3	49.3
WFA TIP SPEED	410000	49.4	49.5	49.5	49.3	49.3	49.3	49.3	49.3	49.3	49.3	49.3	49.3
WFA TIP SPEED	420000	49.4	49.5	49.5	49.3	49.3	49.3	49.3	49.3	49.3	49.3	49.3	49.3
WFA TIP SPEED	430000	49.4	49.5	49.5	49.3	49.3	49.3	49.3	49.3	49.3	49.3	49.3	49.3
WFA TIP SPEED	440000	49.4	49.5	49.5	49.3	49.3	49.3	49.3	49.3	49.3	49.3	49.3	49.3
WFA TIP SPEED	450000	49.4	49.5	49.5	49.3	49.3	49.3	49.3	49.3	49.3	49.3	49.3	49.3
WFA TIP SPEED	460000	49.4	49.5	49.5	49.3	49.3	49.3	49.3	49.3	49.3	49.3	49.3	49.3
WFA TIP SPEED	470000	49.4	49.5	49.5	49.3	49.3	49.3	49.3	49.3	49.3	49.3	49.3	49.3
WFA TIP SPEED	480000	49.4	49.5	49.5	49.3	49.3	49.3	49.3	49.3	49.3	49.3	49.3	49.3
WFA TIP SPEED	490000	49.4	49.5	49.5	49.3	49.3	49.3	49.3	49.3	49.3	49.3	49.3	49.3
WFA TIP SPEED	500000	49.4	49.5	49.5	49.3	49.3	49.3	49.3	49.3	49.3	49.3	49.3	49.3
WFA TIP SPEED	510000	49.4	49.5	49.5	49.3	49.3	49.3	49.3	49.3	49.3	49.3	49.3	49.3
WFA TIP SPEED	520000	49.4	49.5										

Table 24

MODEL SOUND PRESSURE LEVELS (59°F, 70% Relative Humidity, Day)

Angles from Inlet in Degrees (and Radians)

		10°	20°	30°	40°	50°	60°	70°	80°	90°	100°	110°				
		(0.17)	(0.35)	(0.52)	(0.70)	(0.87)	(1.05)	(1.22)	(1.40)	(1.57)	(1.75)	(1.92)				
NON-POROUS CHAMBER (DOORS TO FILTER HOUSE OPEN) CORRECTED SPEED = 69%																
- PNL																
RADIATOR	17.5°	90	81.3	78.3	72.3	59.9	57.6	55.5	71.3	71.5	71.2	70.1	68.6	66.1	104.4	
VEHICLE	45.1	130	31.3	79.3	75.3	73.1	71.3	72.3	73.5	73.5	72.7	73.1	70.1	69.1	105.6	
COV-F16	35.6	125	31.3	79.3	75.3	73.1	71.1	71.1	69.3	58.5	69.3	55.2	57.9	68.1	67.6	103.0
COV-SCHENECTADY	230	73.3	79.3	75.3	73.1	73.6	74.0	72.8	72.3	69.4	70.0	71.0	71.0	71.0	106.7	
DATE 7/1/76	230	31.3	81.3	80.3	79.9	77.9	77.6	75.5	75.2	73.5	71.9	71.6	70.3	68.1	109.2	
RUN 225/2	310	32.3	52.3	41.3	31.9	28.6	27.5	26.0	24.5	22.2	20.6	19.1	17.6	16.6	109.9	
TAPE	400	31.0	30.0	25.0	20.3	15.1	10.1	7.5	4.0	2.0	0.0	0.0	0.0	0.0	107.6	
BAR 29.4 13	577	74.3	77.1	75.1	75.1	74.5	74.9	72.7	71.3	68.9	68.3	65.3	63.8	63.8	105.8	
(295.0 14.2)	550	79.3	79.3	75.3	73.3	76.1	75.1	73.0	72.3	70.1	59.1	67.1	65.3	65.3	107.4	
TAPE 41.0 35.2	430	72.3	79.3	79.3	78.1	74.8	75.2	73.5	71.5	59.6	58.3	67.4	65.6	65.6	107.3	
(300. 75.4)	330	74.2	75.5	75.3	77.3	75.9	75.5	72.7	71.0	69.1	65.3	53.9	63.3	63.3	106.1	
TAPE 75.0 35.2	1250	74.5	75.6	75.5	75.6	74.3	73.2	71.5	69.3	60.9	54.8	62.4	60.3	60.3	104.8	
(297. 75.0 4)	1600	75.1	76.3	76.3	76.1	74.1	74.0	72.5	69.6	66.9	64.8	65.9	61.3	61.3	105.2	
TAPE 19.8 34.4 3	2300	74.3	79.3	77.6	77.9	75.5	75.7	74.7	71.8	68.4	66.3	64.6	63.5	63.5	107.3	
(-0.01985 42/43)	2300	73.5	80.3	79.6	81.5	79.3	78.2	76.9	74.1	69.9	58.7	60.5	64.3	64.3	109.6	
VFA 11345. 2P4	3100	32.0	32.1	81.0	82.6	81.0	82.2	81.2	78.3	70.1	72.2	68.3	68.7	68.7	112.6	
(11381. 240/350)	4000	33.7	84.7	84.7	84.6	84.2	84.8	84.3	81.5	77.8	76.1	71.8	71.4	71.4	115.6	
VFC 11113. 3P4	5700	33.4	85.7	85.5	85.5	85.6	86.1	85.2	82.9	79.0	76.0	73.0	72.1	72.1	116.8	
(11104. 247/352)	5600	93.2	65.9	67.7	89.3	88.9	88.9	87.9	85.9	61.2	78.1	75.3	74.5	74.5	119.5	
VFD 11100. 2P4	9300	94.5	97.1	95.8	102.5	104.4	105.9	105.1	105.7	101.1	95.4	94.5	91.1	91.1	137.0	
(1586. 240/350) 10000	87.8	98.3	99.0	92.3	93.2	94.8	94.2	93.2	87.8	43.9	51.5	79.0	125.2			
VC. DS. 3. BLUES 44	12000	37.3	83.4	89.3	80.7	91.8	91.1	90.2	88.4	53.2	78.0	75.7	73.7	122.0		
TAPE 52.5 20	15000	97.0	95.4	94.6	95.6	97.5	98.3	97.8	97.0	91.1	86.9	82.6	80.6	129.7		
95.4 2T/350	27000	35.9	89.5	89.5	91.4	91.1	91.1	89.6	88.2	82.3	77.4	72.5	70.7	122.7		
	23000	53.6	87.3	91.7	94.4	93.5	94.1	93.0	91.4	85.9	78.0	74.9	72.1	126.3		
	31500	82.7	84.7	87.1	91.3	90.5	89.9	89.1	85.5	80.2	72.9	68.1	65.2	122.9		
	40000	79.0	79.3	82.7	85.3	85.5	85.3	84.7	82.1	75.3	58.1	62.5	62.0	119.9		
	53000	76.1	75.2	79.4	81.6	81.4	82.4	81.8	79.5	72.0	54.2	60.1	63.0	118.4		
	53000	72.0	72.8	73.5	77.3	78.1	79.4	78.3	75.6	65.8	62.0	60.0	64.0	117.5		
	80000	53.2	58.2	70.1	71.0	70.6	71.5	71.5	59.2	62.7	58.5	56.7	56.4	115.0		
		0.744-1.04-0.74-0.77-1.01-1.5	1.01-1.3	1.02-1.5	1.03-1.3	1.05-1.4	1.06-1.3	1.07-1.5	1.06-1.9	1.02-0.0	0.7-0.0	0.9-0.0	0.2-0.0	1.38-0.0		

Table 25
MODEL SOUND PRESSURE LEVELS (59° F, 70% Relative Humidity, Day)

Angles from Inlet in Degrees (and Radians)														
VEHICLE	FREQ. (C.)	0.	10.	20.	30.	40.	50.	60.	70.	80.	90.	100.	110.	
		0.17	0.35	0.52	0.70	0.87	1.05	1.22	1.40	1.57	1.75	1.92	PWL	
NON-POROUS CHAMBER (DOORS TO FLOOR HOUSE OPEN) CORRECTED SPEED = 86%														
RADIAL 12. FT.														
RADIAL 12. FT.	0.1	52.0	83.5	72.0	67.5	62.8	71.3	72.5	72.5	71.5	71.0	71.0	69.0	106.3
VEHICLE R-11	125	81.5	91.3	73.5	69.5	77.0	71.0	72.5	71.5	71.3	72.3	70.0	69.0	105.9
204-13 35.5	150	79.5	76.3	70.5	68.1	71.8	72.5	72.5	72.8	69.5	70.6	71.0	70.3	105.5
204-14-15 35.5	200	73.5	75.5	74.8	74.5	74.5	74.0	73.7	75.2	74.0	73.0	65.0	71.1	107.6
204-15 77.1/75	200	81.0	79.3	81.5	81.0	81.7	79.5	81.0	83.2	84.2	83.8	76.0	60.0	115.5
204-16 25/3	510	79.0	79.0	77.5	75.5	75.2	74.2	73.5	72.2	69.0	68.0	68.0	68.0	106.6
204-17 44.5	400	79.0	79.0	75.5	75.5	75.2	75.0	74.5	73.0	68.5	68.5	68.5	68.5	106.7
204-18 29.5 43 (99896. 47/12)	300	77.0	75.5	75.5	74.5	74.5	74.3	73.7	73.2	72.2	68.7	70.0	68.6	105.7
204-19 63.0 2	630	78.5	77.5	77.0	76.5	75.5	75.5	74.2	73.0	70.2	70.3	67.4	65.3	107.1
204-20 52.0 2	500	77.5	77.5	76.0	77.1	77.3	77.0	74.7	73.2	71.0	72.0	68.0	65.5	107.9
204-21 52.0 2 (301. 52.0 2)	1500	73.5	77.5	78.0	79.0	80.2	80.0	78.0	76.2	75.2	72.0	69.4	67.0	110.6
204-22 52.0 2	1200	82.0	79.5	81.0	82.0	82.7	84.4	84.2	81.5	81.5	78.0	72.4	72.0	115.0
204-23 52.0 2 (29.5 52.0 2)	1500	81.1	79.5	80.6	82.5	83.0	83.7	82.5	80.5	78.5	73.5	74.2	72.3	114.0
204-24 18.53 34/13	2000	54.3	84.3	83.3	53.9	84.5	85.0	88.2	83.8	82.5	77.7	77.5	76.2	117.6
204-25 18.53 43/13 (201853. 43/13)	2500	82.8	82.5	83.1	84.1	84.7	87.7	89.2	80.0	68.5	84.7	79.5	80.5	120.4
204-26 14157. 2P4	3150	84.0	85.5	85.8	85.9	88.0	95.1	97.9	100.0	95.2	94.9	89.8	88.2	129.4
204-27 1432. 2AD/SEC	4000	93.0	93.7	94.9	93.3	97.6	104.1	109.3	109.4	105.4	103.0	101.0	100.0	139.0
204-28 14453. 2P4	5000	94.9	94.7	98.1	98.8	101.8	105.2	111.2	111.4	108.6	104.2	101.5	99.5	140.9
204-29 1453. 2AD/SEC	5100	94.0	92.4	95.0	96.2	98.5	102.1	105.8	106.3	102.9	99.7	94.3	92.5	135.9
204-30 14177. 2P4	6000	93.5	95.1	95.8	97.5	98.6	100.3	103.5	104.4	95.6	95.6	92.7	88.1	134.0
204-31 1585. 44/3/SEC	10000	103.3	103.9	107.2	108.1	108.1	108.7	109.0	108.6	103.4	98.9	95.0	93.0	140.2
204-32 14157. 2P4	12500	94.1	95.4	97.3	96.5	99.3	110.3	113.0	102.3	97.8	94.0	89.7	88.0	133.4
204-33 14177. 2P4	15000	92.2	93.7	90.8	97.0	98.7	100.1	101.0	101.0	96.7	91.0	88.0	84.1	132.3
204-34 14177. 2P4/SEC	12250	93.5	95.7	96.9	93.4	99.8	99.4	99.8	98.2	93.7	99.2	83.0	80.0	131.6
204-35 99.4	99.4	99.7	92.5	94.0	94.7	96.0	95.8	92.1	92.0	95.4	79.0	77.4	128.8	
204-36 99.1	89.1	91.0	92.4	92.6	94.1	93.7	93.0	98.4	91.0	74.7	74.0	127.4		
204-37 93.9	94.9	94.8	87.2	88.0	88.7	89.8	90.5	99.0	84.8	77.0	70.2	72.1	124.9	
204-38 93.0	89.0	82.2	84.2	84.9	85.6	85.8	87.8	87.0	91.0	73.0	67.0	72.0	123.9	
204-39 75.9	77.4	80.2	80.9	82.8	84.2	84.3	83.4	79.9	78.0	67.6	73.0	123.5		
204-40 70.0	70.7	74.4	73.3	78.5	83.0	86.0	79.1	73.0	57.0	68.0	73.0	123.4		
OVERALL CAL-CD-4142 105.0 105.0 104.0 110.7 111.2 113.3 115.2 115.3 112.7 108.0 105.5 104.0 146.6														

Table 26

MODEL SOUND PRESSURE LEVELS (59°F, 70% Relative Humidity, Day)

Angles from Inlet in Degrees (and Radians)

		0°	10°	20°	30°	40°	50°	60°	70°	80°	90°	100°	110°	PRL	
PREL = (1.0, 1.0, 1.0, 1.0, 1.0, 1.0, 1.0, 1.0, 1.0, 1.0, 1.0, 1.0, 1.0, 1.0, 1.0)															
NON-POROUS CHAMBER (DOORS TO FILTER HOUSE OPEN) CORRECTED SPEED = 90%															
2401A1 17. ST.		80													
VEHICLE R-11	100	85.1	84.5	72.3	65.1	69.3	71.3	71.5	72.0	70.0	71.1	70.5	69.6	106.3	
BOVING SF 5	120	93.0	81.3	72.8	67.1	69.5	70.3	71.0	72.0	71.8	72.3	70.3	69.0	105.9	
LOC SCHEVESTADY	150	91.3	79.3	73.8	65.9	71.5	72.3	72.5	73.3	70.5	71.3	72.3	71.3	106.0	
DATE 7/1/76	200	91.1	79.3	71.8	69.9	71.2	71.3	71.5	70.7	67.0	67.0	66.3	66.1	104.1	
REV 26/4	250	94.0	83.5	78.3	79.4	79.2	78.7	76.5	77.2	79.5	80.8	78.3	77.0	112.6	
TAP2	310	73.0	75.1	74.3	73.1	73.0	72.7	71.7	70.2	67.0	67.0	66.8	65.3	104.7	
BAR 59.4 43	400	77.5	75.0	73.5	73.1	73.2	73.2	72.2	72.0	66.5	66.0	65.0	65.0	104.7	
(39985, 4/12)	500	77.1	74.8	74.7	73.8	74.0	73.9	72.7	70.5	59.0	68.0	64.3	66.3	104.9	
TAP3 41° 02.0	550	83.0	79.8	81.5	77.5	77.5	74.2	75.0	71.5	70.0	68.0	65.9	67.0	105.5	
(300, DEG 4)	600	77.0	75.5	76.5	76.5	76.3	75.3	74.7	74.0	74.0	69.5	69.2	66.6	67.3	106.7
NET 74, DEG 4	1000	75.0	79.5	74.0	79.5	82.2	81.4	80.5	80.0	78.4	70.5	73.6	74.5	112.5	
(295, 72.5)	1200	89.5	80.3	79.0	80.8	83.2	84.7	81.5	85.3	83.5	75.7	79.4	77.0	116.1	
(295, 72.5)	1500	85.5	81.8	84.6	84.4	82.3	86.0	88.2	86.8	85.0	79.5	81.2	79.3	118.3	
HACTRA 93 3/4/73	2000	84.5	93.5	93.8	90.5	93.2	100.7	103.5	102.3	99.0	96.0	94.8	92.2	132.7	
(-01383, 4/4/73)	2500	85.0	85.3	86.1	91.9	94.2	98.7	101.9	101.3	98.0	96.4	91.6	91.0	131.5	
NFA 14795, R-1	3150	84.0	87.1	87.0	92.4	90.2	99.1	102.9	102.2	98.5	93.9	91.6	90.4	131.9	
(1542, 240/SEC)	4000	92.0	92.7	93.2	93.8	93.6	104.3	106.6	106.7	103.4	99.0	97.0	95.0	136.0	
NFA 14491, R-1	5000	94.4	95.4	97.4	101.3	102.5	107.0	109.5	108.9	105.1	100.5	99.3	96.5	139.0	
(1517, 240/SEC)	5300	93.2	94.4	96.0	99.0	99.0	100.0	103.1	102.4	103.8	100.4	96.4	92.8	91.7	134.8
NFD 14100, R-1	5700	92.9	94.5	94.5	97.3	97.8	100.0	100.7	100.5	102.1	97.9	93.1	90.5	86.4	132.0
(1535, 240/SEC)	10000	105.1	103.0	105.4	107.1	107.1	107.5	109.2	109.1	105.1	100.9	97.5	93.2	140.2	
NO. 25 3-AUG-44 12000	12000	99.0	99.5	100.8	102.0	101.8	102.5	103.7	104.3	99.5	95.0	91.7	87.9	135.2	
F-44 112 3-SEC	15000	93.0	94.1	95.8	93.1	99.9	100.4	101.0	100.9	96.7	91.1	86.4	83.8	132.4	
1281. F17SEC	20000	94.2	95.4	95.6	97.9	98.6	99.5	99.8	99.7	94.7	99.4	84.0	80.0	131.9	
	22200	92.9	91.2	93.8	93.0	93.5	96.7	97.8	96.9	92.5	85.0	80.0	77.4	129.8	
	31500	94.3	89.5	90.7	92.9	93.8	94.1	94.4	93.7	89.1	81.7	76.1	73.2	127.8	
	40000	83.3	84.7	85.6	88.2	89.1	90.3	91.3	91.0	85.8	77.7	70.9	71.0	125.7	
	50000	41.5	92.1	83.6	85.3	85.8	87.7	88.2	88.1	83.0	75.5	68.5	72.1	124.6	
	53000	75.7	78.0	79.0	80.8	82.7	84.5	85.0	85.0	80.1	71.0	67.2	73.5	124.1	
	80300	70.5	71.5	72.7	73.1	78.6	80.2	81.4	80.4	74.6	68.0	68.0	72.7	123.8	

$$S_v = 44.11 \cdot 0.620 \cdot 4.70 \cdot 109.7 \cdot 108.5 \cdot 109.3 \cdot 111.0 \cdot 111.3 \cdot 113.8 \cdot 115.8 \cdot 115.5 \cdot 111.6 \cdot 107.4 \cdot 104.9 \cdot 102.4 \cdot 146.2$$

Table 27
MODEL SOUND PRESSURE LEVELS (59° F, 70% Relative Humidity, Day)
 Angles from Inlet in Degrees (and Radians)

Table 28

MODEL SOUND PRESSURE LEVELS (59°F, 70% Relative Humidity, Day)

Angles from Inlet in Degrees (and Radians)

	1°	10°	20°	30°	40°	50°	60°	70°	80°	90°	100°	110°	PML	
FREQ. (Hz)	(0.17)	(0.35)	(0.52)	(0.70)	(0.87)	(1.05)	(1.22)	(1.40)	(1.57)	(1.75)	(1.92)			
NON-POROUS CHAMBER (DOORS TO FILTER HOUSE OPEN) CORRECTED SPEED = 86% (REPEAT)														
°D °S														
RADIAL 17. FT. E. 5. 11	120	55.3	54.3	71.5	66.9	69.5	70.1	72.3	73.0	71.8	71.0	74.9	69.8	106.7
VE410-E 3-11	125	53.5	51.1	73.4	59.3	43.8	70.3	72.3	71.8	73.1	70.3	69.1	106.0	
COV-F13 OF 6 -03 SCHEMATIC	150	51.1	73.3	70.0	53.1	70.3	71.3	71.0	72.0	69.8	70.3	71.3	70.4	105.1
DATE 7/1/75	200	31.8	79.3	74.4	73.4	74.2	94.2	72.0	74.7	75.0	73.0	67.3	70.0	118.1
RUN 25/5	220	57.3	79.3	81.5	81.5	82.5	79.0	79.2	83.5	84.0	83.0	74.0	79.0	115.4
TAPE	400	72.1	79.5	75.8	75.1	75.0	74.2	73.5	72.7	58.5	58.0	66.3	65.3	106.4
342 29.5 42 (09896, 1112)	500	77.3	75.3	75.0	75.1	74.3	74.3	73.2	71.5	63.2	56.0	65.0	64.5	105.5
TA43 80. OF 3 F (300, OF 3 1)	800	77.3	77.0	77.0	77.3	77.0	76.7	75.5	73.2	71.2	71.4	69.1	66.8	107.8
TWE 74. OF 3 F (246, OF 3 1)	1000	77.5	77.3	78.0	79.3	80.5	81.2	78.2	76.7	75.9	71.4	69.9	68.0	110.9
440/19.13 RPM (.01913 RPM)	1200	51.3	80.1	80.8	82.3	83.0	85.2	84.5	82.0	82.0	78.0	73.0	72.0	115.4
440/19.13 RPM (.01913 RPM)	1500	51.3	79.5	80.2	82.2	83.3	83.2	82.5	80.0	78.2	74.0	71.0	71.0	113.8
440/19.13 RPM (.01913 RPM)	2000	54.1	84.1	82.8	83.9	83.2	85.7	87.0	84.0	81.7	77.4	77.0	75.0	116.7
440/19.13 RPM (.01913 RPM)	2500	53.3	83.1	83.1	84.4	85.5	89.2	90.9	91.8	90.0	87.2	81.1	82.0	122.0
NFA 14135. RPM (1480, 840/SEC)	3100	53.4	87.1	85.8	86.9	89.2	96.9	99.4	101.0	99.2	76.1	90.6	89.6	130.6
NFA 13850. RPM (1451, 840/SEC)	4000	93.2	94.3	94.7	98.3	97.3	105.9	110.3	110.2	105.9	+03.0	101.0	100.0	139.7
NFA 13850. RPM (1451, 840/SEC)	5000	95.3	94.9	98.9	99.5	101.0	105.5	112.0	111.8	108.6	103.0	102.0	100.0	141.3
NFA 13850. RPM (1451, 840/SEC)	5300	94.7	93.2	94.7	95.5	98.3	102.4	107.2	107.3	102.0	100.2	94.0	93.4	136.7
NFO 16100. RPM (1685, 840/SEC)	10000	93.3	94.5	95.5	97.3	98.3	99.5	103.8	104.6	99.9	96.8	93.0	89.6	134.0
40. OF 3-AUFS 44	12000	94.3	95.5	97.3	98.7	99.0	100.5	102.2	103.1	99.3	94.5	90.4	87.4	133.4
FAV TIP SPEED 1224. F 1/3 SEC	15000	92.7	94.1	96.0	97.6	98.6	100.5	101.3	100.9	95.9	91.0	87.0	84.0	132.4
FAV TIP SPEED 1224. F 1/3 SEC	20000	94.2	95.7	96.5	98.6	99.8	100.0	99.8	99.1	93.9	88.9	84.0	80.0	131.0
FAV TIP SPEED 1224. F 1/3 SEC	25000	89.9	92.4	92.5	94.5	94.7	95.2	97.2	95.3	92.0	85.6	80.0	72.0	129.0
	31000	89.3	89.3	90.9	92.5	92.8	94.1	94.4	93.4	88.3	81.9	76.1	74.4	127.6
	40000	84.3	84.3	87.0	89.4	89.3	91.2	90.7	89.9	85.2	77.4	71.1	72.2	125.0
	50000	81.1	81.7	83.7	85.0	85.9	87.5	88.4	87.3	81.0	74.7	67.0	71.0	124.3
	63000	77.1	77.9	83.2	83.4	82.8	85.2	84.8	84.4	78.9	71.3	62.1	73.4	124.0
	50000	71.4	73.1	74.8	72.9	73.7	80.1	80.9	80.0	73.4	67.0	68.0	71.0	123.4
Overall Calculated	105.7	108.1	109.0	111.7	111.0	113.6	115.8	116.7	112.7	109.0	106.2	104.0	147.0	

Table 29
MODEL SOUND PRESSURE LEVELS (59°F, 70% Relative Humidity, Day)

Angles from Inlet in Degrees (and Radians)													
		0°	10°	20°	30°	40°	50°	60°	70°	80°	90°	100°	110°
RADIAL 17' FT		0.00	1.73	3.47	5.20	6.93	8.66	10.39	12.12	13.85	15.58	17.31	19.04
VEHICLE R-11		120	72.3	78.5	75.5	73.1	71.6	73.3	73.3	73.0	72.9	74.1	71.3
COVE 6		150	75.3	75.3	71.3	71.1	71.3	72.3	68.9	69.0	67.9	68.1	67.8
LOC SIGHTING STATION		200	77.3	78.5	76.5	73.4	74.3	77.5	72.8	72.5	69.4	71.1	71.8
DATE 7/1/75		250	81.3	81.1	80.8	80.1	77.8	76.5	75.2	73.3	72.2	71.0	70.5
RUN 26/7		310	82.3	82.0	81.3	81.1	78.8	77.5	76.2	74.5	71.4	70.0	69.3
TAPE		410	81.1	80.3	79.3	79.1	76.8	76.1	74.2	72.8	70.2	68.6	65.6
BAR 22.5 13		500	79.0	77.0	75.0	75.3	74.3	73.8	72.7	71.0	69.1	67.3	65.3
(33895 7/1/75)		530	80.0	79.5	79.0	78.3	74.3	76.3	73.7	72.3	70.1	68.8	67.4
1413 80.0 0 0		800	79.5	79.3	78.5	78.6	77.1	76.2	74.0	72.3	69.4	69.4	67.6
(3300 DEG 5)		1000	77.8	75.8	76.0	77.0	75.1	77.7	73.5	70.3	68.6	66.8	64.1
TAP 76.0 0 0		1200	75.3	75.3	75.5	75.3	74.6	78.0	72.2	69.6	65.9	65.0	63.7
(1295 373 5)		1500	77.8	76.3	76.6	76.1	74.8	75.0	72.5	70.1	69.7	65.3	62.0
FACT 19.13 54/43		2000	75.3	79.3	78.6	78.4	77.6	80.2	75.0	72.1	68.4	66.3	63.0
(111913 53/43)		2500	80.1	80.5	79.8	80.9	79.3	81.3	76.9	73.8	70.9	68.2	67.3
VFA 11.325. 234		3100	81.8	82.5	82.3	82.5	81.5	82.7	81.2	79.0	75.1	72.2	68.0
(1135. 740/SEC)		4000	83.7	84.5	84.2	84.6	84.2	84.3	83.8	81.2	77.1	75.6	72.1
VFK 11132. 234		5000	84.7	85.7	85.9	86.0	85.8	85.5	85.5	82.4	79.0	76.0	73.5
(1162. 740/SEC)		5300	85.0	87.2	85.0	89.0	89.1	89.2	89.4	85.6	81.0	77.2	75.3
VFD 15130. 234		9000	95.3	97.1	99.3	102.0	103.4	105.5	105.6	104.7	100.8	95.4	94.2
(1685. RAD/SEC)		10000	83.1	89.3	90.4	92.1	92.6	94.3	94.0	92.4	97.5	92.9	81.0
VD. OF 3. AUES 44		12500	87.3	88.4	90.0	91.5	90.3	90.1	90.0	87.9	82.5	78.1	75.4
-AV TIP 33250		15000	94.0	96.1	94.8	95.3	97.2	98.4	97.8	96.5	90.6	86.6	82.4
991. 21/SEC		20000	97.4	89.9	89.4	91.4	97.9	91.3	89.5	87.7	81.8	76.9	73.0
		25000	84.3	87.7	91.5	94.5	93.9	94.2	93.5	90.4	86.2	79.1	74.3
		31000	94.0	84.5	87.9	90.1	90.1	90.8	89.4	86.2	80.5	73.2	68.4
		40000	74.8	83.4	83.5	85.1	85.4	87.3	85.2	82.4	75.4	67.9	62.8
		50000	75.7	77.3	79.7	81.5	81.5	84.4	81.9	78.8	72.5	64.0	60.7
		60000	72.6	73.1	76.2	77.4	78.2	81.2	78.6	75.4	69.1	62.1	60.0
		80000	58.0	58.1	71.0	70.9	70.7	73.5	71.2	69.3	52.5	58.9	59.1
OVERALL CALCULATED 101.9 101.8 102.8 105.0 105.7 109.1 107.9 106.0 101.8 96.6 95.1 92.1 138.6													

Table 30

MODEL SOUND PRESSURE LEVELS (59°F, 70% Relative Humidity, Day)

Angles from Inlet in Degrees (and Radians)

	0.	10.	20.	30.	40.	50.	60.	70.	80.	90.	100.	110.	0.	0.
FREQ. (0. 1 (0.17) (0.35) (0.52) (0.70) (0.87) (1.05) (1.22) (1.40) (1.57) (1.75) (1.92) (0. 1 (0. 1 (0. 1	50													
	63													
		BASELINE CLEAN CHAMBER (REPEAT)												PWL
		CORRECTED SPEED = 54%												
<u>RADIAL 17- FT.</u>	50													
(5. M)	60													
VEHICLE R-11	100	70.0	69.3	68.8	66.8	65.3	65.6	67.7	68.5	68.1	68.0	66.9	65.8	101.1
CONFIG CF 5	125	75.7	75.3	75.1	72.3	71.3	71.9	73.2	73.3	73.1	72.7	72.2	70.8	106.4
LCC SCHENECTADY	150	69.2	68.0	66.8	67.3	68.8	67.1	66.9	70.0	72.3	65.7	70.7	72.0	103.4
DATE 8/11/76	200	72.7	75.0	74.3	72.1	71.1	70.6	68.7	68.8	67.8	66.7	63.9	63.0	103.0
RUN 30/3	250	78.5	77.5	77.8	76.8	75.8	73.6	72.7	70.5	70.3	70.5	68.4	65.5	106.6
TAPE	315	79.0	79.8	78.6	77.5	77.1	75.1	73.2	71.8	69.8	68.7	66.9	66.0	107.3
BAR 29.9 HG	400	74.0	74.3	73.8	72.8	71.8	70.4	68.4	66.3	64.6	64.5	62.2	59.3	102.3
(C1039. N/M2)	500	71.2	71.0	71.5	70.8	69.8	69.1	67.9	66.5	64.8	64.0	61.0	58.5	100.9
TAMH 84. DEG F	630	72.7	73.3	73.1	72.5	71.8	69.9	67.9	66.3	65.0	64.7	62.5	59.5	102.0
(302. DEG K)	800	72.7	72.5	72.6	72.2	71.6	69.8	67.9	65.8	64.5	64.4	62.7	59.5	101.8
THET 75. DEG F	1000	69.2	69.8	70.3	70.2	69.8	68.3	66.4	63.8	61.3	58.9	58.2	56.5	99.6
(297. DEG K)	1250	73.0	71.1	71.6	71.3	70.3	68.3	66.4	64.0	61.8	59.7	58.8	56.0	100.2
MACT 18.88 GM/M3	1600	71.0	71.3	72.1	71.0	70.8	69.3	67.4	64.8	62.3	61.2	58.4	57.0	100.8
(.01888 KG/M3)	2000	73.5	74.6	74.4	74.3	73.6	72.6	71.1	67.6	64.3	63.1	60.2	60.0	103.7
NFA 9901. RPM	2500	76.7	77.3	76.4	76.6	76.3	75.1	73.1	70.0	67.1	64.9	62.4	60.9	106.1
(932. RAD/SEC)	3150	79.0	79.3	78.6	79.1	79.2	79.3	77.6	73.8	70.5	67.6	66.0	64.9	109.4
NFK 8694. RPM	4000	80.6	81.2	81.5	81.8	81.9	81.7	80.0	76.5	72.5	70.2	68.2	67.6	112.0
(910. RAD/SEC)	5000	63.1	83.9	84.2	85.0	84.6	83.1	80.9	76.4	73.2	71.1	68.9	67.5	113.9
NFD 16100. RPM	6300	94.7	94.2	95.5	95.9	96.4	95.3	93.6	89.6	85.9	84.9	81.7	80.4	125.9
(1686. RAD/SEC)	10000	84.0	85.2	86.0	86.0	88.1	87.4	84.9	80.2	75.5	73.1	71.4	70.2	117.4
NO. OF BLADES 44	12500	94.5	92.4	93.8	94.7	93.6	93.2	92.9	87.9	83.4	80.0	77.8	75.9	124.5
FAN TIP SPEED	15000	84.2	85.2	87.1	88.1	88.2	86.3	85.5	81.0	75.5	72.6	69.8	69.6	118.2
771. FT/SEC	20000	63.4	85.4	87.0	89.0	94.6	91.2	88.3	84.2	79.0	74.1	71.4	69.4	122.6
	25000	66.6	82.3	84.6	85.	86.8	87.4	85.5	80.7	74.1	68.8	66.5	65.6	118.5
	31500	77.8	76.1	81.0	83.1	83.5	83.0	81.9	76.6	69.0	64.9	60.6	61.7	115.7
	40000	75.8	74.5	77.5	78.7	80.3	79.5	77.8	72.1	64.7	61.0	58.1	59.6	113.3
	50000	74.8	72.2	75.0	75.3	76.2	75.7	73.8	68.3	61.6	58.8	57.3	58.7	111.4
	63000	72.0	68.4	70.7	71.1	71.9	71.6	69.0	63.2	59.0	58.0	56.2	58.6	109.9
	80000	72.4	62.7	65.0	64.5	64.9	64.1	62.8	59.2	55.9	53.9	54.1	55.9	107.6
OVERALL CALCULATED	96.9	96.4	99.6	100.4	101.2	99.9	98.4	94.0	89.9	87.9	85.4	84.1	131.0	

Table 31

MODEL SOUND PRESSURE LEVELS (59° F, 70% Relative Humidity, Day)

Angles from Inlet in Degrees (and Radians)

78

Table 32
MODEL SOUND PRESSURE LEVELS (59°F, 70% Relative Humidity, Day)

Angles from Inlet in Degrees (and Radians)

	0.	10.	20.	30.	40.	50.	60.	70.	80.	90.	100.	110.	0.	0.
FREQ. (Hz.)	(0.17)	(0.35)	(0.52)	(0.70)	(0.87)	(1.05)	(1.22)	(1.40)	(1.57)	(1.75)	(1.92)	(0.1)	(0.1)	
	50													
	53													
	30													
RADIAL - 17. FT. (5. M)	100	68.8	68.8	68.3	67.1	66.1	70.8	72.0	72.3	71.8	72.1	71.5	69.6	104.6
VEHICLE R-11	125	72.3	71.8	72.5	69.9	68.3	71.3	73.0	71.5	71.3	72.6	71.0	70.1	105.1
CONFIG OF H	150	59.1	67.8	66.8	67.6	67.6	70.8	71.3	71.8	70.0	70.6	71.0	69.9	104.0
LOC SCHENECTALY	200	73.3	74.8	74.3	73.1	72.8	74.0	73.5	74.2	73.5	71.0	68.0	68.9	106.3
DATE 8/11/76	250	79.0	78.8	80.0	80.5	80.8	79.2	78.0	81.5	83.7	81.0	76.0	78.3	114.1
RUN 30/5	315	78.0	78.3	77.3	77.4	76.1	75.2	74.0	72.2	69.7	69.0	67.5	66.1	107.0
TAPE	400	77.8	77.5	76.5	76.6	75.1	74.7	73.5	72.2	68.7	68.8	66.3	63.3	106.3
BAR 30.0 MG	500	74.5	74.0	75.0	75.1	73.8	74.0	73.5	72.2	69.0	67.8	65.3	62.6	105.5
(01172. V/M2)	630	72.5	77.1	76.0	75.6	75.6	75.0	74.0	72.5	70.2	69.3	66.9	63.3	106.7
TEMP 25. DEG F	800	70.8	70.3	77.0	77.3	76.3	75.5	74.2	73.2	70.5	70.7	69.4	64.3	107.2
(303. DEG K)	1000	75.0	75.0	75.5	77.3	76.6	75.4	73.2	73.0	72.2	68.0	65.4	64.3	106.8
THET 75. DEG F	1250	77.8	78.6	77.8	77.1	76.3	77.5	78.0	74.5	75.5	72.0	66.7	65.6	109.0
(297. DEG K)	1600	78.3	80.0	79.6	78.5	77.8	77.2	76.2	75.0	70.2	71.5	67.5	66.3	108.9
HACT 18.57 GM/M3	2000	59.3	61.5	82.6	80.9	81.3	80.7	81.0	80.5	74.7	77.2	69.3	72.5	112.8
(.01857 KG/M3)	2500	50.6	80.6	81.1	82.1	85.3	88.2	90.7	90.0	85.0	83.7	80.8	78.8	120.2
NFA 14205. RPM	3150	65.8	86.1	83.8	85.1	91.3	96.9	98.9	98.7	95.5	91.1	88.1	87.0	126.6
(1487. RAD/SEC)	4000	91.0	95.8	93.7	97.8	100.9	107.8	109.1	106.9	101.9	99.3	95.8	98.4	137.9
NFK 13862. RPM	5000	95.7	96.7	97.6	99.0	101.6	109.7	112.0	109.1	105.1	101.7	99.8	97.8	140.4
(1451. RAD/SEC)	6300	94.5	93.4	93.7	97.0	98.6	102.9	107.4	105.3	101.4	99.2	94.6	91.0	135.9
NFD 16100. RPM	8000	93.1	94.1	94.6	97.0	96.9	98.1	102.3	101.1	97.9	94.3	90.5	88.6	131.9
(1686. RAD/SEC)	10000	102.6	105.4	105.7	107.8	108.2	109.3	107.5	106.9	101.6	97.9	95.0	92.3	139.5
NO. OF BLADES 44	12500	94.6	94.9	96.3	98.5	99.6	100.1	102.5	101.1	96.8	93.3	90.7	85.9	132.7
FAN TIP SPEED	16000	92.5	93.4	94.6	96.9	98.0	99.9	100.6	99.0	94.5	90.9	87.1	82.9	131.3
1230. FT/SEC	20000	94.2	94.7	96.2	97.2	98.4	100.3	99.1	96.7	91.7	87.4	83.8	79.7	131.0
	25000	94.4	90.5	92.1	93.5	94.6	96.8	96.8	94.2	89.6	84.4	80.9	75.5	128.5
	31500	88.6	89.2	90.3	91.7	92.5	93.7	93.8	91.1	86.4	79.8	74.7	71.1	126.6
	40000	84.7	85.3	87.0	87.4	88.9	90.4	89.7	87.1	81.9	76.1	69.8	67.7	124.2
	50000	81.2	81.8	83.3	84.0	85.0	87.2	86.7	83.6	78.4	72.0	66.7	66.9	122.7
	61000	77.5	77.5	78.8	79.3	80.6	83.3	82.7	80.8	74.3	68.4	66.5	65.6	121.5
	68000	70.2	71.4	73.4	72.3	73.1	80.6	80.5	79.1	71.8	69.2	69.7	63.4	122.6
OVERALL CALCULATED	100.4	107.4	108.2	110.3	111.3	114.9	116.3	114.2	109.9	106.7	103.7	102.6	145.9	

BASELINE CLEAN CHAMBER (REPEAT)

CORRECTED SPEED = 86%

PWL

Table 33
MODEL SOUND PRESSURE LEVELS (59° F, 70% Relative Humidity, Day)

Angles from Inlet in Degrees (and Radians)

		0.	10.	20.	30.	40.	50.	60.	70.	80.	90.	100.	110.	0.	0.
FREQ.	(0.)	(0.17)	(0.35)	(0.52)	(0.70)	(0.87)	(1.05)	(1.22)	(1.40)	(1.57)	(1.75)	(1.92)	(0.)	(0.)	
	50														PWL
	63														
RADIAL 12. FT.	80														
(5. ft)	100	68.1	64.0	65.8	64.4	70.3	70.8	71.0	71.0	70.0	70.3	69.8	69.1	103.6	
VEHICLE R-11	125	70.1	69.5	70.8	67.9	70.3	70.8	72.0	71.8	70.8	72.1	71.3	70.4	104.8	
CONFIG CF 6	160	67.8	66.3	66.0	66.1	70.5	70.8	71.3	72.0	70.3	71.1	71.8	70.6	104.4	
LOC SCHENECTADY	200	70.6	71.8	71.0	69.9	72.7	72.5	73.0	71.2	67.5	68.0	67.0	63.9	104.0	
DATE 8/11/76	250	70.5	78.3	76.5	77.1	76.7	78.2	79.7	78.7	79.7	82.5	81.0	74.1	113.1	
RUN 30/6	315	75.5	75.3	73.8	73.9	73.7	73.5	72.2	70.7	67.2	68.0	67.3	64.6	104.8	
TAPE	400	74.5	73.5	73.3	73.1	73.2	72.5	71.7	70.2	66.7	67.0	65.1	61.8	104.0	
BAR 30.0 KG	500	73.3	72.5	72.8	72.6	73.8	74.0	72.5	70.2	67.7	65.8	64.3	63.6	104.3	
(01172. N/M2)	630	80.5	80.1	79.0	77.6	76.5	71.2	73.5	71.8	67.7	67.0	64.9	63.6	107.0	
TAMB 85. DEG F	800	75.5	74.0	74.8	74.8	75.0	74.2	73.5	73.2	70.0	69.0	66.4	63.1	105.9	
(303. DEG K)	1000	75.3	73.5	73.0	74.3	76.2	75.9	73.2	74.2	72.9	69.2	68.4	68.3	106.8	
THET 74. DEG F	1250	77.5	76.6	76.3	78.1	80.3	81.5	81.0	81.5	80.2	75.5	72.4	72.1	112.7	
(296. DEG K)	1600	80.6	81.6	82.1	83.9	86.5	90.2	90.5	88.3	84.2	82.7	82.0	81.3	120.2	
HACT 17.61 GM/M3	2000	85.3	85.1	86.3	85.9	95.2	100.2	102.2	100.0	96.7	94.5	94.0	91.0	131.2	
(+01761 KG/M3)	2500	80.1	85.1	84.8	87.6	95.2	98.7	100.4	98.8	94.7	95.2	90.6	89.0	129.9	
NFA 14848. RPM	3150	85.5	89.1	83.3	84.6	95.4	99.6	100.1	98.0	94.2	89.4	88.8	87.0	129.4	
(1555. RAD/SEC)	4000	89.2	90.3	90.7	97.8	104.1	107.6	106.8	103.9	100.7	97.3	97.3	95.9	136.6	
NFK 14489. RPM	5000	94.9	95.4	95.9	98.5	106.8	111.5	111.2	107.1	103.8	100.0	100.3	99.1	140.3	
(15117. RAD/SEC)	6300	94.5	93.7	96.2	96.0	100.3	106.9	108.9	105.1	101.9	99.9	94.8	93.8	137.3	
NFD 16100. RPM	8000	92.3	93.3	93.5	96.8	97.6	102.6	103.6	101.1	96.9	93.6	90.7	88.6	132.9	
(1686. RAD/SEC)	10000	105.9	104.7	105.9	107.1	107.3	107.8	110.5	107.6	103.9	100.7	96.0	96.0	140.1	
NO. OF BLADES 44	12500	100.1	99.2	100.3	102.0	103.0	103.3	106.0	102.9	99.1	95.1	92.0	89.5	135.6	
FAN TIP SPEED	16000	93.3	93.7	95.3	97.9	99.7	100.4	102.3	99.0	95.3	90.4	87.4	83.4	132.3	
1286. FT/SEC	20000	93.8	95.0	96.0	98.0	98.9	99.9	100.6	98.0	93.5	89.0	85.1	81.5	131.7	
	25000	91.2	91.8	93.1	94.6	96.1	97.6	98.9	96.0	90.9	86.0	82.2	77.3	130.0	
	31500	88.2	89.0	90.3	92.6	93.0	94.8	95.3	92.4	87.3	82.1	76.8	72.9	127.7	
	40000	84.1	85.2	86.4	88.0	89.7	91.3	91.8	89.2	83.3	77.2	71.7	69.6	125.5	
	50000	81.4	81.4	83.0	85.2	86.6	88.9	89.1	87.0	80.8	74.6	68.7	68.3	124.7	
	63000	78.0	77.8	78.8	79.9	82.7	85.3	85.5	83.6	77.6	70.4	67.0	67.1	123.7	
	60000	73.6	71.8	73.7	73.6	79.6	81.3	81.9	80.2	73.6	69.5	70.0	64.0	124.0	

OVERALL CALCULATED 108.2 107.6 108.7 110.4 113.0 116.1 117.1 113.9 110.3 107.2 105.0 103.7 146.6

Table 34
MODEL SOUND PRESSURE LEVELS (59° F, 70% Relative Humidity, Day)

Angles from Inlet in Degrees (and Radians)

Table 35
MODEL SOUND PRESSURE LEVELS (59° F, 70% Relative Humidity, Day)

Table 36

MODEL SOUND PRESSURE LEVELS (59° F, 70% Relative Humidity, Day)

Angles from Inlet in Degrees (and Radians)

Appendix III

REFERENCES

1. Feiler, C.E., and Merriman, J.E.: Effects of Forward Velocity and Acoustic Treatment on Inlet Fan Noise. NASA TM X-71591, 1974 (also AIAA Paper No. 74-946).
2. Merriman, J.E., and Good, R.C.: Effect of Forward Motion on Fan Noise. Paper No. 75-464, AIAA 2nd Aero-Acoustics Conference, 1975.
3. Roundhill, J.P., and Schaut, L.A.: Model and Full Scale Test Results Relating to Fan Noise In-Flight Effects. Paper No. 75-465, AIAA 2nd Aero-Acoustics Conference, 1975.
4. Kazin, S.D., and Volk, L.J.: LF336 Lift Fan Modification and Acoustic Test Program. NASA CR-1934, 1971.
5. Hodder, B.K.: The Effects of Forward Speed on Fan Inlet Turbulence and Its Relation to Tone Noise Generation. NASA TM X-62381, 1974.
6. Lowrie, B.W.: Simulation of Flight Effects on Aero Engine Fan Noise. Paper No. 75-463, AIAA 2nd Aero-Acoustics Conference, 1975.
7. Cumpsty, N.A., and Lowrie, B.W.: The Cause of Tone Generation by Aero-Engine Fans at High Subsonic Tip Speeds and the Effect of Forward Speed. ASME J. Eng. Power, vol. 96, no. 3, 1974, pp. 228-234.
8. Povinelli, F.P., Dittmar, J.H. and Woodward, R.P.: Effects of Installation Caused Flow Distortion on Noise from a Fan Designed for Turbofan Engines. NASA TN D-7076, 1972.
9. Hodder, B.K.: Investigation of the Effect of Inlet Turbulence Length Scale on Fan Discrete Tone Noise. NASA TM X-62300, 1973.
10. Hanson, D.B.: The Spectrum of Rotor Noise Caused by Atmospheric Turbulence. J. Acoust. Soc. of America, vol. 56, no. 1, 1974, pp. 110-126.
11. Hanson, D.B.: Measurements of Static Inlet Turbulence. Paper No. 75-467, AIAA 2nd Aero-Acoustics Conference, 1975.
12. Hanson, D.B.: A Study of Subsonic Fan Noise Sources. Paper No. 75-468, AIAA 2nd Aero-Acoustics Conference, 1975.
13. Pickett, G.F.: Effects of Non-Uniform Inflow on Fan Noise. Acoust. Soc. of America, Spring Meeting, New York, April 1974.
14. Hodder, B.K.: An Investigation of Possible Causes for the Reduction of Fan Noise In Flight. Paper No. 76-585, AIAA 3rd Aero-Acoustics Conference, 1976.
15. Goldstein, M., Unified Approach to Aerodynamic Sound Generation in the Presence of Solid Boundaries, J. Acoust. Soc. of America, vol. 56, no. 2, 1974, pp. 497-509.
16. Goldstein, M., Dittmar, J., and Gelder, T., A Combined Quadrupole-Dipole Model for Inlet Flow Distortion Noise from a Subsonic Fan. NASA TN D-7676, 1974.
17. Mani, R.: Noise Due to Interaction of Inlet Turbulence with Isolated Stators and Rotors. J. Sound Vib. vol. 17, no. 2, 1971, pp. 251-260.

18. Mani, R.: Isolated Rotor Noise Due to Inlet Distortion or Turbulence. NASA CR-2479, 1974.
19. Mani, R., and Bekofske, K., Experimental and Theoretical Studies of Subsonic Fan Noise. NASA CR-2660, 1976.